



**The Effect of Low-Intensity Pulsed Ultrasound on Extracellular Matrix and its cross-linking and organisation.**

**Yazeed Almukhlifi**

A thesis submitted in partial fulfilment of the requirements for the degree of  
Doctor of Philosophy

The University of Sheffield  
Faculty of science  
Department/School of Biosciences

Submission Date

October 2024

## Acknowledgment

I would like to express my appreciation to my supervisor Dr Mark Bass, for the invaluable guidance, encouragement and support throughout my PhD journey. Your insights, patience and expertise have been crucial in shaping both my research and personal development as a scientist. I would like, also, to thank Majmaah university for supporting me in this journey. Also, many thanks to my advisors Dr Elena Rainero and Dr Stephen Brown for providing invaluable feedback and support.

I am also deeply thankful to have such an amazing and supportive family; my father, mother, my big brother and my sisters, for their love, encouragement and belief in me. Your endless support has been my source of strength during the most challenging times of this journey.

To my beloved wife **Noura**, your patience, understanding and constant motivation have been a true blessing. You have been by my side through every late night, every challenge I have gone through and even during the many weekends when I was completely absorbed in my lab work. Your belief in me more than anyone else has kept me going. As we eagerly await the arrival of our little baby in just a few months, I am filled with gratitude for the incredible journey we have already been on together and I look forward to the joy and new challenges that lie ahead as we embark on this next chapter of our lives.

I would also like to extend my heartfelt appreciation to my current and previous colleagues at the lab: Dr Amani, Dr Salma, Dr Elghazali, Weronika Buczek, Nataya, Dr Hatoon Alamri, Michelle King and Nadia. Your friendship and constant support made this journey much easier and more fulfilling. Whether it was sharing knowledge or providing encouragement, each of you contributed to the success of this work in your own way. I would like to especially thank Bass lab colleague Xianhui Wei, your support and encouragement were truly invaluable. I deeply appreciate our friendship, collaboration and the countless times you lifted my spirits when things seemed overwhelming.

Thank you all for being part of this journey and for making it an unforgettable and inspiring experience.

## **Abstract**

Chronic wounds are characterised by their inability to heal within the expected time frame, significantly impacting patient welfare and even life expectancy, while also imposing considerable financial burdens on the healthcare system. The extracellular matrix (ECM) plays an essential role by interacting with growth factors and providing the physical substrate over which cells migrate during healing. However, in chronic wounds, the ECM components often appear to be dysfunctional. Low-intensity ultrasound, as a form of mechanical stimulation, has shown promising results at the cellular level.

This project aims to investigate the effect of Low-Intensity Pulsed Ultrasound (LIPUS) on gene expression, matrix deposition, cross-linking, and the organisation of specific ECM molecules.

In this study, two cell lines were used, human foreskin fibroblast (HFF) and telomerase-immortalized fibroblasts (TIF). Then, I performed western blot, Quantitative PCR, Immunofluorescence, migration assay and traction force microscopy to investigate the protein and gene expression changes, matrix alignment and contractility and cell migration after the LIPUS treatment. 1.5-MHz frequency, a 20% duty cycle pulse to generate a 30 mW/cm<sup>2</sup> spatial average and temporal average (SATA) were applied to the treatment group. The treatment was performed for 20 minutes per day for five days.

The results indicate that matrix composition was altered by LIPUS, with specific effects on ECM molecules involved in healing. Transforming growth factor-beta (TGF- $\beta$ ) and collagen type I showed a reduction in protein expression in the conditioned medium, whereas lysyl oxidase (LOX), collagen type III, and fibronectin exhibited increased expression. These findings reveal that LIPUS treatment changes the composition of secreted matrix by altering the expression profiles of several components and regulatory factors in a manner that is far more nuanced than simply promoting expression.



LIPUS treatment also altered fibronectin fibre curvature, leading to more random alignment. This is significant as it suggests that a 20-minute treatment can have long-lasting healing effects by modifying ECM architecture. Traction Force Microscopy revealed reduced cellular contractility after LIPUS treatment, likely due to changes in TGF- $\beta$  expression, which explains the altered ECM alignment. Overall, these findings show that LIPUS influences both ECM structure and cellular mechanical properties, potentially improving tissue repair and healing outcomes.

Together, these findings indicate LIPUS's potential as a therapeutic tool to enhance wound healing and reduce the scar effect, particularly in cases of chronic wounds where ECM dysfunction is common. Also, this project suggests that LIPUS can affect ECM dynamics, showing changes in protein expression and ECM organisation.

***Declaration***

*I, the author, confirm that the Thesis is my own work. I am aware of the University's Guidance on the Use of Unfair Means ([www.sheffield.ac.uk/ssid/unfair-means](http://www.sheffield.ac.uk/ssid/unfair-means)). This work has not been previously been presented for an award at this, or any other, university.*

## Table of Contents

<b>Chapter 1 Introduction.....</b>	<b>17</b>
<b>1.1 Overview .....</b>	<b>17</b>
<b>1.2 Structure and Function of Intact Skin .....</b>	<b>17</b>
1.2.1 Skin as a Protective Barrier.....	17
1.2.2 Skin Structure and Function.....	18
1.2.3 Role of Fibroblasts in Skin Integrity .....	19
<b>1.3 Healing Processes and Scar Formation .....</b>	<b>21</b>
1.3.1 Objectives of Wound Healing .....	21
1.3.2 Acute vs. Chronic Wounds.....	21
1.3.3 Scar Formation and Types .....	22
1.3.4 Cellular and Molecular Mechanisms in Scar Formation .....	24
<b>1.4 Chronic Wounds .....</b>	<b>26</b>
1.4.1 Definition and Prevalence .....	26
1.4.2 Characteristics of Chronic Wounds .....	28
1.4.3 Challenges in Chronic Wound Healing .....	30
<b>1.5 Wound Healing Stages .....</b>	<b>31</b>
1.5.1 Haemostasis Stage.....	31
1.5.2 Inflammatory Stage .....	31
1.5.3 Proliferative Phase .....	32
1.5.4 Remodelling Stage .....	32
<b>1.6 The Extracellular Matrix in Wound Healing .....</b>	<b>33</b>
1.6.1 Overview of the ECM.....	33
1.6.2 ECM's Role in Wound Healing Stages.....	34
1.6.3 Collagen .....	35
1.6.4 Transforming Growth Factor-Beta (TGF- $\beta$ ) .....	38
1.6.5 Fibronectin.....	39
1.6.6 Lysyl Oxidase.....	41
<b>1.7 Ultrasound as a Therapy Tool.....</b>	<b>44</b>
1.7.1 Overview of Ultrasound .....	44
1.7.2 Types of Therapeutic Ultrasound .....	44
1.7.3 Low-Intensity Pulsed Ultrasound (LIPUS).....	45
1.7.4 Mechanisms of LIPUS .....	47
1.7.5 LIPUS in Fracture Healing .....	49
1.7.6 LIPUS in Musculoskeletal Studies.....	50
1.7.7 LIPUS in Wound Healing Studies.....	52
<b>1.8 Research Gap and Thesis Aims .....</b>	<b>54</b>
<b>1.9 Significance of this PhD Project.....</b>	<b>55</b>
<b>1.10 Hypothesis and Objectives: .....</b>	<b>55</b>
<b>Chapter 2 Materials and Methods .....</b>	<b>57</b>
<b>2.1 Investigation of published data sets to define the candidate proteins .....</b>	<b>57</b>

<b>2.2 Cell Lines.....</b>	<b>59</b>
<b>2.3 LIPUS stimulation parameters .....</b>	<b>61</b>
<b>2.4 Storing cells.....</b>	<b>65</b>
<b>2.5 Thawing cells.....</b>	<b>65</b>
<b>2.6 Quantitative polymerase chain reaction .....</b>	<b>66</b>
<b>2.7 Analysis of Protein Expression by Western blot .....</b>	<b>67</b>
<b>2.8 Mammalian cell transfection for RNAi .....</b>	<b>71</b>
<b>2.9 Immunofluorescence .....</b>	<b>72</b>
<b>2.10 Migration Assay .....</b>	<b>75</b>
<b>2.11 Traction Force Microscopy .....</b>	<b>77</b>
<b>2.12 Statistical Analysis.....</b>	<b>79</b>
<b><i>Chapter 3 Identification of matrix proteins involved in wound healing by data mining ...</i></b>	<b>81</b>
<b>3.1 Introduction to the role of Extracellular Matrix in wound healing .....</b>	<b>81</b>
<b>3.2 Results.....</b>	<b>82</b>
3.2.1 Matrix metalloproteinases .....	82
3.2.2 Extracellular Matrix.....	88
<b>3.3 Discussion .....</b>	<b>91</b>
3.3.1 Why Collagens as a Target for Ultrasound Therapy But not MMPs? .....	91
3.3.2 The Importance of Fibronectin in Wound Healing.....	94
3.3.3 Lysyl Oxidase as a Cross Linker for Collagen .....	95
3.3.4 Transforming Growth Factor-Beta: A Key Growth Factor Target for Ultrasound Therapy .....	96
3.3.5 Limitations of Microarray Data and Alternative Approaches .....	98
<b>3.4 Conclusion .....</b>	<b>98</b>
<b><i>Chapter 4 Effect of LIPUS on Matrix Deposition.....</i></b>	<b>101</b>
<b>4.1 Introduction .....</b>	<b>101</b>
<b>4.2 Results.....</b>	<b>102</b>
4.2.1 Period of LIPUS stimulation .....	102
4.2.2 Fibronectin .....	103
4.2.3 Collagens .....	104
4.2.4 Matrix alignment.....	111
<b>4.3 Discussion .....</b>	<b>113</b>
<b><i>Chapter 5 Effect of LIPUS on matrix cross-linking and cell contractility.....</i></b>	<b>119</b>
<b>5.1 Introduction .....</b>	<b>119</b>
5.1.1 Cell-Derived Matrix (CDM) .....	120
5.1.2 The role of Lysyl Oxidase (LOX) in matrix cross-linking .....	120
5.1.3 Transforming growth factor-beta (TGF- $\beta$ ) .....	121
5.1.4 Traction Force microscopy .....	121

<b>5.2 Result .....</b>	<b>123</b>
5.2.1 LIPUS-stimulation increase abundance of secreted Lysyl Oxidase. ....	123
5.2.2 Effects of LIPUS on TGF- $\beta$ Expression.....	125
5.2.3 Cell-derived matrix.....	126
5.2.4 Collagen III knockdown CDM .....	127
5.2.5 Traction Force Microscopy .....	132
<b>5.3 Discussion .....</b>	<b>135</b>
5.3.1 Alternative mechanisms for regulating matrix organisation .....	135
5.3.2 The role of Lysyl Oxidase (LOX) in matrix cross-linking .....	135
5.3.3 Transforming growth factor-beta (TGF- $\beta$ ) affects scarring .....	136
5.3.4 CDM migration.....	138
5.3.5 Traction Force Microscopy .....	139
<b>Chapter 6 Discussion .....</b>	<b>143</b>
<b>6.1 Effect of LIPUS as a therapy tool on fibroblast.....</b>	<b>143</b>
<b>6.2 Exploring the Impact of LIPUS on Extracellular Matrix Composition and Alignment .145</b>	
6.2.1 Regulation of fibronectin expression highlights changes in ECM structure and function .....	145
6.2.2 Differential Regulation of Collagen I and III Reflects ECM Composition Changes .....	147
6.2.3 LIPUS Effect on Matrix Alignment .....	148
<b>6.3 Impact of LIPUS on matrix cross-linking and cellular mechanics: insights into LOX activity, TGF-<math>\beta</math> signaling, and cell-matrix interactions.....</b>	<b>150</b>
6.3.1 Altered LOX Expression Reflects Changes in ECM Remodeling Dynamics.....	150
6.3.2. LIPUS modulates cell migration dynamics on cell-derived matrices, highlighting ECM influence on cellular behaviour.....	151
6.3.3 Modulation of TGF- $\beta$ expression highlights changes in fibrotic signalling pathways .....	153
6.3.4 Traction force analysis reveals altered force generation following LIPUS stimulation.....	155
<b>6.4 Limitations.....</b>	<b>157</b>
<b>6.5 Future Direction .....</b>	<b>158</b>
<b>6.6 Conclusion .....</b>	<b>159</b>
<b>Chapter 7 Appendices .....</b>	<b>160</b>
<b>References .....</b>	<b>165</b>

## List of figures

Figure 1.1 The structural layers of human skin include the epidermis, dermis, and hypodermis. ....	19
Figure 1.2 Comparison between normal wound healing to chronic wounds.....	29
Figure 1.3 Stages of wound healing repair. ....	33
Figure 1.4 Extracellular matrix structure. (Image created in BioRender.com.) .....	34
Figure 1.5 The proposed roles of LOX in response to various factors (image reproduced from Voloshenyuk et al., 2011). ....	43
Figure 1.6 Pulsed and continuous ultrasound waveforms. ....	46
Figure 2.1 DAVID page showing how to specify the Extracellular Matrix proteins amongst the other proteins. ....	58
Figure 2.2 Showing DAVID Gene Report of the Extracellular Matrix proteins involved on genome-wide microarray study, involving 25 biopsies from SSG yielded more than 2-fold change.....	58
Figure 2.3 Fast Read 102® chambers for cell counting .....	61
Figure 2.4 Flowchart of the process of LIPUS treatment and control samples (Image created using Biorender). ....	63
Figure 2.5 Flow chart Showing summary of the cell culture and LIPUS stimulation steps...	64
Figure 2.6 The Western blot process (Image created using Biorender). ....	71
Figure 2.7 A summary of the protocol for the generation of CDMs (image created using Biorender). ....	77
Figure 3.1 the different biopsy stages. ....	83
Figure 3.2 Time-course expression of key ECM-related genes during wound healing.....	91
Figure 3.3 Skin sections at 72 hours post-wounding. ....	98
Figure 4.1 Time scale of LIPUS stimulation. ....	103
Figure 4.2 Protein expression of fibronectin conditioned medium and cell lysate.....	104
Figure 4.3 Protein expression of collagen I conditioned medium. ....	106
Figure 4.4 Protein expression of collagen I conditioned medium. ....	107
Figure 4.5 Immunofluorescence analysis of collagen I showing the mean intensity. ....	109
Figure 4.6 Protein expression of Collagen III conditioned medium. ....	110
Figure 4.7 Immunofluorescence analysis of fibronectin.....	112
Figure 4.8 The result of different curvature windows used.....	113
Figure 5.1 A depiction of cell migration and CTFs (Image Created in BioRender.com). ...	122
Figure 5.2 Protein expression of LOX cell lysate and conditioned medium. ....	124
Figure 5.3 Protein expression of TGF- $\beta$ . ....	126
Figure 5.4 Cells migrating over the sham-treated and LIPUS-stimulated matrix .....	128
Figure 5.5 Cells migration over 16 hours with and without Collagen III knockdown. ....	129
Figure 5.6 Bar chart of the total cells' directional persistence. ....	130
Figure 5.7 Cells migrating on matrix. ....	131
Figure 5.8 Cells total distance.....	132
Figure 5.9 TFM experiment.....	134

Figure 5.10 Mechanical (ultrasound) and chemical (fibronectin) stimuli activate Rac1.....	139
Figure 5.11 Summary of the LIPUS effect on the candidate proteins.....	141
Figure 6.1 Sham- or ultrasound (US)-treated wild-type (a–c). (Images are from Roper et al., 2015) .....	152
Figure 6.2 The amount of TGF- $\beta$ in the epidermis .....	154
Figure 7.1 $\alpha$ SMA Western blot gel with GAPDH.....	160
Figure 7.2 Collagen 4 Western blot gel with GAPDH. ....	160
Figure 7.3 qPCR of LOX (n=2). ....	161
Figure 7.4 qPCR of collagen 1 (n=2). ....	161
Figure 7.5 qPCR of fibronectin (n=2). ....	161
Figure 7.6 qPCR of collagen 6 (n=2). ....	162

## List of tables

Table 1.1 Comparison of Key Features and Characteristics of Normal Skin, Hypertrophic Scars, and Keloids. ....	25
Table 2.1 Cell culture materials.....	60
Table 2.2 LIPUS stimulation period.....	62
Table 2.3 Buffers used in western blot and preparations. ....	69
Table 2.4 Antibodies used for western blot tests, the species in which they were raised and their dilution factors. ....	70
Table 2.5 siRNA transfection reagents. ....	72
Table 2.6 TWOMBLI Parameters.....	75
Table 2.7 Traction Force Microscopy procedure timeline. ....	79
Table 3.1 List of ECM proteins in order from highest to lowest fold change for up-regulation in different phases of wound healing. ....	84
Table 3.2 List of ECM proteins in order from highest to lowest fold change for down-regulation in different phases of wound healing. ....	86
Table 3.3 Relative expression levels at each time point (Intact, Acute, 3 POD, and 7 POD) were calculated using fold-change values from pairwise comparisons. ....	90
Table 5.1 The period of LIPUS treatment. ....	124



## **List of abbreviations**

3POD – Third Postoperative Day

7POD – Postoperative Day

ADAMs – Adamalysins

AFM – Atomic force microscopy

$\alpha$ -SMA – alpha-smooth muscle actin

BM – Basement membrane

BSA – Bovine Serum Albumin

Ca<sup>2+</sup> – Calcium ions

CAF – Cancer-associated fibroblasts

CDM – Cell-derived matrix

COL1A1 – Collagen type 1 A1

Cx43 – Connexin43

DAVID – Database for Annotation, Visualization, and Integrated Discovery

DFU – Diabetic foot ulcer

DFUFs – Diabetic foot ulcer fibroblasts

DMEM – Dulbecco's Modified Eagle Medium

DMSO – Dimethyl Sulfoxide

ECM – Extracellular matrix

EGF – Epidermal growth factor

EMT – Epithelial-mesenchymal transition

FAs – Focal adhesions

FBS – Foetal bovine serum

FGF – Fibroblast growth factor

FNs – Fibronectins

FTTC – Fourier transform traction cytometry

GAGs – Glycosaminoglycans

GFs – Growth factors

HDF – Human dermal fibroblasts

HFFs – Human foreskin fibroblasts  
HGF – Human gingival fibroblasts  
HIFU – High-intensity focused ultrasound  
KDF – Keloid dermal fibroblasts  
LIUS – Low-intensity ultrasound  
LIPUS – Low-intensity pulsed ultrasound  
LOX – Lysyl oxidase  
LOXL – Lysyl oxidase-like  
MMPs – Matrix metalloproteinases  
MuSCs – Muscle stem cells  
MSCs – Mesenchymal stem cells  
NDF – Normal dermal fibroblasts  
NFFs – Normal foot fibroblasts  
NPC – Nuclear pore complex  
PAA – Polyacrylamide  
PBS – Phosphate-buffered saline  
PCNA – Proliferating cell nuclear antigen  
PDGF – Platelet-derived growth factor  
PIV – Particle Image Velocimetry  
pFn – Plasma Fibronectin  
PUs – Pressure ulcers  
qPCR – quantitative polymerase chain reaction  
ROI – Region of interest  
ROS – Reactive oxygen species  
SATA – Spatial average temporal average  
siRNA – Small interfering RNA  
SSG – Split-thickness skin grafts  
TGF- $\beta$  – Transforming growth factor-beta  
TIFs – Telomerase Immortalised Fibroblasts

TIMP1 – Matrix metalloproteinase 1

TGase – Tissue transglutaminases

TWOMBLI – The Workflow of Matrix BioLogY Informatics

US – Ultrasound

VLUs – Venous leg ulcers

# Chapter 1

## Introduction

# Chapter 1 Introduction

## 1.1 Overview

Wound healing is a critical biological process involving a complex interaction of cells, growth factors, and extracellular matrix (ECM) components. This process is necessary for restoring tissue integrity and function after injury. It is crucial to understand the mechanisms involved in wound healing for developing therapeutic strategies to improve outcomes in both acute and chronic wounds. The following sections will explore the role of the skin in wound healing, the process of wound healing and scar formation, the stages of wound healing, the importance of the extracellular matrix in these processes, and investigate the potential of low-intensity pulsed ultrasound (LIPUS) as a therapeutic tool to influence ECM cross-linking and organisation, aiming to enhance wound healing outcomes.

## 1.2 Structure and Function of Intact Skin

### 1.2.1 Skin as a Protective Barrier

The skin, as the body's largest organ, accounts for over 10% of total body weight and acts as a vital border between the human body and the external environment (Walters and Roberts, 2002). It plays a critical protective and homeostatic role, primarily through its barrier function, allowing humans to survive in a variety of environmental conditions, including fluctuating temperatures, humidity, and exposure to hazardous substances such as chemicals, bacteria, and radiation. The skin is also crucial in maintaining body homeostasis, including functions like blood pressure control, and excretion. Additionally, it serves as a major sensory organ, detecting environmental changes such as pressure and microbial presence, while continuously regenerating and repairing itself (Xue and Jackson, 2015; Walters and Roberts, 2002).

Although the skin's protective system is highly effective in preventing infection, one limitation is its inability to fully restore its original state post-injury. Only about 80% of the skin's original structure and function is regained after a wound heals, primarily due to the formation of scars

(Stadelmann et al., 1998; Sorg et al., 2017). Thus, proper wound healing is vital for survival, enabling the closure of wounds and the restoration of the skin's barrier function.

### 1.2.2 Skin Structure and Function

Structurally, the skin is composed of four distinct layers: the stratum corneum (non-viable epidermis), the viable epidermis, the dermis, and the subcutaneous tissues (Figure 1.1) (Walters and Roberts, 2002). The epidermis is the outermost layer and is crucial for protection, while the dermis lies beneath, providing strength and elasticity to the skin. The epidermis varies in thickness depending on its location and function and consists of multiple layers of keratinised stratified squamous epithelium. This layer acts as a selective barrier, safeguarding the body from harmful substances and bacterial invasion (Benson, 2012). The dermis, deeper within the skin, contains both cellular and fibrous components, contributing to the skin's structural integrity and viscoelastic properties through a complex network of collagen and elastin fibres bound by proteoglycans. The dermis is further divided into the superficial papillary dermis and the deeper reticular dermis (Ng et al., 2015; Smith and Dean, 1998).

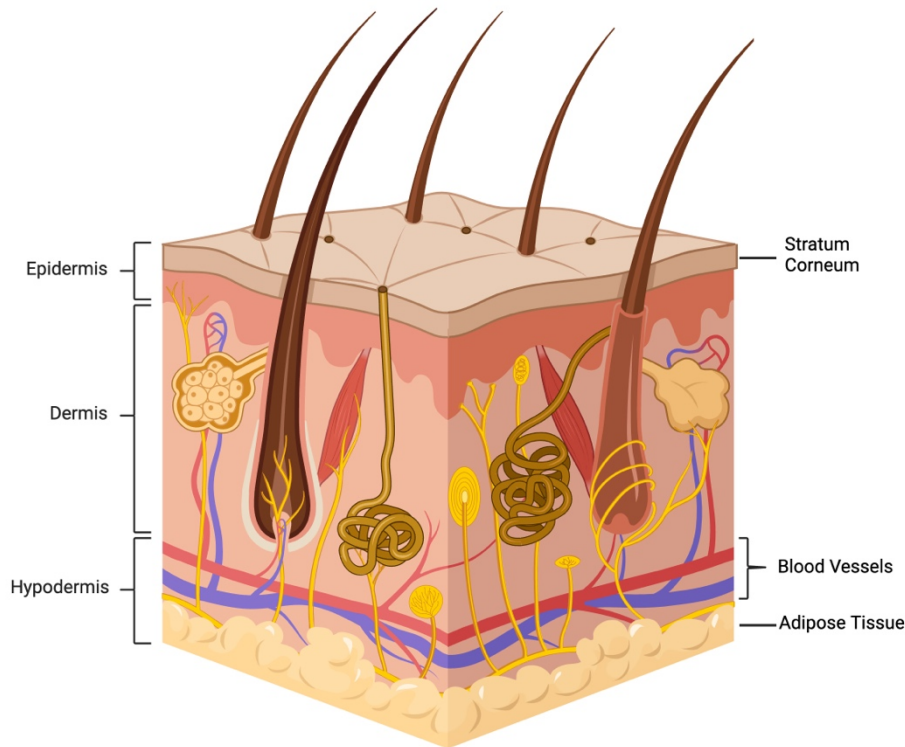


Figure 1.1 The structural layers of human skin include the epidermis, dermis, and hypodermis. (image generated using Biorender.com).

### 1.2.3 Role of Fibroblasts in Skin Integrity

Human skin cells, particularly fibroblasts and keratinocytes, are pivotal in the production of dermal substitutes due to their integral roles in skin physiology and repair processes (Pittenger et al., 2019). Fibroblasts, typical mesenchymal cells found throughout the body, are key players in maintaining the ECM, which is essential for the structural support of soft connective tissues. These cells not only synthesise and support the ECM but also secrete cytokines and growth factors that are vital for cellular communication and signalling. This signalling is crucial for the function of stem cell niches and the broader context of tissue remodelling, including wound healing and the pathological processes of fibrosis and cancer (Boraldi et al., 2024).

The fragmentation of collagen, caused by the interactions of physical and functional process between fibroblasts and the ECM, plays a central role in skin ageing. Fibroblasts produce collagen constitutively, which serves as the primary structural component of connective tissue. Through integrins, which span the cell membrane, fibroblasts attach to matrix proteins like type I collagen. In this way, integrins link the matrix outside the cell to the cytoskeleton, creating focal adhesions (Fisher et al., 2008).

Fibroblast ensures effective wound healing; however, any dysregulation can have significant consequences. The structural organisation, tensile strength, and elasticity of the skin, as well as its response to various intrinsic and extrinsic stimuli, can vary significantly depending on the specific area of the body. Also, mechanical signals which often originate from changes in the protein composition of the ECM, leading to either increased tension or alterations in the ECM's structure (Angelini et al., 2020). For example, reduced fibroblast activity may lead to chronic, non-healing wounds, while excessive activity can result in abnormal fibrosis, such as keloid scar formation (Potekhaev et al., 2021). This balance of fibroblasts is important in response to injury to achieve the desirable wound healing outcome.

The use of primary skin fibroblasts as models in research is particularly valuable for studying how therapy can promote tissue repair. This is because fibroblasts not only respond to particular therapies, but also play a direct role in tissue remodelling, making them ideal candidates for investigating therapeutic interventions (Tottoli et al., 2020; Zhou et al., 2004). Understanding these mechanisms further explain the critical roles fibroblasts play, not only in maintaining skin integrity but also in the broader context of therapeutic advancements in wound healing and tissue engineering (LeBleu and Neilson, 2020).



## 1.3 Healing Processes and Scar Formation

### 1.3.1 Objectives of Wound Healing

The primary objective of skin wound healing is to restore the skin's barrier function, thereby preventing further damage or infection. This process is initiated immediately upon injury and involves a highly coordinated interaction between various cells and signalling molecules. However, when wound healing is either prolonged or excessively aggressive, it can impede normal healing and lead to scarring (Sorg et al., 2017).

Upon injury, the body activates several mechanisms to prevent foreign bodies from penetrating the skin and causing infection. These mechanisms are typically divided into four phases: the haemostasis phase, where a fibrin clot forms to stop bleeding; the inflammatory phase, during which invading microbes are eliminated; the proliferative phase, which involves the formation of a new extracellular matrix; and finally, the remodelling phase, in which tissue function and integrity are restored to their original state (Potekhaev et al., 2021). The successful progression through these stages relies on the efficient delivery of inflammatory cells, chemokines, cytokines, matrix molecules, and nutrients to the wound site, which are crucial to meet the increased metabolic demands during healing (Han and Ceilly, 2017).

### 1.3.2 Acute vs. Chronic Wounds

Wounds can arise from a variety of causes, including surgical procedures, injuries, external factors such as burns and cuts, or underlying pathological conditions like diabetes and vascular diseases. Depending on their causes and outcomes, wounds are classified as either acute or chronic. Acute wounds generally follow a well-organised repair process, leading to the restoration of both anatomical and functional integrity. In contrast, chronic wounds fail to heal optimally, leaving the skin unable to fully restore its structure and function (Hurlow and Bowler, 2022). The healing process is influenced by the nature and extent of the pathological process, as well as the host and environmental conditions. Systemic factors, such as the

presence of vasculature, age of the patient, metabolic, or autoimmune diseases and ongoing treatments, can significantly impact wound healing (Tottoli et al., 2020).

### 1.3.3 Scar Formation and Types

Throughout the wound healing process, the ideal outcome is functional and scarless healing (Martin, 1997). However, the process can range from excessive healing, resulting in pathological scarring, to insufficient healing, leading to chronic wounds (Penn et al., 2012). Keloids and hypertrophic scars are examples of abnormal skin healing, characterised by excessive collagen deposition in the dermis and subcutaneous tissues following injury. In these conditions, the collagen fibres are thicker and aligned in the same direction as the epidermis, unlike in normal skin, where they are randomly arranged (Tuan and Nichter, 1998). Different studies have confirmed that in scar tissue, collagen fibres undergo hyperplasia, leading to a disordered tissue structure and poor mechanical tension (Corr and Hart, 2013; Jones, 2010).

#### *1.3.3.1 Hypertrophic scars*

Histopathologically, the key features of hypertrophic scars and keloids include the increased production and accumulation of ECM components within the dermal connective tissue following trauma, inflammation, or burns (Huang et al., 2013; Szauter et al., 2005). In a study by Yang et al. (2016), their results showed that scar tissue exhibited histological changes, including a significant reduction of collagen IV and the absence of integrin  $\beta 4$  in the basal layer. Additionally, keratinocytes in scar tissue were more proliferative than in normal skin. These findings suggest that alterations in basement membrane (BM) formation during wound healing may influence keratinocyte proliferation and tissue remodelling, contributing to scar formation.

The outcome of wound healing can vary not only between different individuals, genders, and ages but also within the same person (Guo et al., 2010). Hypertrophic scarring is more commonly observed after certain types of injuries, such as burns, delayed epithelialisation, or

wounds in areas subjected to high tension, like the shoulder, sternal regions, or areas with significant movement. The depth of a wound may be linked to the development of hypertrophic scarring, as fibroblasts from the deep dermis resemble those found in hypertrophic scars (Mustoe et al., 2002; Wang et al., 2008). These scars are characterised by their raised appearance, abnormal pigmentation, and potential to cause itching or unusual sensations. Unlike keloids, hypertrophic scars remain confined within the boundaries of the original injury and may gradually diminish over time. These scars contain a higher concentration of collagen type III fibres, typically aligned parallel to the epidermal surface (Slemp and Kirschner, 2006). This variation in scar outcomes demonstrate the complex interaction between injury type, wound depth, and individual healing responses.

#### *1.3.3.2 Keloid Scars*

Keloids are clinically characterised by elevated, firm, and nodular papules, as well as poorly defined plaques with varying pigmentation, including erythematous, violaceous, or brown hues (Thornton et al., 2021). Several factors during early wound management have been linked to the formation of keloid scars, such as delayed debridement, severe inflammation, and excessive wound tension, which can disrupt normal healing processes (Thornton et al., 2021). In keloid development, there is a close association between inflammatory cell infiltrates and fibroblasts actively producing collagen type I. Factors derived from inflammatory cells, such as transforming growth factor-beta (TGF- $\beta$ ), interferons, and interleukins, stimulate the expression of certain ECM genes, including collagen, leading to the clinical appearance of dermal fibrosis (Uitto and Kouba, 2000).

Unlike normal and hypertrophic scars, keloids extend beyond the borders of the original injury and do not regress over time. They are composed of disorganised type I and III collagen bundles, often making them symptomatic with pain and itching (Ghazawi et al., 2018; Trace et al., 2016). During the early phase of wound healing, inflammatory cells, epithelial cells, and

fibroblasts migrate into the wound matrix, playing crucial roles in scar remodelling. Specifically, fibroblasts and myofibroblasts are responsible for producing a collagen-rich ECM, which must maintain a delicate balance between synthesis and degradation to ensure proper healing. An imbalance between collagen production and ECM degradation contributes to scar formation. A pro-inflammatory microenvironment, driven by dysregulated levels of TGF- $\beta$  isoforms (TGF- $\beta$ 1, TGF- $\beta$ 2, and TGF- $\beta$ 3) and cytokines from the Th2 immune response interleukin-4 (IL-4), IL-5, IL-10, and IL-13, is believed to play a role in keloid development (Ekstein et al., 2021; Kiritsi and Nystrom, 2018). Therefore, keloid scars are characterized by their extension beyond the original wound boundaries, persistent nature, and disorganized collagen buildup due to a pro-inflammatory environment and disrupted healing processes. In contrast, hypertrophic scars stay within the original injury site and may diminish over time, illustrating the complex interactions of inflammation, fibroblast activity, and extracellular matrix regulation in scar formation.

#### 1.3.4 Cellular and Molecular Mechanisms in Scar Formation

Keloid fibroblasts show higher levels of growth factor receptors and respond more rapidly to platelet-derived growth factor (PDGF) and TGF- $\beta$  compared to normal skin fibroblasts. These growth factors can activate keloid fibroblasts early in the wound healing process, potentially contributing to keloid formation (Mari et al., 2015). Additionally, increased expression of elastin and fibrillin-1 is linked to scar elasticity (Cohen et al., 2017). Keloid fibroblasts, also, reveal different force generation and stiffness of actin filament compared to normal fibroblasts, which may explain their tendency to extend beyond the original wound margins (Jusman et al., 2023; Hsu et al., 2018). These fibroblasts also produce excess ECM when cultured on stiff substrates, which may partly explain the higher risk of keloid formation in high-tension areas of the body, such as the chest and upper back (Hsu et al., 2018). Scar contracture is another significant complication of wound healing, distinct from keloids and hypertrophic scars,

resulting from the excessive contraction of ECM by fibroblasts in the wound and often seen in hypertrophic scars. Myofibroblasts, which are rich in alpha-smooth muscle actin ( $\alpha$ -SMA), play a crucial role in this process. The contracture process is characterised by  $\alpha$ -SMA expression, the formation of  $\alpha$ -SMA stress fibres, and the generation of large traction forces (Grinnell, 1994). TGF- $\beta$  plays a vital role in scar formation by stimulating the production of collagen and fibronectin (Ignatz and Massague, 1986). Desmoulière et al. (1993) demonstrated that the local administration of TGF- $\beta$ 1 induces  $\alpha$ -SMA expression and plays a major role in myofibroblast differentiation. This understanding of cellular and molecular dynamics is crucial for developing targeted therapies for different types of scars. Table 1.1 summarises the important features comparing normal skin, hypertrophic, and keloid scars.

Table 1.1 Comparison of Key Features and Characteristics of Normal Skin, Hypertrophic Scars, and Keloids.

Feature	Normal	Hypertrophic	Keloid
<b>Collagen Arrangement</b>	Randomly arranged	Aligned parallel to the epidermis	Disorganized, thicker, and aligned with the epidermis
<b>Fibroblast Activity</b>	Normal fibroblast activity	Increased activity, especially in deeper wounds	Highly active, with elevated growth factor receptors
<b>Inflammatory Response</b>	Controlled, normal response	Localised, may involve higher inflammation	Pro-inflammatory microenvironment with dysregulated cytokines
<b>TGF-<math>\beta</math> and Cytokine Levels</b>	Normal levels	Elevated, especially TGF- $\beta$ 1	Highly elevated, with dysregulated TGF- $\beta$ isoforms and Th2 cytokines

<b>Appearance</b>	Smooth, normal pigmentation	Raised, abnormal pigmentation	Elevated, firm, nodular with varying pigmentation (erythematous, violaceous, brown)
<b>Symptoms</b>	None	May cause itching or unusual sensations	Often symptomatic with pain and itching
<b>ECM Components</b>	Balanced ECM production and degradation	Increased ECM components	Excessive ECM production and reduced degradation
<b>Scar Contracture</b>	N/A	Common, due to myofibroblast activity	Rare, but can occur if associated with hypertrophic components
<b>Risk Factors</b>	N/A	More common in high-tension areas, deep wounds	High-tension areas, chest, upper back, certain racial and genetic predispositions

## 1.4 Chronic Wounds

### 1.4.1 Definition and Prevalence

Chronic wounds are characterised by a prolonged healing process that exceeds the expected time frame (Falanga et al., 2022). In the United States, around 8 million people suffer from chronic wounds, which represent approximately 2% of the population, with similar prevalence rates reported in European countries (Sen, 2021; Järbrink et al., 2017; Phillips et al., 2016). Chronic wounds typically affect the adult population and arise due to complications such as venous insufficiency, diabetes, neuropathies, immobility and/or spinal cord injuries leading to pressure ulcers (PUs) and arterial insufficiency. There are also various other clinical scenarios

where the initial injury is attributed to genetic factors (such as the range of epidermolysis bullosa in children) or exposure to radiation, whether accidental or therapeutic (Falanga et al., 2022). Furthermore, dysfunction of the immune system plays a significant part in the development of certain chronic ulcers. In less developed countries, the causes may differ considerably from those in developed nations, including factors such as nutritional deficiencies, parasitic and chronic fungal infections, and leprosy (Falanga et al., 2022).

PU are a global issue, particularly among patients who are infirm. The prevalence of PUs is heavily influenced by factors such as the patient's place of residence (e.g., hospital or nursing home), individual patient characteristics, and age (Mervis et al., 2019). A Portuguese multicentre study by Lopes et al. (2020) found that point prevalence rates of PUs were 5.76% among hospitalised individuals, 4.03% among residents of nursing homes, and 0.02% within the community population. In the UK, a comprehensive study by Drew et al. (2007), which included 1,644 patients suffering from either single or multiple wounds, reported that 42% of those diagnosed with foot or leg ulcers remained unhealed for more than six months. Additionally, 27.5% of these patients experienced non-healing for over a year. Similarly, a meta-analysis conducted by Margolis et al. (2000) on five prospective diabetic foot ulcer (DFU) trials found that only 23.9% of patients with DFUs healed within 12 weeks, while 32.8% showed healing within 20 weeks following standard treatment. This suggests that approximately two-thirds of the patients continued to suffer from DFUs even after 20 weeks. Furthermore, it is essential to recognise that diabetes has become the eighth leading cause of the global disease burden and is the fastest growing among them (Lazzarini et al., 2023). This anticipated increase in diabetes prevalence may result in a corresponding rise in the incidence of chronic wounds (Kang et al., 2024). Thus, the escalating connection between the growing prevalence of chronic conditions and the challenges associated with wound healing indicate needs for extra wound care and management strategies.

### 1.4.2 Characteristics of Chronic Wounds

Chronic wounds are characterised by their failure to progress normally through the stages of healing, often stalling in the inflammatory phase. These wounds exhibit constant inflammation, impaired angiogenesis, difficulties in re-epithelialisation, dysregulated levels of cytokines and growth factors, and increased protease activity (Las Heras et al., 2020). When wound healing is ineffective, skin damage can escalate, leading to serious medical conditions, such as DFUs and venous leg ulcers (VLUs) (Yeung and Kelly, 2021). This connection between chronic wounds and severe health complications highlights the critical need for effective wound management.

In a normal wound healing process, the wound progresses through distinct phases: bleeding and haemostasis, inflammation, proliferation, and remodelling, ultimately leading to wound closure and scar formation. In contrast, chronic wounds stall during the inflammatory phase, resulting in delayed or incomplete healing, with the wound remaining open and vulnerable (Figure 1.2).



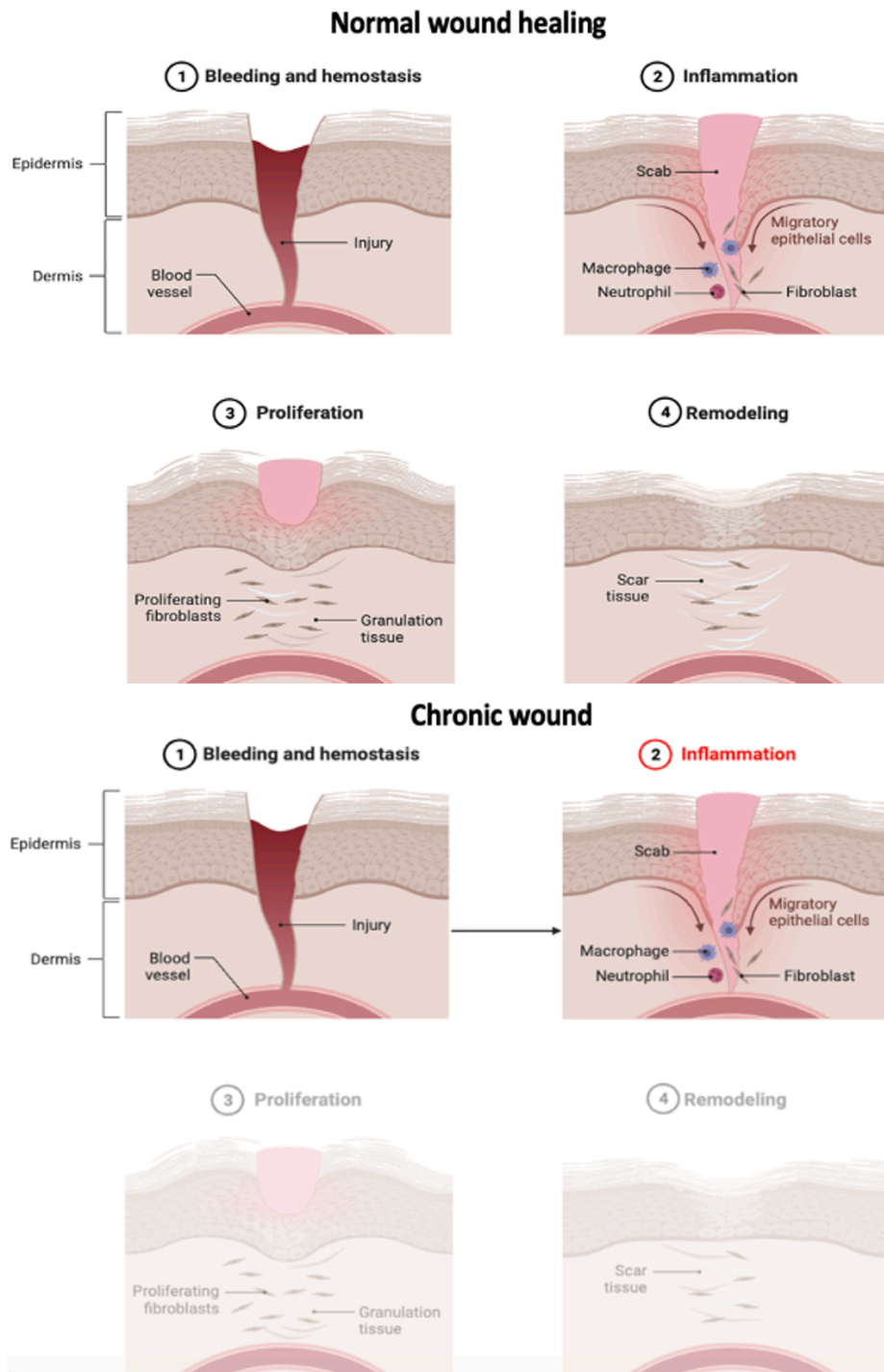


Figure 1.2 Comparison between normal wound healing to chronic wounds.

In normal healing, the process moves from bleeding and haemostasis (1), through inflammation (2), proliferation (3), and finally remodelling (4), leading to wound closure and scar formation. In chronic wounds, the process stalls during the inflammatory phase (2). (image generated using BioRender website).

In chronic wounds, the persistent accumulation of inflammatory cells results in elevated levels of reactive oxygen species (ROS), which cause damage to ECM proteins and contribute to

premature cellular ageing (Ben-Porath and Weinberg, 2005). Excessive exudation, constant infection and necrosis are physical signs of chronic wounds all of which complicate wound management and care. Wound exudate indicates the physiological condition of the wound bed and mirrors the microenvironment of the injured tissue. It serves as an indicator of the chronic nature of a wound or the effectiveness of treatment. Evidence suggests that in chronic wounds, exudate components, which are corrosive, can exacerbate the injury by causing ongoing degradation of the ECM (Widgerow et al., 2015; Jahromi et al., 2018).

Bacterial invasion of injured skin is often unavoidable, and, in some cases, the immune response may be insufficient, causing complications or even fatalities, particularly in individuals with significant chronic skin lesions (Rajpaul, 2015). Necrosis occurs when an infection remains unresolved or when the tissue sustains irreparable damage. Superficial infections can spread into deeper tissue layers, potentially reaching bone tissue and impacting systemic pathways, which may result in bacteraemia and generalised sepsis. While skin necrosis is more commonly associated with vascular occlusion than with external factors (Tottoli et al., 2020). The interconnected nature of infection, inflammation, and wound healing failure in chronic wounds emphasises the complexity of treating these conditions.

### 1.4.3 Challenges in Chronic Wound Healing

When fibroblast function is compromised, it can lead to unresolved inflammation and the development of chronic wounds. Additionally, conflicts in macrophage roles may further contribute to abnormal repair processes (Las Heras et al., 2020; Wall et al., 2008). These dysfunctions disrupt ECM deposition and granulation tissue formation, which are critical for proper wound healing, thereby leading to chronic wound formation. As a result, various therapeutic approaches have been developed to address these defects, including debridement, electrical stimulation (ES), drugs such as antiseptics or antimicrobials, and low-frequency ultrasound (Las Heras et al., 2020). The systemic impact of conditions like diabetes further

complicates the wound healing process, making it a significant concern in the context of chronic wounds (Han and Ceilly, 2017).

## 1.5 Wound Healing Stages

### 1.5.1 Haemostasis Stage

When skin damage occurs, four healing stages begin to protect and repair the damaged area (Figure 1.3). The first stage, haemostasis, begins immediately after the injury and aims to prevent significant blood loss. This is accomplished through the narrowing of blood vessels and the formation of fibrin clots, which not only prevent bleeding but also provide a matrix for the invasion of cells necessary for wound healing (Velnar et al., 2009). Platelets interact with the blood to release clotting factors that facilitate the formation of the clot which composed of fibronectin, fibrin, vitronectin, and thrombospondin (Velnar et al., 2009). Additionally, the clot and the surrounding tissue release pro-inflammatory cytokines and growth factors, including transforming growth factor (TGF)- $\beta$ , platelet-derived growth factor (PDGF), fibroblast growth factor (FGF), and epidermal growth factor (EGF) (Guo and DiPietro, 2010).

### 1.5.2 Inflammatory Stage

The inflammatory stage begins once bleeding has been controlled, which characterised by increased vascular permeability and vasodilation. These changes allow inflammatory cells to migrate to the wound site (Han and Ceilly, 2017). This stage is marked by the serial infiltration of neutrophils, macrophages, and lymphocytes, all of which work to prevent infection (Gosain and DiPietro, 2004). Neutrophils are primarily responsible for clearing invading microbes from the wound area, and they are attracted to the injured site by PDGF and pro-inflammatory cytokines (Hantash et al., 2008). Macrophages have a multifaceted role in wound healing. They release cytokines that amplify the inflammatory reaction in the early phase by the activation of leukocytes (Guo and DiPietro, 2010). Also, they initiate the growth of granulation tissue by releasing various of pro-inflammatory cytokines (IL-1 and IL-6) and growth factors (FGF,

EGF, TGF- $\beta$ , and PDGF) (Barrientos et al., 2008). The inflammatory stage not only addresses immediate threats but also prepares the wound environment for the subsequent proliferative stage.

### 1.5.3 Proliferative Phase

Following haemostasis and the resolution of inflammation, the proliferative phase begins. During this phase, a newly synthesised extracellular matrix is formed, accompanied by the migration of fibroblasts, which act as a replacement for the provisional network of fibrin and fibronectin. Also, angiogenesis and the formation of granulation tissue is observed during this period (Velnar et al., 2009). Fibroblasts are the main cells responsible for forming granulation tissue. Molecules released by macrophages, such as PDGF-bb, TNF- $\alpha$ , IL-1, and IL-6, can trigger fibroblasts to produce substances that help with skin repair (Ellis et al., 2018). The proliferative phase marks the transition from initial damage control to the active reconstruction of tissue, prior to the final healing stages.

### 1.5.4 Remodelling Stage

The remodelling stage is the final step in wound healing and is responsible for the growth of new epithelial tissues and the formation of scar tissue (Velnar et al., 2009). In this phase, collagen plays a crucial role in restoring tissue strength and integrity. The tensile strength of the wound area increases as collagen accumulates. Collagen remodelling persists for months after the wound has closed, gradually increasing the tensile strength of the repaired tissue to approximately 80–85% of that of normal tissue (Mathew-Steiner et al., 2021). The remodelling stage combines the earlier phases of wound healing, finally restoring the functional integrity of the tissue.

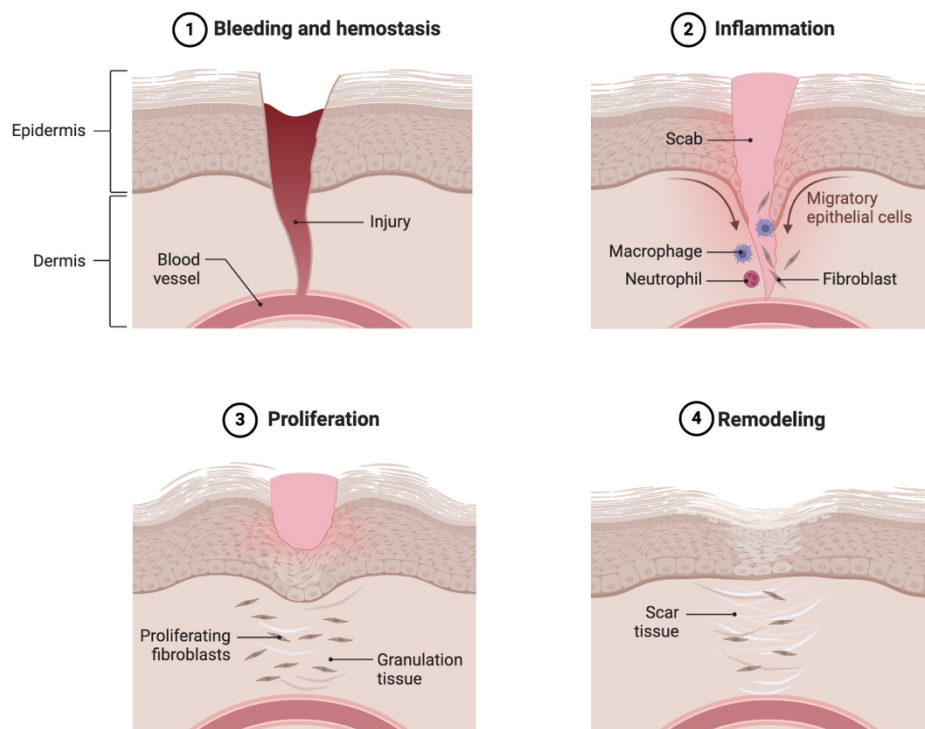


Figure 1.3 Stages of wound healing repair.

This illustration summarizes the stages of wound healing (Image created using Biorender).

## 1.6 The Extracellular Matrix in Wound Healing

### 1.6.1 Overview of the ECM

Historically, the ECM was considered an inert substance that merely provided structural support to cells. However, as more data revealed from basic and clinical studies, it became evident that the ECM plays a central role in the cellular microenvironment. ECM actively participates in wound healing by influencing cell behaviour, including proliferation, adhesion, and migration. Additionally, the ECM regulates cell differentiation and death through interactions with growth factors, cytokines and integrins (Potekae et al., 2021). The ECM is a three-dimensional, non-cellular structure that provides essential support for tissue integrity and elasticity (Bonnans et al., 2014). The ECM plays a vital role in maintaining cellular processes such as proliferation, migration, and differentiation. It is composed of multiple proteins, including collagen, fibronectin, elastin, laminins, tenascins, and other components

such as growth factors (GFs) and matrix metalloproteinases (MMPs) (Kular et al., 2014). The ECM links connective cells together, maintaining the strength and integrity of tissues (Figure 1.4) (Geiger and Yamada, 2011).

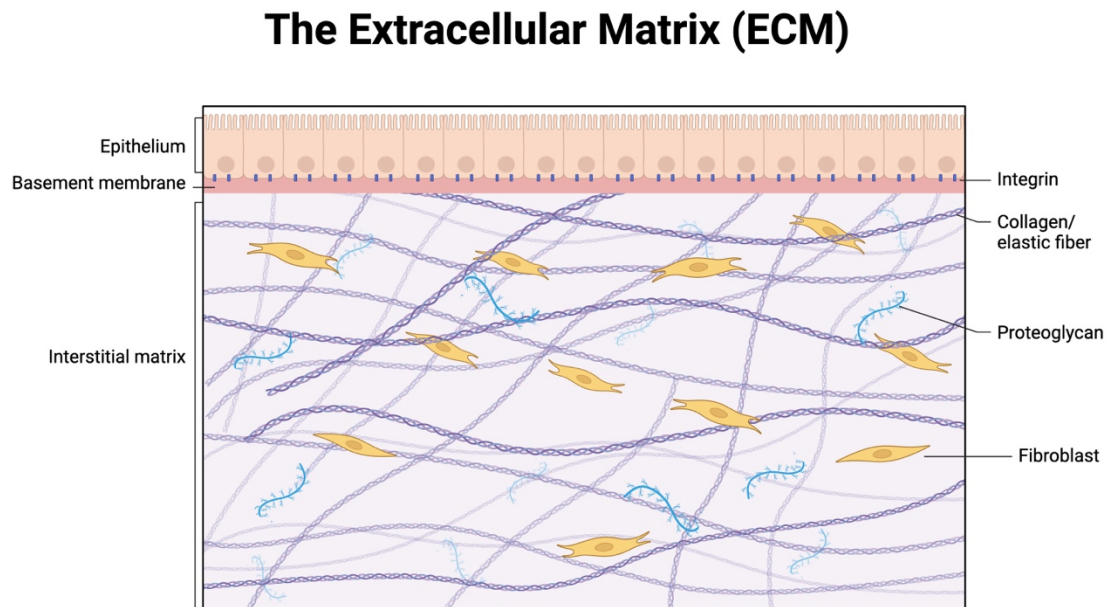


Figure 1.4 Extracellular matrix structure. (Image created in BioRender.com.)

### 1.6.2 ECM's Role in Wound Healing Stages

In each of the four stages of wound healing, the ECM plays an essential role by interacting with growth factors and providing the physical substrate over which cells migrate during healing. The ECM's role in cellular processes is evident as it links individual cells together to form functional tissues and organs, while also providing a scaffold for cells during tissue repair (Rolfe and Grobbelaar, 2012). Abnormal remodelling of the ECM could result in uncontrolled cell invasion and proliferation, apoptosis disruption, impaired differentiation, and physiological processes dysfunction in the skin. ECM not only affects ageing, migration and fibroblast gene expression but also plays a crucial role in their differentiation into various cell types. The properties of a fibroblast are shaped by the surrounding extracellular matrix (Potekaev et al., 2021). Dysregulated ECM remodelling is associated with various pathological conditions, including impaired wound healing and excessive scarring (fibrosis), where the

excessive deposition of dysfunctional ECM hinders tissue regeneration and prevents the complete restoration of structure and function (Wang et al., 2023; Lichtman et al., 2016). The diverse roles of different ECM proteins, such as the tensile strength provided by fibrillar collagens and elastin, and the connector functions of fibronectin and laminin, indicate the importance of understanding matrix behaviour for controlling matrix deposition (Vakonakis and Campbell, 2007). This emphasises the interrelated of ECM components in supporting both the structure and function of tissues during healing.

### 1.6.3 Collagen

Collagen is considered as the most abundant protein in the ECM, forming fibres which provides tensile strength to ECM (Chang, 2016). Collagen fibrils play a crucial mechanical role in the ECM of many multicellular organisms, providing a strong structural framework for tissue architecture. These fibrils resist tension within a complex fibre-composite system, organised into a tissue-specific hierarchical structure to meet mechanical requirements (Holmes et al., 2018). Collagen is composed of three polypeptide  $\alpha$  chains that form a triple helical structure. There are 28 collagen types, categorised based on their structure and function, fibril-forming, network-forming and fibril-associated collagens (Yue, 2014). Specifically, collagen consists of straight, elongated, cable-like fibril structures and a characteristic band periodicity of 64–67 nm. It plays a significant role in providing mechanical support and ensuring dimensional stability (Sowbhagya et al., 2024).

Collagens play a crucial role in skin injury by contributing to wound contraction, cellular differentiation, angiogenesis, protein synthesis, collagen induction, and ECM deposition (Chattopadhyay and Raines, 2014; Rangaraj et al., 2011). However, factors such as diabetes, smoking, and ageing can impair collagen metabolism, leading to poor wound healing and tissue breakdown. Hyperglycaemia in diabetes reduces normal collagen production, resulting in the formation of abnormal, rigid collagen (Black et al., 2003). Similarly, smoking and age can

decrease collagen synthesis rates and increase collagen degradation (Knuutinen et al., 2002). Intrinsic factors, including alterations in oxygen tension, can also impact collagen production and fibroblast proliferation (Falanga et al., 2002). These influences on collagen metabolism further demonstrate the complexity of wound healing and the importance of managing these factors to promote effective tissue repair.

In most connective tissues, collagen fibrils have uniform sizes and arrangements. For instance, embryonic tendons have fibrils 30–35 nm in diameter, arranged in hexagonal bundles. As tendons mature, the uniformity in fibril size and order decreases, leading to increased strength and stiffness. On the other hand, the corneal layer maintains consistent fibril size and organisation into adulthood (Sowbhagya et al., 2024). Collagen types I–III are predominantly found in elastic soft tissues such as the dermis. The healthy dermis comprises about 80% type I collagen and 20% type III collagen. However, acute wound granulation tissue shows an increase in the percentage of type III collagen which can reach to 40% (Velnar et al., 2009).

Collagen Type III plays a crucial role in preserving the structural integrity of organs, skin elasticity and blood vessels. Type III collagen is also vital in wound healing, as it provides a scaffold for new tissue growth and aids in the regeneration process. Collagen type III is a fibrous protein that is abundant in connective tissues making it one of the most common collagen types. Its key benefits include enhancing skin elasticity and firmness, reducing wrinkles and fine lines (Sowbhagya et al., 2024; Xue and Jackson, 2015). The dynamic changes in collagen type, quantity, and organisation during wound healing affect skin tensile strength. Initially, collagen III is produced and later replaced by collagen I, with covalent cross-linking by lysyl oxidase enhancing collagen deposition in granulation tissue. After the wound is closed, collagen continues to remodel for several months, allowing the regenerated tissue to regain 80–85% of its original tensile strength. Throughout this process, collagen fibres are realigned to restore structural integrity (Mathew-Steiner et al., 2021).



Angiogenesis, which is essential for both physiological processes like development and wound healing and pathological processes like cancer, is regulated by a balance between stimulators and inhibitors. ECM remodelling is crucial for vascular development, with collagens playing a significant role in this process. They can either promote or inhibit angiogenesis depending on the collagen type, (Senk and Djonov, 2021). Collagen I is known to strongly stimulate angiogenesis both in vitro and in vivo by engaging integrin receptors, with its C-propeptide fragment recruiting endothelial cells and potentially triggering angiogenesis in healing wounds (Mathew-Steiner et al., 2021). Type IV collagen, an essential part of the basement membrane, is vital for maintaining tissues and organ's structure and function. It plays a key role in preserving the integrity for different parts such as blood vessels, kidney filtration mechanism (Abreu-Velez and Howard, 2012).

Collagen types I and III are essential components of the extracellular matrix that play a pivotal role in wound healing by influencing cellular behaviours through signalling pathways. Their interaction with cell surface receptors, such as integrins, initiates intracellular signalling cascades, notably the PI3K/Akt/mTOR pathway, which regulates vital cellular processes including migration, proliferation, and survival (Kasowanjete et al., 2023). These pathways are crucial for cellular proliferation and survival under both normal and pathological conditions (Kasowanjete et al., 2023). In a study conducted by Zhang et al. (2016) on human dermal fibroblast cells, Notoginsenoside Ft1 was found to enhance cell proliferation and collagen synthesis via the PI3K/Akt/mTOR signalling pathway. Another study by Bao et al. (2022) demonstrated that bovine collagen oligopeptides significantly promote fibroblast migration and proliferation, which are crucial for tissue repair. This effect is mediated through the activation of the PI3K/Akt/mTOR signalling pathway, suggesting that bovine collagen oligopeptides could be effective agents in accelerating the wound healing process.

An imbalance between collagens I and III can lead to pathological scarring. Recent research indicates that TGF- $\beta$ 1-induced connexin43 (Cx43) expression promotes scar formation via the Erk/MMP-1/collagen III pathway (Li et al., 2020). Specifically, the upregulation of Cx43 activates the extracellular signal regulated kinases (Erk) signalling cascade, which increases MMP-1 expression. Elevated MMP-1 degrades collagen I, leading to a relative increase in collagen III deposition. This shift enhances scar tissue formation due to the fibrotic properties of collagen III. Therefore, the TGF- $\beta$ 1/Cx43-mediated signalling pathway critically regulates the collagen I to III ratio, presenting potential therapeutic targets for controlling excessive scar formation (Li et al., 2020).

#### 1.6.4 Transforming Growth Factor-Beta (TGF- $\beta$ )

TGF- $\beta$ , a multifunctional growth factor, plays key roles in wound healing, including regulating cell migration, differentiation, ECM production, and immune response. TGF- $\beta$  exists in three isoforms (TGF- $\beta$ 1, TGF- $\beta$ 2 and TGF- $\beta$ 3). It is secreted in a latent complex that binds to the ECM and is activated by proteases, enabling its various regulatory functions (Lichtman et al., 2016).

TGF- $\beta$  primarily signals through the Smad pathway, which is associated with fibrosis, as its activation can lead to excessive fibroblast proliferation and increased deposition of ECM (Sun et al., 2023). TGF- $\beta$  plays a key role in scarring by driving the excessive deposition of dysfunctional ECM, which hinders tissue regeneration. Targeting the TGF- $\beta$  pathway may improve wound healing and reduce scarring (Finnsen et al., 2013). When TGF- $\beta$  binds to certain ligands on cell surface receptors, it stimulates the keratinocytes production, fibroblasts, neutrophils, and macrophages, which in turn trigger the release of pro-inflammatory cytokines like IL-1 $\alpha$ , IL-1 $\beta$ , IL-6, and TNF- $\alpha$  (Sun et al., 2023).

TGF- $\beta$ 2 has similar effects to TGF- $\beta$ 1, and its downregulation can lead to reduce scar formation (Lichtman et al., 2016). Wounds treated with antibodies against TGF- $\beta$ 1 and TGF- $\beta$ 2 has been

demonstrated to restore skin's structure to a state similar to that in healthy skin (Denton et al., 2007). This indicates that inhibiting TGF- $\beta$ 1 and TGF- $\beta$ 2 might help reduce scarring. Additionally, the level of TGF- $\beta$ 1 expression vary between young and adults individual, with higher levels observed in adults (Sun et al., 2023). The effect of TGF- $\beta$  on cell migration, proliferation, and ECM production influences the alignment of collagen fibres, a significant indicator of scar quality (Dallon et al., 2001). Additionally, TGF- $\beta$  controls the formation of myofibroblasts, which are necessary for the differentiation of fibroblasts into myofibroblasts, identified by inducing expression of alpha-smooth muscle actin ( $\alpha$ -SMA) (Satish et al., 2011). Thus, TGF- $\beta$  plays a crucial role in controlling scar formation. Its ability to regulate collagen alignment and promote fibroblast differentiation further emphasises its significance in affecting scar outcomes.

#### 1.6.5 Fibronectin

Fibronectins (FNs) are a family of multifunctional glycoproteins that play significant roles in wound healing, cell adhesion, migration and maintaining tissue integrity (Moretti et al., 2007). FN is required for fibroblast adhesion to fibrin, with adhesion being strongest when FN is crosslinked to fibrin. It exists in two forms: plasma in the blood and cellular proteins formed by fibroblasts (Kular et al., 2014). The biological function of FN is ultimately determined by the molecular conformation of the molecules that make up the fibronectin fibres (Zollinger and Smith, 2017). FN interacts with a variety of ECM proteins, growth factors, glycosaminoglycans (GAGs) and cell surface receptors to deliver essential mechanical and chemical signals that control cellular behaviours, such as differentiation and epithelial-mesenchymal transition (EMT). Dysregulation of these processes can result in scarring, tumorigenesis, and developmental abnormalities (Schwarzbauer et al., 2011; Sible et al., 1994; Bae et al., 2013). FN's connections with proteins like collagen, tenascin-C, fibrin, fibrillin, and bacterial wall

proteins illustrate its diverse role in the ECM, supporting structural integrity and modulating cell adhesion, migration, and signalling pathways (Dalton and Lemmon 2021).

During wound healing, maintaining tensile homeostasis in the skin is believed to play a role in the mechanics of wound signalling, as a wound disrupts the normal tensile balance (Wong et al., 2013). The pericellular matrix of FN, assembled by fibroblasts, is responsible for sensing strain (Lutz et al., 2010). FN matrices initiate the ECM structure, which is later replaced by collagen to strengthen the matrix (Kubow et al., 2015). FN exists throughout all stages of wound healing. Plasma FN plays a crucial role in the early phase, helping to form the clot and assemble a cell-ECM matrix (Patten and Wang, 2021). Platelets facilitate the assembly of plasma-derived FN into fibrillar matrices by increasing the expression of platelet binding sites. In the later stages of tissue remodelling, cellular-derived FN is responsible for local FN assembly. Although these two types of FN are well-studied, they have limited ability to perform each other's functions, and not all FN isoforms can be compensated for if absent (Patten and Wang, 2021). After a clot is formed and bleeding stops, platelets accumulate and adhere to the damaged endothelial surface. FN's role is to provide strength to the clot by forming a fibrin–FN network called the fibrin–FN provisional matrix (Lenselink, 2015). During the proliferation stage of wound healing, FN is associated with the collagen III matrix within granulation tissue. Over time, this temporary FN matrix is remodelled into a collagen I matrix (Patten and Wang, 2021).

FN regulates the expression of matrix metalloproteinases, influencing ECM remodelling in chronic wounds, which can lead to unintended effects in FN- or platelet-rich plasma therapies. Additionally, in chronic wounds the expression of FN mRNA is upregulated significantly compared to both normal wounded and unwounded dermis (Ongenaes et al., 2000). In acute wounds, the fluid from the wound tissue contains full-length FN. However, in chronic wounds, FN fragments smaller than 125 kDa are present, with some retaining similar but reduced

binding abilities (Grinnell et al., 1992). Impaired clearance of the temporary FN matrix is often observed in chronic wounds and this cause alteration to the ECM structure and likely exacerbates the chronic nature of the wound (Patten and Wang, 2021).

Grinnell et al. (1981) suggested that FN may influence wound healing by contributing to the formation of a proper substratum for cell migration and growth during the development and organisation of granulation tissue. Also, during the remodelling of the connective tissue matrix. The involvement of FN in all phases of wound healing shows its indispensable role in the repair process.

### 1.6.6 Lysyl Oxidase

Lysyl oxidase (LOX) are secreted amine oxidases that contribute to the formation of the ECM in a copper-dependent process (Finney et al., 2014). The LOX precursor, which is 50 kDa in size and primarily secreted by smooth muscle cells and fibroblasts, undergoes hydrolysis to become the catalytically active, mature form of LOX (30 kDa) along with a non-catalytic peptide (18 kDa). Once activated, LOX plays a crucial extracellular role by facilitating the crosslinking of ECM components, including elastin and collagen types I – III, consequently, convert them into an insoluble form (Wei et al., 2020).

During development, LOXs act as intermediaries between the ECM and cells. The crosslinking of fibrous macromolecules is vital for tissue formation, as a well-constructed ECM provides the optimum rigidity and stiffness. LOXs play an important role in shaping the structure of cells and in transmitting signals and responses between external forces and the cells within tissues during growth and remodelling stages. This structural support is essential for ensuring the correct form and appropriate functioning of organs (Wei et al., 2020). The expression of LOX is concentrated within keratinocytes in the basal layer, with a reduced role in the suprabasal layer (Szauter et al., 2005).

Active LOX is closely linked to fibrosis in tissues such as the lungs, arteries, heart, skin, and kidneys. It is also important in cellular fibrotic processes, including platelet-driven EMT and the conversion of fibroblasts into myofibroblasts, particularly in wounds that undergo repeated injury and repair cycles (Laczko and Csiszar, 2020). In the development of fibrosis, the signalling pathway involving transforming growth factor- $\beta$ 1 TGF- $\beta$ 1 and Smad3 leads to a marked increase in LOX mRNA, protein expression, and activity in fibroblasts, osteoblasts, epithelial cells, and aortic smooth muscle cells (Laczko and Csiszar, 2020). For instance, upregulation in LOX expression was observed in an in vivo model TGF- $\beta$ -induced synovial fibrosis (Remst et al., 2014).

The collagen type I A1 and A2 genes and LOX contain TGF- $\beta$  response promoter elements which regulate their coordinated expression (Hong et al., 2002). In adult rat cardiac fibroblasts, TGF- $\beta$ 1 stimulates the upregulation of LOX mRNA, protein, and activity, alongside increased expression of collagen types I and III, as well as BMP-1. This process is mediated through various signalling pathways, including PI3K, Smad3, p38-MAPK, JNK, and ERK1/2, indicating a convergence of the PI3K/Akt and Smad pathways (Figure 1.5). Additionally, the upregulation of LOX via TGF- $\beta$ /Smad2/3 signalling plays a key role in promoting myocardial fibrosis and chronic heart failure. In this model, TGF- $\beta$ /Smad2/3 signalling also activates C-jun, a component of the AP-1 transcription factor, further inducing LOX gene expression (Laczko and Csiszar, 2020). Additionally, inhibiting LOX with  $\beta$ -Aminopropionitrile (BAPN) has been demonstrated to reduce TGF- $\beta$ -mediated downstream effects (Lu et al., 2019).

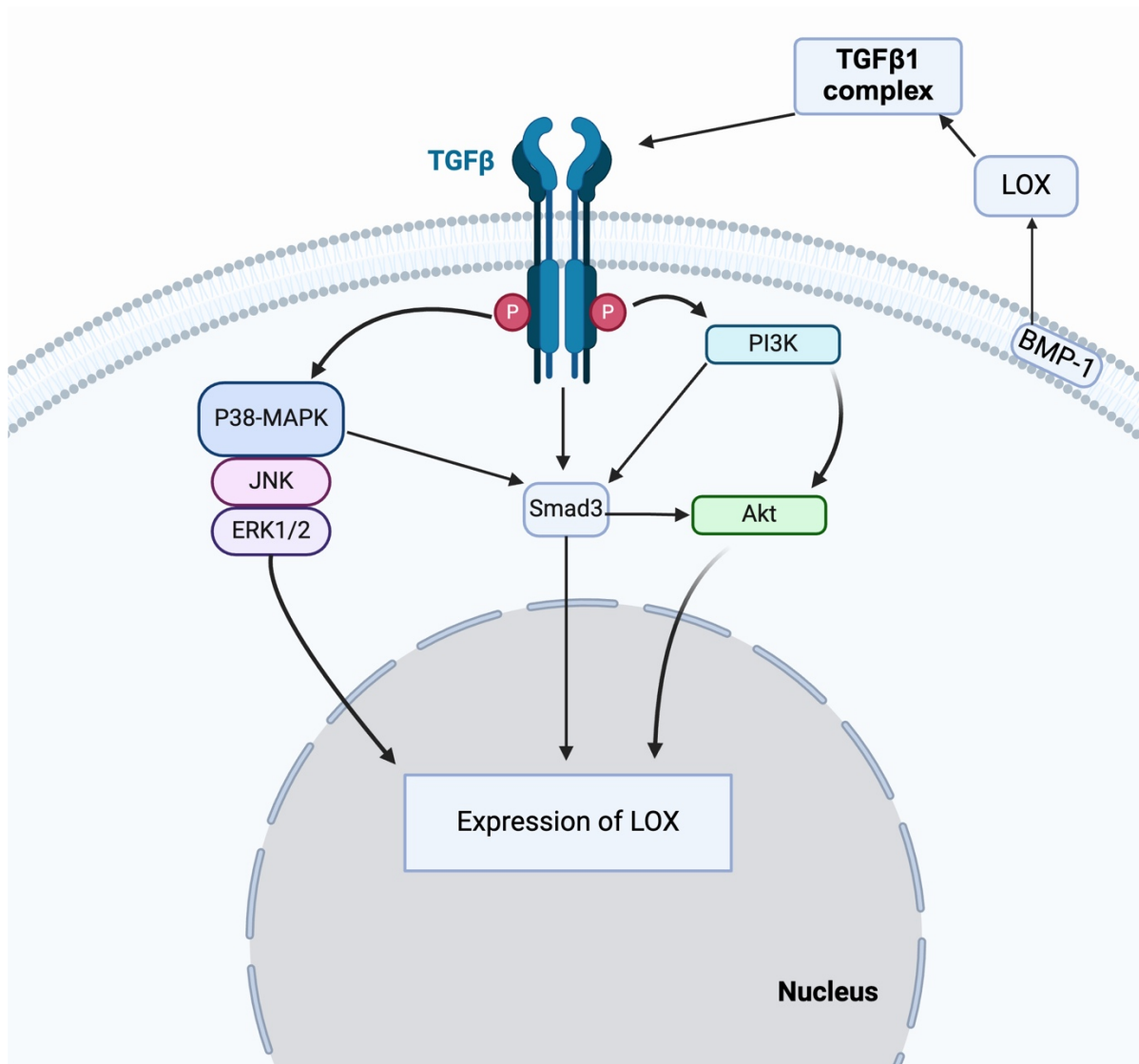


Figure 1.5 The proposed roles of LOX in response to various factors (image reproduced from Voloshenyuk et al., 2011).

TGF- $\beta$ 1 initiates signal transduction, leading to an increase in LOX mRNA and activity. This process is regulated through the phosphatidylinositol-3-kinase (PI3K)/protein kinase B (Akt), Smad3, and mitogen-activated protein kinase (MAPK) pathways (Image created in BioRender.com).

The role of LOX in forming crosslinks in collagen fibrils is crucial for maintaining and repairing the ECM (Kumari et al., 2017). LOX and LOXL are linked to various disease conditions, including fibrosis, which occurs due to the excessive buildup of insoluble collagen

fibres. Elevated levels of these enzymes have been associated with multiple fibrotic diseases (Kagan et al., 2000). It has been observed that in aged skin, the activity of LOX/LOXL is significantly higher in both the epidermis and dermis compared to younger skin. This implies that LOX/LOXL may play a role in the formation of abnormal cross-links and could contribute to age-related tissue stiffening (Langton et al., 2013). Therefore, the covalent cross-linking of LOX in the ECM is vital for strengthening and stabilising the ECM, which is highly related to wound healing and scarring effects.

## 1.7 Ultrasound as a Therapy Tool

### 1.7.1 Overview of Ultrasound

Ultrasound (US) is widely used in medical diagnostics and therapeutic applications, including surgery, ophthalmology, and physiotherapy. US refers to sound waves with frequencies higher than those audible to humans ( $>20$  kHz) (Wu and Nyborg, 2008). Mechanical forces are generated as these US waves travel through a medium. The applications of medical ultrasound depend on various parameters, including frequency, duty cycle, wavelength, energy, power, and intensity. These factors affect the way ultrasound waves are transmitted, absorbed, and reflected as they pass through tissues (Uddin et al., 2021). The intensity level (power per unit area) is crucial in US applications. For short intervals, intensities below  $0.1 \text{ W/cm}^2$  are used for Doppler effects, while intensities between  $0.1$  and  $1 \text{ W/cm}^2$  are employed for diagnostic imaging (Carovac et al., 2011).

### 1.7.2 Types of Therapeutic Ultrasound

There are different types of ultrasound modalities available, such as high-intensity focused ultrasound (HIFU) and low-intensity pulsed ultrasound (LIPUS). HIFU has been researched for its use in drug delivery, as it can heat targeted tissue areas region of interest (ROI) while minimizing thermal effects on surrounding healthy tissue (Tavakkoli and Sanghvi, 2011). In contrast, LIPUS operates at lower power, generating low acoustic intensity beam over a larger



ROI (Hornsby et al., 2023). Intensities above 10 W/cm<sup>2</sup> produce substantial heat, making high-HIFU primarily suitable for cancer treatment and surgical applications (Cheung, 2018). In contrast, LIPUS operates at lower power, generating low acoustic intensity, ranging from 20 to 1000 mW/cm<sup>2</sup>, beam over a larger ROI (Hornsby et al., 2023). It can be categorised into pulsed and continuous forms based on the duty cycle. Pulsed US involves ON/OFF cycles of ultrasound waves, while continuous US delivers uninterrupted acoustic waves (Figure 1.6) (Uddin et al., 2021; Jiang et al., 2018).

### 1.7.3 Low-Intensity Pulsed Ultrasound (LIPUS)

LIPUS is described as mechanical energy that travels through tissue in the form of acoustic pressure waves (Claes and Willie, 2007). The first reported use of low-intensity ultrasound to accelerate fracture healing in humans was by Duarte in 1983 (Harrison and Alt, 2021). This success led to clinical trials in the United States, culminating in the U.S. Food and Drug Administration's (FDA) 1994 approval of EXOGEN for the accelerated healing of specific fresh fractures. In 2000, the product also received approval for treating established non-unions (Harrison et al., 2016).

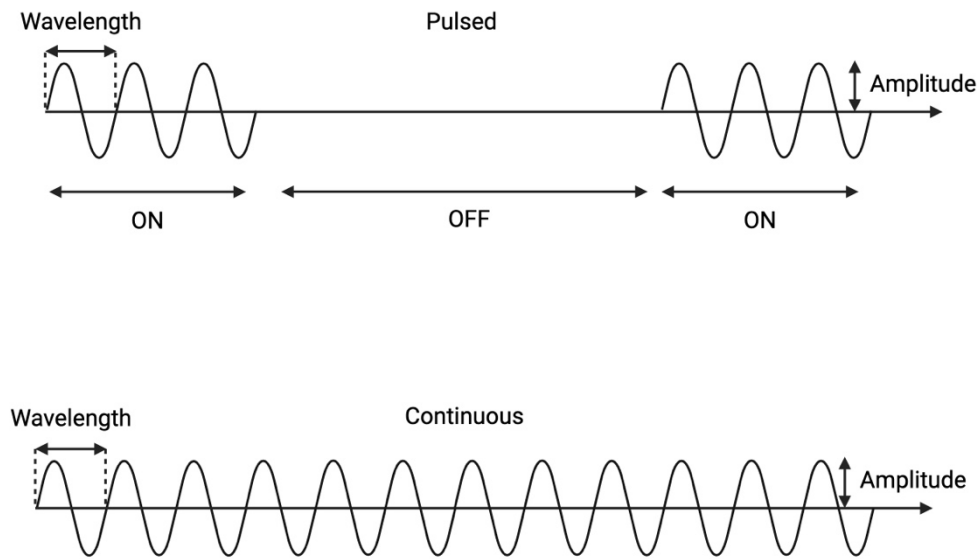


*Figure 1.6 Pulsed and continuous ultrasound waveforms.*

The illustration highlights the major difference between pulsed and continuous ultrasound waveforms. The top part of the image shows a pulsed ultrasound waveform, characterized by alternating ON/OFF cycles. The bottom part depicts a continuous ultrasound waveform, which is a steady wave without ON/OFF cycles, indicating continuous energy delivery.

Its growing importance is due to its low cost, inherent safety, and ability to deliver non-invasive treatments to targeted areas within the body, providing therapeutic effects without leaving scars (Xin et al., 2016; Fontana et al., 2021). Frequency is a critical factor in LIPUS stimulation. It is defined as the number of compression and rarefaction cycles a particle undergoes per second. Additionally, ultrasound can cause vibrations in particles found within extracellular fluids, intracellular fluids, and cell membranes (Xin et al., 2016; Abu-Zidan et al., 2011). Another important concept related to ultrasound is the ultrasonic beam, which exhibits variations in energy concentration, with areas of both higher and lower energy density. The absorption of ultrasound energy is proportional to the density of the tissue through which it passes (Schortinghuis et al., 2003; Xin et al., 2016).

### 1.7.4 Mechanisms of LIPUS

The biophysical effects of US can be divided into thermal and non-thermal effects. Thermal effects, such as a rise in tissue temperature, can result from continuous wave exposure, while non-thermal effects, such as cavitation, result from pulsed-wave exposure. However, both thermal and non-thermal effects produce heat through the interaction of sound waves with tissue, with the pulsed-wave ratio and rising temperature being proportionally related (Baker et al., 2001).

#### *1.7.4.1 Thermal Effects*

Ultrasound is produced when energy is transferred from a source, such as an ultrasound probe, to an object. This energy causes cyclic vibrations of compression and expansion, typically in the direction of wave propagation. As energy is transferred from one location to another, it can lead to a temperature increase within the medium. The extent of this temperature rise depends on the initial energy of the acoustic beam (Furusawa et al., 2014). Therefore, adjusting US parameters, such as frequency, intensity, time and the area being sonicated, can either enhance or reduce the thermal effects on objects within the wave propagation field. For instance, equipment that emits HIFU is used in cancer ablation therapy in some clinics worldwide. A focused beam of high-intensity US, ranging from 100 to 10,000 W/cm<sup>2</sup>, is directed at a tumour area to rapidly increase its temperature to over 60°C, which will result in cancer cell death. Thermal US is also used in physiotherapy to alleviate pain and reduce swelling, where heat is produced, by the continuous US beam, to the soft tissues. The application of heat to the affected tissues enhances blood flow, elasticity, and metabolic processes (Furusawa et al., 2014).

#### *1.7.4.2 Non-Thermal (Mechanical)/Intracellular Bioeffects*

The mechanical (non-thermal) effects are partly caused by the transfer of some of the beam's momentum to the surrounding medium, which leads to a convective movement known as "acoustic streaming" (Furusawa et al., 2014). The main effect of non-thermal US are seen on the cell membrane, leading to cellular deformation, mild disruptions and cell lysis (van Wamel

et al., 2006; Hassan et al., 2010). Additionally, due to the complex network of mechanotransduction that transmits extracellular physical forces into the cell's interior, ultrasound can trigger various intracellular events. These include initiating biochemical reactions and altering gene expression. Together, increased cell proliferation or activation of apoptosis may result from these bioeffects, suggesting that US could play a role in accelerating wound and bone fracture healing, as well as in cancer treatment (Furusawa et al., 2014).

Sustained effects are observed in more intense exposure level that may cause cell lysis. When there is significant membrane damage, it is understandable that ultrasound can penetrate deeper into intracellular targets. However, at lower exposure levels, where cell viability appears to be maintained, the observed cellular functions and gene expression changes remain harder to explain (Furusawa et al., 2014; Schlicher et al., 2010). However, this could be explained by rapid increase in intracellular calcium ions ( $\text{Ca}^{2+}$ ) due to  $\text{Ca}^{2+}$  influx when the membrane's permeability is disrupted. This influx helps prevent the reduction of intracellular  $\text{Ca}^{2+}$ , including those within the cisternae of the nuclear membrane (Furusawa et al., 2014). As a result, the nuclear pore complex (NPC) stays open, allowing macromolecules to pass through (Maitra, 2005). Furthermore, it has been suggested that increased  $\text{Ca}^{2+}$  levels may activate a group of cytoplasmic enzymes called tissue transglutaminases (TGase), which are known for their ability to crosslink proteins, particularly those in the extracellular matrix, a process associated with wound healing and the formation of intracellular 'clots' (Hassan et al., 2010).

Another non-thermal effect is cavitation, which is defined as a physical process that occurs when US interacts with a liquid. This effect involves the formation, oscillation and collapse of gas-filled cavities (bubbles) within tissue in response to varying pressure gradients in the ultrasound wave field (Li et al., 2023; Tang et al., 2015). Cavitation can be classified into two types: inertial cavitation and stable cavitation. In stable cavitation, bubbles oscillate in response to the ultrasound wave, expanding during the negative pressure phase and contracting during

the positive pressure phase. Unlike inertial cavitation, stable cavitation does not result in the violent collapse of bubbles or the production of reactive oxygen species (ROS) (Tang et al., 2015). In contrast, during inertial cavitation, bubbles can expand to 2–3 times their resonant size before collapsing in the subsequent compression half-cycle (Izadifar et al., 2019).

### 1.7.5 LIPUS in Fracture Healing

The role of LIPUS in bone fracture and tendon healing has been extensively investigated, and it has been commonly used in clinics for fracture treatments since the 1990s. The U.S. FDA has approved the use of LIPUS to enhance bone regeneration in humans, though the precise molecular processes behind its therapeutic effects are not yet fully understood (Zhong et al., 2024). LIPUS waves create nanomotion at the fracture site, converting mechanical signals into biochemical signals within cells. This process, involving integrins and focal adhesions, leads to the production of Cyclooxygenase-2 (COX2), which likely increases PGE2 levels and drives osteogenic gene expression, promoting increased mineralisation and enhanced endochondral ossification that aids in fracture healing (Harrison et al., 2016).

A review by Claes and Willie (2007) concluded that LIPUS demonstrated positive results for bone regeneration and improved fracture healing processes. Another study by Fung et al. (2014) explored the effect of LIPUS beam direction and depth on bone fracture healing, finding that beam strength at the fracture site is critical, with a closer LIPUS beam providing better healing. Lee et al. (2024) investigated the role of LIPUS in 38 four-month-old male Sprague Dawley rats, randomly divided into four groups: Sham, Sham + US, osteoarthritis (OA), and OA + US. LIPUS was administered to the medial side of the right knee using a 3.3 MHz pulse frequency, 0.1 W/cm<sup>2</sup> peak intensity, and a 20% duty cycle. The treatment was applied for 20 minutes per day, 5 days a week, for 4 weeks. The study found that early intervention with LIPUS offers protective benefits against the progression of knee OA, including reduced tissue degradation, alleviated pain, improved subchondral bone structure, and decreased sensory innervation. Also,

Yang et al. (1996) studied ultrasound's effects on gene expression in a rat femur fracture model and found that LIPUS enhanced aggrecan expression during fracture healing, suggesting a role in endochondral ossification. Therefore, while LIPUS is an effective way to treat bone fractures, the precise location of the fracture should be accurately identified to deliver the best treatment.

LIPUS treatment is typically administered in one 20-minute session per day with 1.5 MHz waves, an average intensity of 30 mW/cm<sup>2</sup>, and a pulse width of 200 ms (Claes and Willie, 2007). However, these parameters can vary, and different machines offer different settings depending on the depth and site of the injury. For example, Heybeli et al. (2002) used a 7.5 MHz frequency and an 11.8 mW/cm<sup>2</sup> total output intensity, successfully stimulating bone fracture healing. In a cohort study by Zura et al., (2015), they found that LIPUS treatment resulted in a high healing rate of 86.2% in 767 non-union fractures that had not healed for at least a year before treatment. This healing rate is well within the range typically seen with surgical revision, indicating that LIPUS may offer a similar benefit to surgery.

#### 1.7.6 LIPUS in Musculoskeletal Studies

For decades, therapeutic US has been researched and used for the treatment of musculoskeletal injuries, such as injuries to tendons, skeletal muscles. Different studies have shown its effect on the recovery of soft tissue (Enwemeka et al., 1990; Junior et al., 2011; Ng et al., 2003). Enwemeka et al. (1990), investigated the effect of low-intensity ultrasound on the right tendo calcaneus (Achilles) tendon of 28 rabbits was investigated. The results suggested that after 10 days of 5-minute daily sessions, ultrasound increased tensile strength and tensile stress. Similarly, Júnior et al. (2011) performed calcaneus tendon tenotomy and tenorrhaphy on 28 Wistar rats and concluded that LIPUS treatment for 28 days at a frequency of 1 MHz and an intensity of 0.1 W/cm<sup>2</sup> positively influenced the calcaneus tendon healing process in rats. Rantanen et al., (1999) concluded in their study that while pulsed ultrasound treatment can

enhance the proliferation phase of satellite cells during muscle regeneration (by around 96%), it does not appear to significantly impact the overall structural aspects of muscle repair. A study by Chan et al. (2010) demonstrated that LIPUS therapy significantly enhances the regeneration of myofibers, leading to improved physiological function in lacerated mouse muscles, especially during the first four weeks after surgery. The therapy also resulted in a notably higher proliferation rate and increased cell numbers on days 6 and 8. Another study by Tsai et al. (2006) provided new data on the molecular events linked to the stimulation of collagen expression in tendon cells affected by ultrasound. This study showed that ultrasound significantly stimulates collagen type I and III expression and TGF- $\beta$  secretion in tendon cells. In their experiments, tendon cells at 50% to 60% confluence were exposed to a single LIPUS treatment for 5 minutes, with subsequent experiments conducted 24 hours later. Another study by Wood et al., (2010) showed that after 5 days of LIPUS stimulation they found an increase in expression of type I collagen. On the other hand, type III collagen, did not show significant changes in its expression levels following these treatments.

LIPUS has also been shown to influence inflammation in tendon injury (Li et al., 2023). In a study by Gan et al., (1995) where they used chicken model, they found that after pulsed ultrasound applied to zone 2 flexor tendons. The results showed increased movement, a reduction in the inflammatory phase, and improved scar maturation compared to the control group. A study by Fu et al., (2010) found in a rat patellar tendon injury model, LIPUS was applied at various stages of the healing process. The results showed that after a single LIPUS session the TGF- $\beta$  and collagen type I and III expression increased when administered on the fourth day post-injury, with no significant effect observed when applied at other times. However, a recent study by Icenogle et al. (2021), using a rat Achilles tendon injury model, found that after 14 days of LIPUS treatment, no statistically significant difference was observed

in TGF- $\beta$ 1 expression. However, a significant increase in collagen type 3 and a reduction in collagen type 1 were observed following the LIPUS treatment.

While therapeutic ultrasound has demonstrated various beneficial effects on the healing of musculoskeletal injuries, including enhanced cellular proliferation and collagen expression (Li et al., 2023), its impact can vary depending on the timing, duration, and specific tissue being treated, highlighting the need for further research to optimise its therapeutic applications.

### 1.7.7 LIPUS in Wound Healing Studies

An animal study by Maeda et al. (2013) investigated the effect of LIPUS on 28 rats with palatal excisional wounds, exposing them to LIPUS for 15 days. The LIPUS group showed better wound epithelialisation and reduced wound size compared to the control group. A recent study by Zhong et al. (2024) found that LIPUS enhances the wound healing of diabetic rats by boosting the effects of adipose-derived stem cell (ADSC) derived exosomes. Specifically, LIPUS increases the uptake of these exosomes by the cells in the wound area, making the healing process more effective.

LIPUS has shown promising results at the cellular level in various studies. Atherton et al. (2017) demonstrated that LIPUS is detected by cell-matrix adhesions via vinculin, which subsequently regulates the Rab5-Rac1 pathway, influencing ultrasound-mediated endocytosis and cell movement. This aligns with Mahoney et al. (2009), who also found that LIPUS activates Rac1. However, Mahoney's study revealed that LIPUS could activate Rac1 independently of the Syndecan-4 signaling pathway, suggesting an alternative mechanism for influencing cell migration. Both studies highlight the role of Rac1 in cell movement, supporting LIPUS as a valuable tool in wound management through mechanosensitive pathways.

Building on these findings, Roper et al. (2015) explored how ultrasound can promote fibroblast migration by activating the calcium/CamKinaseII/Tiam1/Rac1 pathway, specifically in



diabetic and aged mice. Their study showed that ultrasound could compensate for impaired fibronectin signaling, significantly reducing healing times by 30%. These results complement those of Atherton and Mahoney, as they all highlight Rac1 activation as a key factor in LIPUS-induced cell migration, particularly under challenging healing conditions like aging or diabetes.

On the other hand, Samuels et al. (2013) took a different approach by focusing on how LIPUS promotes wound healing through increased cellular metabolism and proliferation. While their results suggest that LIPUS is effective at boosting healing at the cellular level, they pointed out the need for further studies on collagen assays, given collagen's key role in the ECM. This focus on metabolism and proliferation differs from Atherton et al.'s emphasis on cytoskeletal changes and cell-ECM adhesion, indicating that LIPUS may impact wound healing through multiple pathways depending on the cellular context.

Bohari et al. (2015) and Mostafa et al. (2009) provided additional nuance to these findings. Mostafa et al. (2009) found no significant changes in cell viability, proliferation, or the expression of proliferating cell nuclear antigen (PCNA) and collagen-I in human gingival fibroblasts (HGF) after 4 weeks of treatment. Whereas Bohari et al. (2015) showed that LIPUS increased cell numbers in human dermal fibroblasts (HDF) only in the absence of TGF- $\beta$ 1 and ascorbic acid, suggesting that these factors may influence how LIPUS affects cell proliferation. These studies highlight how the effects of LIPUS can vary based on the presence of growth factors, cell type, and treatment duration, indicating that LIPUS's influence may be context dependent.

Shiraishi et al. (2011) demonstrated that LIPUS enhances the expression of connective tissue growth factors (CCN2/CTGF) in gingival cells, which in turn promotes wound healing. This aligns with the general view that LIPUS can positively affect growth factors to enhance healing. However, Cárdenas-Sandoval et al. (2023) found more nuanced results. They applied LIPUS

to ligament fibroblasts and discovered that while it improved cell migration at lower doses, the higher dose decreased migration. Moreover, after 5 days of ultrasound stimulation, none of the groups expressed sufficient collagen protein, making the results inconclusive in terms of collagen-related wound healing. This contrasts with Shiraishi's findings on connective tissue growth factors, suggesting that while LIPUS may promote growth factor expression, its impact on collagen production and overall healing may depend on the dose and treatment conditions.

Overall, these studies present a complex understanding of LIPUS, where its effectiveness in enhancing cell migration and wound healing is influenced by various factors such as cell type, growth factors, and treatment conditions. While several studies support its role in activating pathways like Rac1 to improve cell movement, others raise questions about its impact on proliferation and collagen production, indicating the need for further investigation into how LIPUS affect different ECM molecules that directly related to wound healing.

#### *1.7.7.3 Gaps in the Literature*

While numerous studies have highlighted the effectiveness of ultrasound in wound healing, there remain significant gaps in our understanding of its effects at the cellular level. In particular, it is not yet fully understood which specific ECM proteins are influenced by LIPUS nor how ECM organisation is altered following LIPUS stimulation. These insights are especially crucial for understanding the role of LIPUS in wound healing and scar formation. Therefore, further research is essential to enhance our knowledge and bridge these gaps in the literature. This PhD thesis seeks to address these issues by specifically investigating the impact of LIPUS on ECM, providing clearer insights into these critical areas.

## **1.8 Research Gap and Thesis Aims**

Although LIPUS shows promising potential in enhancing wound healing, the exact molecular mechanisms behind its impact on ECM remodelling remain unclear, particularly in relation to ECM protein expression, cross-linking, and organisation. Therefore, this thesis aims to:

1. Investigate the effect of LIPUS on the gene expression of specific ECM molecules.
2. Examine the effect of LIPUS on matrix deposition, cross-linking, and organisation.

## 1.9 Significance of this PhD Project

The significance of this PhD lies in its focus on elucidating the molecular expression through which LIPUS affects ECM remodelling. By identifying specific cellular responses activated by LIPUS, the research aims to provide a scientific basis for its application in chronic wound management. Understanding these mechanisms could lead to the development of targeted therapies that not only accelerate wound closure but also improve the quality of the regenerated tissue, reducing scar formation.

## 1.10 Hypothesis and Objectives:

LIPUS will influence the expression level of the candidate proteins either by up or down regulation. Resolving the effects of LIPUS will result in a better understanding of the ECM role in wound management. Additionally, LIPUS will modify ECM organisation and cross-linking, which will have an impact on wound scarring by reducing its effect on the skin after healing. Existing evidence that LIPUS alters cell migration, adhesion, and differentiation provides strong grounds to predict that matrix organisation will be affected.

The hypothesis will be investigated by answering three questions:

1. Does LIPUS affect the expression of the candidate ECM molecules and modifying proteins?
2. How does LIPUS influence the expression of candidate molecules that modify ECM proteins and affect the organisation of the ECM (up/down regulated)?
3. Does LIPUS have an effect in reducing the scar effect after wound healing by investigating matrix alignment?

# Chapter 2

## Materials and Methods

### Methodology

## Chapter 2 Materials and Methods

### 2.1 Investigation of published data sets to define the candidate proteins

Published datasets reporting changes in gene expression during both healthy and impaired healing were analysed using multiple approaches to identify proteins with altered expression under various conditions. Proteins showing differential expression may serve the ideal choice to be investigated by ultrasound to investigate its effect on them. A genome-wide microarray study, involving 25 biopsies from split-thickness skin grafts (SSG), conducted by Nuutila et al. (2012), was explored. The microarray data were imported into Excel for analysis of fold changes yielded more than 2-fold change in extracellular matrix molecules. Statistical significance was assessed in the original publication, and changes in protein expression across different wound healing stages were compared.

The process of selecting candidate proteins was done using the Database for Annotation, Visualization, and Integrated Discovery (DAVID) v 6.8. This tool provides a comprehensive functional annotation to understand the biological meaning of a large list of genes. DAVID was used to select genes that are annotated as being part of the ECM (Figure 2.1 and Figure 2.2). The filtered genes were sorted based on fold change to identify the proteins which have changed between the three conditions.

















Annotation Cluster 29		Enrichment Score: 1.16	 	Count	P_Value	Benjamini
<input type="checkbox"/>	UP_SEQ_FEATURE	LIPID:O-palmitoleoyl serine; by PORCN	<a href="#">RT</a> 	4	5.8E-3	6.1E-1
<input type="checkbox"/>	KEGG_PATHWAY	<a href="#">Melanogenesis</a>	<a href="#">RT</a> 	8	6.3E-3	2.8E-1
<input type="checkbox"/>	GOTERM_BP_DIRECT	<a href="#">cell fate commitment</a>	<a href="#">RT</a> 	6	7.6E-3	5.0E-1
<input type="checkbox"/>	INTERPRO	<a href="#">Wnt_CS</a>	<a href="#">RT</a> 	4	8.2E-3	2.7E-1
<input type="checkbox"/>	INTERPRO	<a href="#">Wnt_C</a>	<a href="#">RT</a> 	4	8.2E-3	2.7E-1
<input type="checkbox"/>	INTERPRO	<a href="#">Wnt</a>	<a href="#">RT</a> 	4	8.2E-3	2.7E-1
<input type="checkbox"/>	SMART	<a href="#">WNT1</a>	<a href="#">RT</a> 	4	9.7E-3	3.5E-1
<input type="checkbox"/>	GOTERM_BP_DIRECT	<a href="#">canonical Wnt signaling pathway</a>	<a href="#">RT</a> 	8	1.1E-2	5.7E-1
<input type="checkbox"/>	KEGG_PATHWAY	<a href="#">Signaling pathways regulating pluripotency of stem cells</a>	<a href="#">RT</a> 	9	1.3E-2	4.4E-1
<input type="checkbox"/>	KEGG_PATHWAY	<a href="#">Hippo signaling pathway</a>	<a href="#">RT</a> 	9	2.1E-2	5.6E-1
<input type="checkbox"/>	KEGG_PATHWAY	<a href="#">Human papillomavirus infection</a>	<a href="#">RT</a> 	13	5.9E-2	8.8E-1
<input type="checkbox"/>	GOTERM_MF_DIRECT	<a href="#">frizzled binding</a>	<a href="#">RT</a> 	4	6.1E-2	1.0E0
<input type="checkbox"/>	KEGG_PATHWAY	<a href="#">Proteoglycans in cancer</a>	<a href="#">RT</a> 	9	7.7E-2	9.3E-1
<input type="checkbox"/>	UP_KW_CELLULAR_COMPONENT	<a href="#">Extracellular matrix</a>	<a href="#">RT</a> 	11	1.0E-1	3.5E-1

Figure 2.1 DAVID page showing how to specify the Extracellular Matrix proteins amongst the other proteins.

Gene Report				<a href="#">Help and Manual</a>
Current Gene List: List_2				
Current Background: Homo sapiens				
159 DAVID IDs				
17 record(s)				<a href="#">Download File</a>
AFFYMETRIX_3PRIME_IVT_ID	GENE NAME	Related Genes	Species	
Wnt family member 4(WNT4)	<a href="#">Wnt family member 4(WNT4)</a>	<a href="#">RG</a>	<a href="#">Homo sapiens</a>	
Wnt family member 5A(WNT5A)	<a href="#">Wnt family member 5A(WNT5A)</a>	<a href="#">RG</a>	<a href="#">Homo sapiens</a>	
asporin(ASPIN)	<a href="#">asporin(ASPIN)</a>	<a href="#">RG</a>	<a href="#">Homo sapiens</a>	
collagen type III alpha 1 chain(COL3A1)	<a href="#">collagen type III alpha 1 chain(COL3A1)</a>	<a href="#">RG</a>	<a href="#">Homo sapiens</a>	
collagen type V alpha 1 chain(COL5A1)	<a href="#">collagen type V alpha 1 chain(COL5A1)</a>	<a href="#">RG</a>	<a href="#">Homo sapiens</a>	
collagen type V alpha 3 chain(COL5A3)	<a href="#">collagen type V alpha 3 chain(COL5A3)</a>	<a href="#">RG</a>	<a href="#">Homo sapiens</a>	
collagen type X alpha 1 chain(COL10A1)	<a href="#">collagen type X alpha 1 chain(COL10A1)</a>	<a href="#">RG</a>	<a href="#">Homo sapiens</a>	
collagen type XI alpha 1 chain(COL11A1)	<a href="#">collagen type XI alpha 1 chain(COL11A1)</a>	<a href="#">RG</a>	<a href="#">Homo sapiens</a>	
dermatopontin(DPT)	<a href="#">dermatopontin(DPT)</a>	<a href="#">RG</a>	<a href="#">Homo sapiens</a>	
hemicentin 1(HMCN1)	<a href="#">hemicentin 1(HMCN1)</a>	<a href="#">RG</a>	<a href="#">Homo sapiens</a>	
lumican(LUM)	<a href="#">lumican(LUM)</a>	<a href="#">RG</a>	<a href="#">Homo sapiens</a>	
matrix metalloproteinase 12(MMP12)	<a href="#">matrix metalloproteinase 12(MMP12)</a>	<a href="#">RG</a>	<a href="#">Homo sapiens</a>	
matrix metalloproteinase 13(MMP13)	<a href="#">matrix metalloproteinase 13(MMP13)</a>	<a href="#">RG</a>	<a href="#">Homo sapiens</a>	
nidogen 2(NID2)	<a href="#">nidogen 2(NID2)</a>	<a href="#">RG</a>	<a href="#">Homo sapiens</a>	
osteomodulin(OMD)	<a href="#">osteomodulin(OMD)</a>	<a href="#">RG</a>	<a href="#">Homo sapiens</a>	
periostin(POSTN)	<a href="#">periostin(POSTN)</a>	<a href="#">RG</a>	<a href="#">Homo sapiens</a>	
spondin 2(SPON2)	<a href="#">spondin 2(SPON2)</a>	<a href="#">RG</a>	<a href="#">Homo sapiens</a>	

Figure 2.2 Showing DAVID Gene Report of the Extracellular Matrix proteins involved on genome-wide microarray study, involving 25 biopsies from SSG yielded more than 2-fold change.

## 2.2 Cell Lines

Telomerase Immortalised Fibroblasts (TIFs) (Munro et al., 2001) were cultured at 37 °C with 5% CO<sub>2</sub> in DMEM supplied with 15% foetal bovine serum (FBS), 4.5 g l<sup>-1</sup> glucose, 25mM HEPES, and 2mM-glutamine. TIFs were used because they are a stable line, and cells continue to divide due to telomerase immortalisation. Also, the non-transformed human foreskin fibroblasts (HFFs) were used. HFFs were cultured at 37 °C with 5% CO<sub>2</sub> in Dulbecco's Modified Eagle Medium (DMEM), 10% FBS, 25mM HEPES, and 2mM-glutamine. HFFs were used to explore the key results if the transformation influences expression changes.

To prepare for the experiments, cells were cultured until they became confluent. Next, they were washed with Dulbecco's Phosphate-buffered saline (PBS) not containing MgCl<sub>2</sub> and CaCl<sub>2</sub>, and then trypsinised using 0.05% Trypsin-EDTA from Gibco by Life Technologies to detach them from the flask. Trypsinised cells were then centrifuged and resuspended in growth medium and counted using Fast Read 102® chamber to maintain an optimum and equal number of cells in each well to be grown during the experiment. By counting 3 squares, the cell calculation for each well in a 6-well plate is given using the equation:

$$\left[ \frac{\text{number of cells in each well (300,000)}}{\left( \frac{\text{Cells count in 3 squares}}{3} \times 10^4 \right)} \right]. \text{ Figure 2.3 showing the counting technique using Fast}$$

Read 102® chambers.

The cells were seeded in 20 ml of medium (details summarised in Table 2.1). Finally, two hours before LIPUS treatment, the cells were seeded into 6-well plates in full culture medium at a density of 3x10<sup>5</sup> cells per well.

Table 2.1 Cell culture materials.

Media/reagents	Suppliers/components	Catalogue number
Culture media	<p>Sigma-Aldrich,</p> <p><u>TIF</u> supplemented with 15% FBS (75ml) and 200mM L-glutamine (10ml).</p> <p><u>HFF</u> supplemented with 10% FBS (50ml) and 200mM L-glutamine (10ml).</p>	D5796
FBS	Sigma-Aldrich	F7524
Trypsin-EDTA	Sigma-Aldrich	59417C
PBS-	Sigma-Aldrich	-



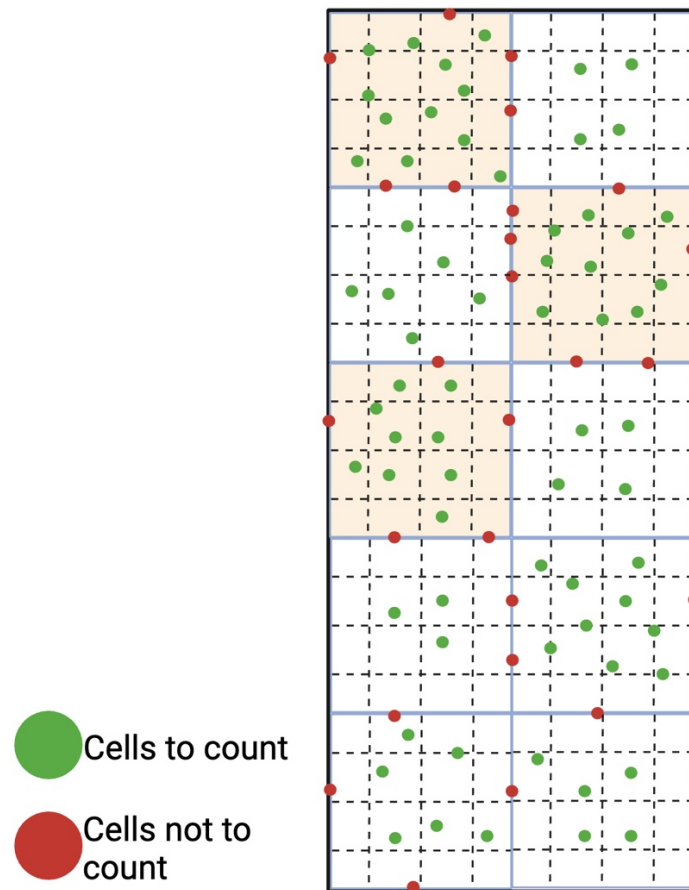


Figure 2.3 Fast Read 102® chambers for cell counting

Cell counting is done by denoting cells that will be counted as green dots and cells that should not be counted as red dots to avoid over counting. (Image Created in BioRender.com.).

## 2.3 LIPUS stimulation parameters

For all experiments, cells were cultured in duplicate plates, one plate treated with LIPUS and the other kept grown as control sample without treatment. LIPUS was applied at the following parameters: 1.5-MHz frequency, a 20% duty cycle pulse, using a 457mVpp signal to generate 30 mW/cm<sup>2</sup> spatial average, temporal average (SATA). Cells were treated for 20 minutes per day for 5 days (Table 2.2). Both samples were subjected to identical conditions, with the incubator consistently maintaining a temperature of 37°C containing 5% CO<sub>2</sub> (Figure 2.4). Although no formal calibration or functionality checks were performed on the LIPUS machine prior to the experiments, the observed changes in gene expression following LIPUS treatment

suggest that the device was functioning as intended. Notably, several target genes exhibited differential expression, while GAPDH, a commonly used housekeeping gene, remained stable across all conditions. The lack of change in GAPDH expression supports the specificity and reliability of the observed effects, as housekeeping genes are expected to remain constant and unaffected by experimental conditions.

'Sham' treatments refer to experimental conditions in which the cell samples underwent identical procedures as LIPUS-treated samples but without the actual activation of ultrasound emission. This is to ensure that any observed effects were due to LIPUS stimulation, eliminating potential confounding variables related to treatment setup.

Figure 2.5 shows an overview flow chart of the cell culture process and the LIPUS stimulation steps.

Table 2.2 LIPUS stimulation period.

Day1	Day2	Day3	Day4	Day5
<ul style="list-style-type: none"> <li>TIF, HFF cells Seeding</li> </ul> LIPUS treatment (20 minutes)	LIPUS treatment (20 minutes)	LIPUS treatment (20 minutes).	<ul style="list-style-type: none"> <li>Change medium to serum free medium.</li> </ul> LIPUS treatment (20 minutes).	<ul style="list-style-type: none"> <li>LIPUS treatment (20 minutes).</li> <li>Cellular lysate</li> </ul> Serum-free medium concentration.

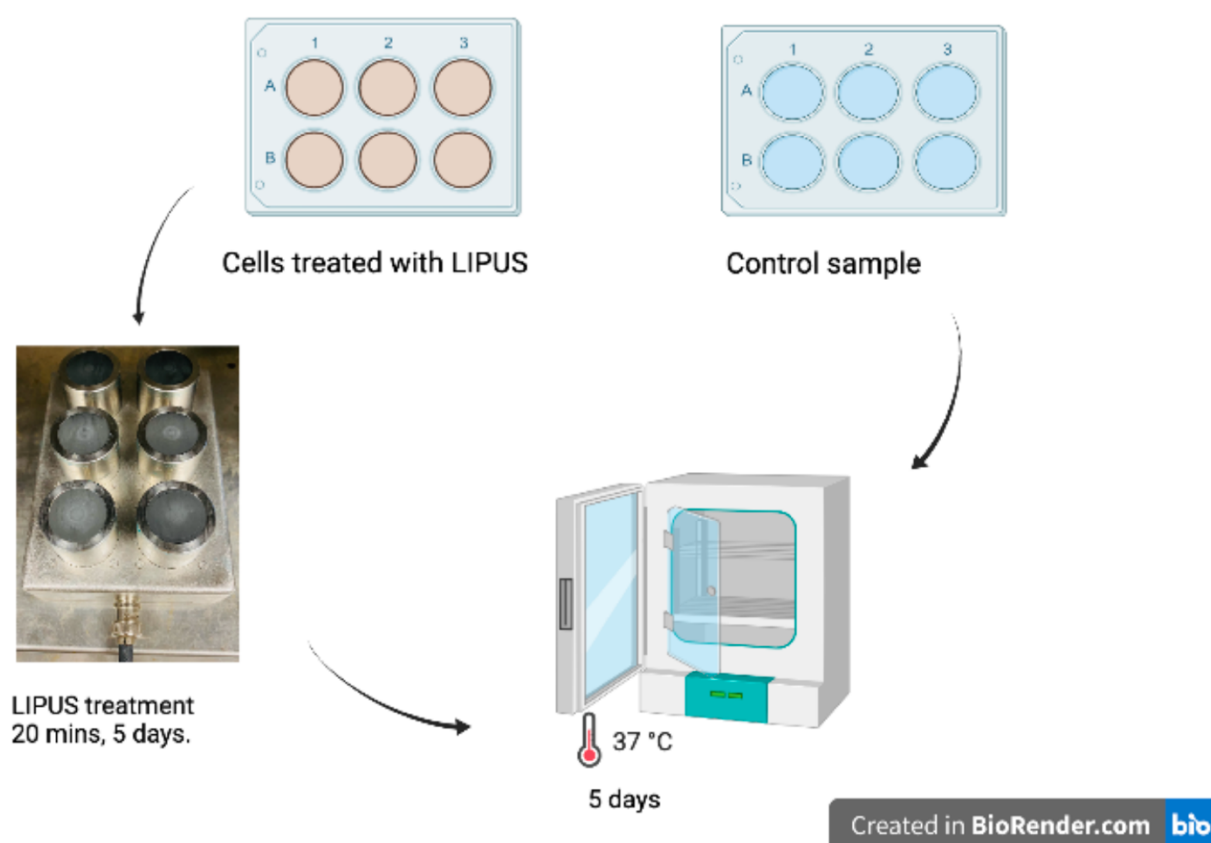


Figure 2.4 Flowchart of the process of LIPUS treatment and control samples (Image created using Biorender).

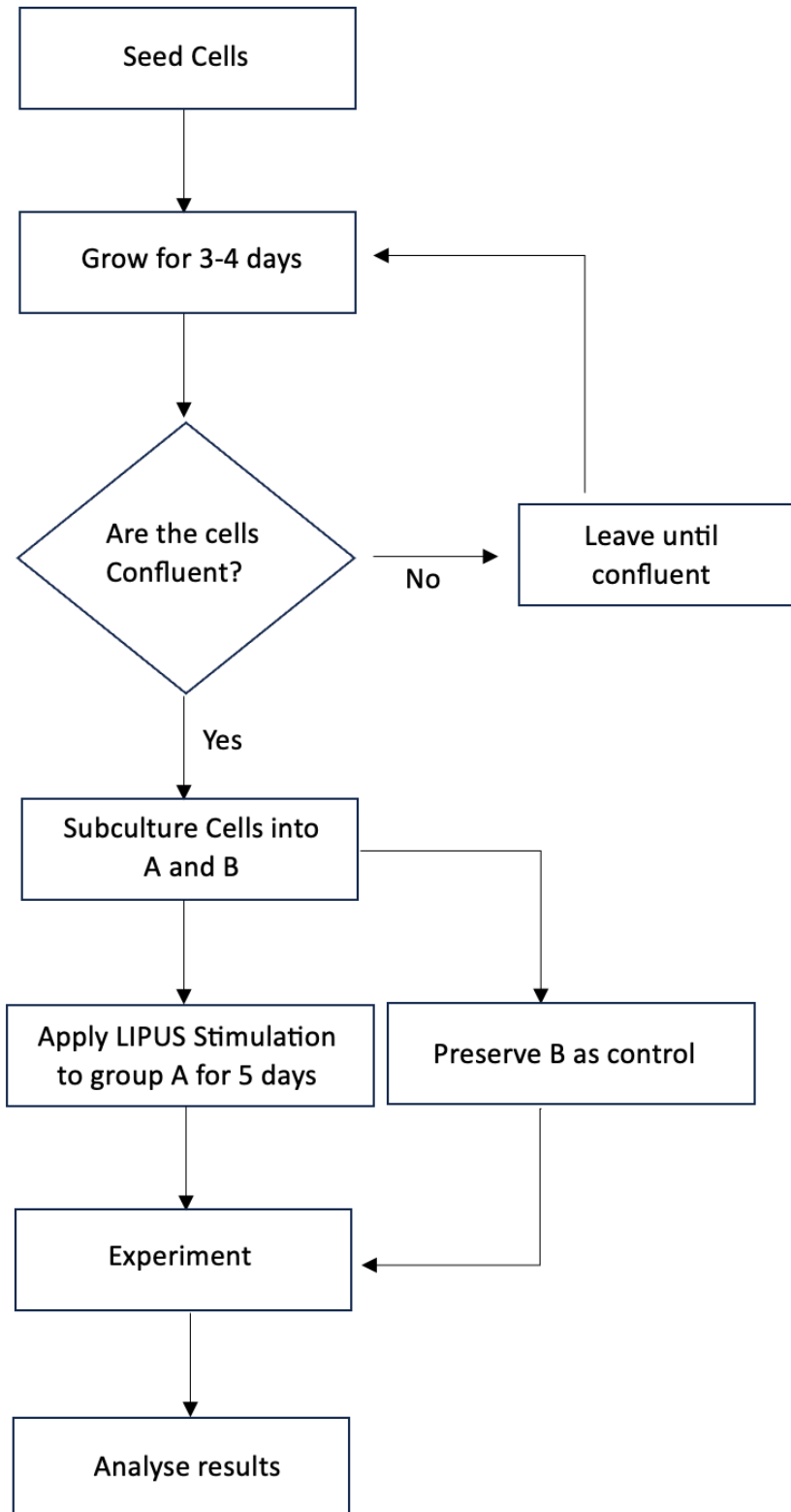


Figure 2.5 Flow chart Showing summary of the cell culture and LIPUS stimulation steps.

## 2.4 Storing cells

First, the cells were trypsinised to detach them from the flask, then centrifuged and resuspended in FBS. An equal volume of 20% Dimethyl Sulfoxide (DMSO) was added to the cell suspension to achieve a final concentration of 10% DMSO. This solution acts as a cryoprotective agent for the cells during the freezing process. Next, the cell suspension was centrifuged at 1500 rpm for 5 minutes to pellet the cells and remove the supernatant. Then, the cell pellet was resuspended with the FBS-DMSO solution to ensure that equal number of cells are divided for cryoprotectant. One milliliter (1ml) was then pipetted into pre-cooled cryovials, taking care to avoid making bubbles which can disrupt cell integrity. These cryovials were then promptly placed in a -80°C freezer and ensuring gradually lowering the temperature of the cells. This will help to minimize the formation of ice crystals that could potentially damage the cell membranes. If extended preservation is needed, the cryovials were then transferred to the liquid nitrogen. Freezing cells is crucial to maintain the integrity of the cell line, and to ensure that the cells are kept viable and healthy for future experiments.

## 2.5 Thawing cells

To revive freeze cells, the cryovials were rapidly thawed in a 37°C water bath. Once completely thawed, the cells were promptly transferred to a 15 ml Falcon tube containing prewarmed medium. Following this, the tube was centrifuged at 1500 rpm for 5 minutes to pellet the cells. The cell pellet was then carefully resuspended in 5 ml of medium and transferred into a T25 flask containing fresh culture medium.

The next day, the culture medium was refreshed to eliminate any floating or nonviable cells, ensuring a healthy and viable cell population for subsequent experiments. This methodical process of freezing and thawing cells is critical for maintaining the integrity and functionality of the cell line, facilitating reliable and reproducible experimental outcomes.

## 2.6 Quantitative polymerase chain reaction

Quantitative PCR (qPCR) was used to quantify changes in expression of a candidate genes in response to LIPUS stimulation (Freitas et al., 2019). The total RNA was extracted from the harvested TIF cells using a commercially available RNA extraction kit, Monarch© Total RNA Miniprep Kit with the following steps:

cells were centrifuged at 500 g for 2 minutes to pellet cells. Then, they were resuspended in 300 µl RNA lysis buffer provided in the kit.

RNA binding and elution: The sample was transferred into a collection tube with a gDNA-removal column (to remove contaminating genomic DNA from RNA before reverse transcription) and spun for 30 seconds at a maximum speed (16000 g). Ethanol was then added to the collection tube, which was transferred into RNA purification and spun for 30 seconds. Then it was washed with an RNA washer. Next, in an Eppendorf tube, 5 µl of DnaseI with 75µl DnaseI-reaction buffer was added to RNA purification, and the sample was incubated for 15 minutes. Following this, 500µl of priming buffer (used to wash bound RNA to remove contaminants, including salts and enzymes) was added and the sample was spun for 30 seconds.

RNA binding and elution: 500 µl of RNA wash buffer is added, and the sample was spun for 30 seconds. After discarding the fluid, this step was repeated but with spinning for 2 minutes. The sample column was then transferred to a microfuge tube. The last step of RNA extraction was to add 100 µl of nuclease-free water to elute and store the sample.

To perform the cDNA part, the RNA concentration was measured using a Nanodrop in each Eppendorf tube for qPCR. After that, 10 µl of (10 ng/µl sample + water) and 10 µl of (4 µl 5x reaction mix + 4 µl water + 2 µl maximum enzymes) were added to a PCR Eppendorf tube. In

the final stage, the forward and reverse primers were added for PCR amplification, followed by adding the green-blue mix to the sample.

## 2.7 Analysis of Protein Expression by Western blot

Western blots were imaged using Odyssey infrared imaging system and quantified using Image Studio Lite software (Li-COR Biosciences). The band intensities of target proteins were measured, and then normalised against the corresponding housekeeping protein (GAPDH). The resulting ratio of the target protein to housekeeping protein expression was used for statistical comparisons between different experimental groups.

In this study, GAPDH from cell lysates was used as a loading control to support the analysis of secreted proteins in conditioned medium. GAPDH is widely used as an internal control in cell lysates because of its stable expression. However, its application in studies involving secreted proteins requires careful consideration. As GAPDH is not secreted, it cannot serve as a direct control for conditioned medium. Currently, there is no universally accepted control for secreted proteins, and normalisation often depends on complementary approaches such as cell viability assays or total protein quantification in the medium. These limitations have been considered when interpreting the secretion data presented here. By analysing GAPDH levels in cell lysates from the same samples, it is possible to infer relative cell numbers and assess consistency across samples, indirectly supporting the interpretation of results from conditioned medium.

Protein abundance changes in both the conditioned medium and cell lysates were assessed using Western blot analysis. Therefore, on the fourth day of cell culture, the serum-containing medium was replaced with 15 ml serum-free medium. Then, after 24 hours, the conditioned medium is concentrated to 300ul using Amicon® Ultra-15 Centrifugal Filters ultracel 3K and centrifuged for 3h at 40 RPM/RCF x 100. Then, 10 ul of conditioned medium were mixed with

protein-dye 1:1 to prepare samples for western blotting. For the cell lysate, cells were scraped using 80  $\mu$ l of lysis buffer, then centrifuged (25,000 $\times$ g for 2 minutes at 4 °C), then 10  $\mu$ l of supernatant were mixed with protein-dye 1:1 to prepare samples for western blotting. Samples were loaded into a precast polyacrylamide BOLT gel (Invitrogen), and NuPAGE™ MES SDS Running Buffer (20X) buffer was used to run the samples at 200 volts for 27 minutes. Gels were transferred onto Amersham Protran 0.45  $\mu$ m nitrocellulose membrane (GE Healthcare Life Sciences A29474092) at 30 volts for 90 minutes. Membranes were blocked for one hour in 10x casein (1ml) diluted in 1xTBS-T (9ml). Primary antibody was added according to the dilutions (*Table 2.4*) in (TBS-T+casein) and then incubated at 4 °C at the lab plate shaker overnight. The next day, membranes were rinsed with TBS-T three times for 5 minutes. Then a secondary antibody was added according to the dilutions in (*Table 2.4*). The samples were incubated in the dark at the lab plate shaker at room temperature for 30 minutes. Then, membranes were rinsed with TBS-T three times for 5 minutes before being scanned. Odyssey infrared imaging system (700 nm and 800 nm channels, 169  $\mu$ m resolution) was used to detect Immunoblotted proteins. Figure 2.6 shows illustration of the Western blot process.

Band intensity was determined by digital- densitometric analysis using a free version of Image Studio version 5.2.5. A housekeeping protein standardisation method was used to adjust for loading variations within an experiment, and fold changes were normalised to the average of datasets with similar conditions across experiments. This will ensure dependable comparisons between different experimental sets. *Table 2.3* and *Table 2.4* list the buffer and antibodies used in the experiments.



Table 2.3 Buffers used in western blot and preparations.

Component	Amount
stock lysis buffer (100ml)	10% Glycerol <b>10ml</b> 20mM HEPES. pH 7.4 <b>2ml</b> 140nM NaCl <b>2.8ml</b> 1% NP40 <b>1ml</b> 0.5% NaDeoxycholate <b>0.5g</b> 4mM EGTA <b>8ml</b> 4mM EDTA <b>8ml</b>
lysis buffer	stock lysis buffer <b>1ml</b> PhoSTOP <b>100ul</b> cOmplete inhibitor <b>10ul</b>
NuPAGE™ MES SDS Running Buffer (20X)	MES SDS Running buffer (20X) <b>25ml</b> dH2O <b>475ml</b>
Protein Loading Buffer Stock	200 mM Tris-HCL (pH6.8) 125mM 30% Glycerol 25% 7% SDS 10% 0.01% Bromophenol Blue 2.5 ml 2-Mercaptoethano per 50 ml final sample
Protein Loading Buffer Working Solution	Protein Loading Buffer Stock <b>900ul</b> 2-Mercaptoethano <b>60ul</b>
1x TBS-T (1000ml)	10 mM Tris pH7.4 <b>1.212g</b> 150mM NaCl <b>8.76</b> 0.1% Tween20 <b>1ml</b>

10x High Western Buffer (1L)	Glycine 192mM <b>30.28g</b>
	SDS 0.1% of the final amount 1g
	Tris Base <b>25mM 144g</b>
	Methanol 20% of the final amount <b>200ml</b>

Table 2.4 Antibodies used for western blot tests, the species in which they were raised and their dilution factors.

Antibody	Species	Dilution	Company	Catalogue number
Primary Antibodies				
GAPDH	Rabbit	1:5000	Cell Signalling	2118
TGF- $\beta$	Rabbit	1:1000	Cell Signalling	3711
Lysyl-oxidase	Rabbit	1:1000	Cell Signalling	58135
Collagen 1 $\alpha$ 1	Rabbit	1:1000	Cell Signalling	39952
Collagen 3 $\alpha$ 1	Rabbit	1:1000	Cell Signalling	66887
Fibronectin	Rabbit	1:1000	Cell Signalling	F3648
Secondary Antibodies				
800 anti-rabbit	Goat	1:10000	Thermo Fisher Scientific, DyLight 680/800 conjugate anti-rabbit, anti-mouse	35571

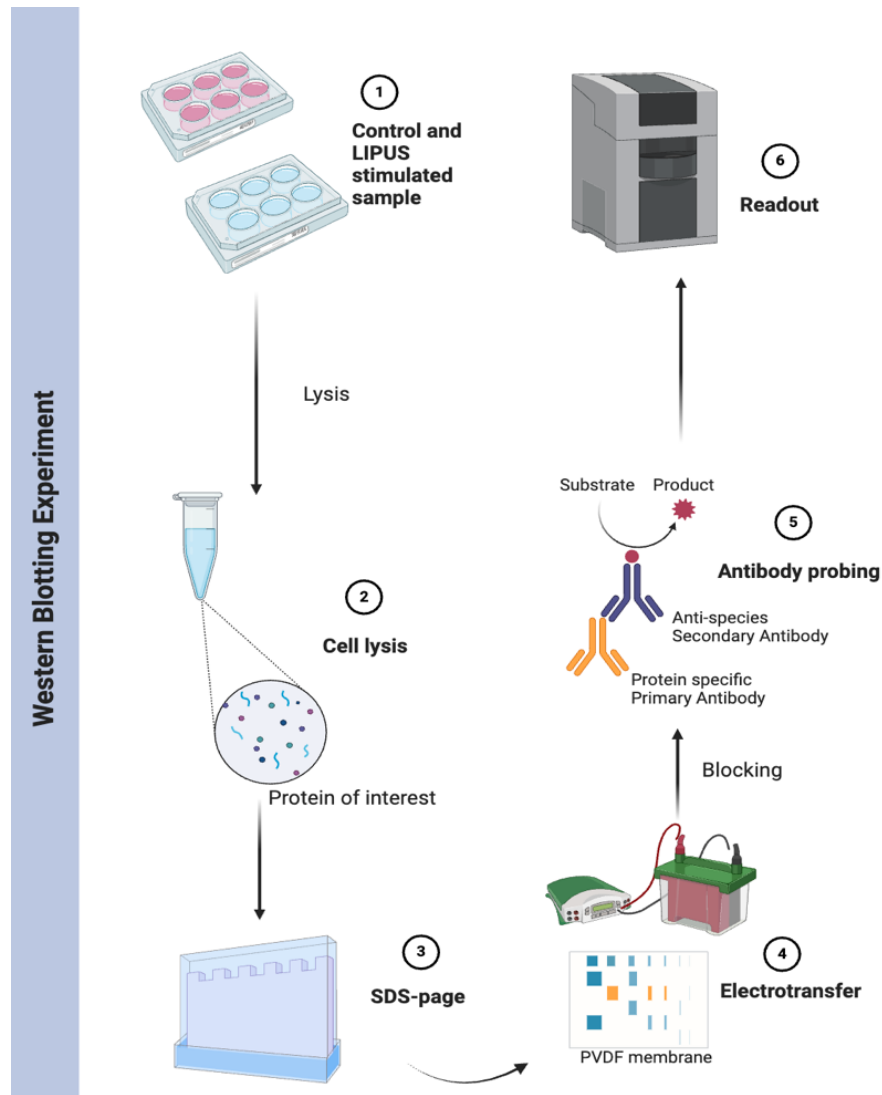


Figure 2.6 The Western blot process (Image created using Biorender).

## 2.8 Mammalian cell transfection for RNAi

Cells were cultured in T-25 flasks until they reached 80-90% confluency before adding RNA oligonucleotides to knockdown the protein expression of interest. For each transfection, a non-targeting small interfering RNA (siRNA) used as a control for knockdown. For every knockdown experiment, Oligos and Dharm2 were Diluted in optimem as follows: two tubes, the first tube contains 300 ul Optimem + 8 ul Oligo (2 nmol dissolved in 100ul 5xRNAi buffer diluted in RNase-free sterile water) and the other contains 300 ul Optimem + 4 ul Dharm2 and were left to incubate for 5 minutes at room temperature. Subsequently, the two tubes were

mixed and incubated for an additional 20 minutes at room temperature. This mixture was then transferred to the T-25 flasks filled with 2.5 ml of fresh culture medium and left to grow overnight. The following day, cells were splitted and left until reaching the same confluency to carry out a second round of transfection 24 hours after splitting. Upon completion of the second round of transfection, cells were utilised for experiments, and the efficacy of knockdown was evaluated through western blotting (Table 2.5 showing siRNA transfection reagents).

Table 2.5 siRNA transfection reagents.

Reagents	Suppliers	Cat number
ON-TARGET plus Human COL3A1 siRNA (knockdown oligo)	Dharmacon	J-011012-07
Opti-MEM® Reduced serum medium	Gibco by Life Technologies	51985026
DharmaFECT 2 Transfection reagent	Dharmacon	T-2002-03
5X siRNA buffer	Dharmacon	-

## 2.9 Immunofluorescence

To prepare coverslips for cell culture, coverslips are placed in a small bottle and covered with MilliQ water. The bottle was boiled while loosely covered on a heating block for approximately 5 minutes or until boiling for cleansing. This boiling process is repeated two more times. The coverslips were then stored in the boiled MilliQ water and autoclaved before use.

For seeding and culturing cells, coverslips were placed into a 24-well plate in a sterile culture hood. Next, cells are trypsinised, pelleted at 500 x g for 5 minutes, and resuspended in growth medium. cells are seeded at a concentration of  $6 \times 10^4$  cells/ml, using 0.5 ml per well in a 24-well plate or 2 ml per well if coverslips placed in a 6-well plate.

To preserve the ECM, cells were fixed using paraformaldehyde to minimize loss of extracellular components. While standard washes may remove soluble ECM, our protocol aimed to retain structural ECM proteins. For fixation, the medium was aspirated from the wells and washed with PBS-. Then, adding 200  $\mu$ l of 4% paraformaldehyde to each well to fix the cells for 12 minutes. Next, cells were washed three times with PBS-, then quenched with 400  $\mu$ l of 0.1M Glycine in PBS-. After another three washes with PBS-, permeabilisation the cells with 200  $\mu$ l of 0.5% Triton in PBS- per well. Afterward, cells were washed again three times with PBS- before adding 500  $\mu$ l of 3% Bovine Serum Albumin (BSA) per well and left for blocking at 4°C overnight.

For staining, the blocking solution was aspirated, and the primary antibody was diluted in 3% BSA in PBS-. A 50  $\mu$ l drop of the diluted antibody was placed onto parafilm, and the coverslip was placed onto the drop while cells side facing down to be stain. Coverslips were left 1 hour at room temperature in a humidity chamber, followed by three washes with PBS-. Then, the secondary antibody and phalloidin (CY2 anti-rabbit at 1/200 in 3% BSA, PBS- and TRITC-phalloidin at 1/200 in 3% BSA, PBS-) were applied in similar way as the primary antibody and coverslips were then incubated for 30 minutes at room temperature in the dark, followed by three washes with PBS- and two washes with MilliQ water.

To mount the coverslips, they were covered with MilliQ water during the mounting process, then, 6  $\mu$ l of Prolong anti-fade with DAPI was placed on a slide, and the coverslip with cells facing down was positioned onto the drop. After two hours, the coverslips were imaged using

the Nikon A1 Confocal Microscope, equipped with an inverted microscope system and an Oko-labs environmental control chamber for live-cell imaging. Imaging was performed with CFI Plan Fluor 10x (NA 0.3) and CFI Plan Fluor 20x MI (NA 0.75) objectives. The system is equipped with 405 nm, 488 nm, 561 nm, and 640 nm laser lines, along with bandpass filters for DAPI (450/25), FITC (525/25), AF568 (595/25), and Cy5. The imaging plane was located using the eyepiece and images were acquired at 0.160 frames per second with a frame time of 6.2 seconds. Data acquisition was carried out using Nikon Elements software. All images were acquired blindly under identical settings to ensure consistency and minimize bias across samples. ImageJ (Fiji) was used for analysing the images using intensity calculation to measure the collagen staining for the control and LIPUS stimulated samples. Also, using The Workflow Of Matrix BioLogY Informatics (TWOMBLI) macro was used to quantify matrix patterns in an ECM image by deriving a range of metrics (Wershof et al., 2021). To assess matrix curvature, Ridge Detection was first applied to all images in the test set, generating binary masks that highlighted the ECM fibres. The Straight-Line tool in FIJI was then used to measure the typical lengths of fibre curves from these masks, while deliberately avoiding regions with branching points or sharp directional changes. Due to the inherent subjectivity in selecting an appropriate window size for curvature analysis, a range of window sizes (40, 50, and 60) was tested. Smaller window sizes allowed for the detection of local waviness within individual fibres, whereas larger windows captured curvature trends on a broader, more global scale. Before commencing the matrix alignment analysis with TWOMBLI, it is necessary to firstly select a series of steps and choose parameters that will be used to generate the matrix mask to be ready for the analysis such as contrast saturation, line width and curvature window (Table 2.6).

Table 2.6 TWOMBLI Parameters.

Step	Function
Contrast Saturation	Represents the saturation level for a given percentage of pixels.
Line Width	Ridge detection creates a mask that identifies matrix fibre bundles with a width in this range
Curvature Window	Measures the change in angle over matrix fibre specified length.

## 2.10 Migration Assay

For the plate coating preparation, the following steps were undertaken: The wells were washed with PBS, then incubated with 0.2% sterile gelatine for an hour at 37°C. Then, the plates were incubated with growth medium for 30 minutes, washed again three times with PBS, and then either used immediately or stored at 4°C. If stored, they will need re-incubate with medium before seeding cells.

Plating cells involves detaching cells with trypsin and resuspending in 10 ml of growth medium to count using a haemocytometer. Cells were plated at ( $10^5$  / ml, plate 2 ml per well) followed by an overnight culture at 37°C with 5% CO<sub>2</sub>. Medium was then changed to one supplemented with 50 µg/ml ascorbic acid, which was renewed every two days until denudation to have a fibronectin-rich matrix and to stabilise the matrix, the medium was changed every other day for nine days culturing. Denuding cells required aspirating the medium and washing with PBS before adding 1.5ml pre-warmed extraction buffer (20 mM NH<sub>4</sub>OH, 0.5% Triton X-100 in PBS). Cells were lysed for about 2 min or until no intact cells visible in the microscope. The matrix was treated gently from this stage on as it is delicate. Then the buffer was aspirated, and

the wells were gently washed twice with PBS containing calcium and magnesium. DNA residue was digested with 10 ug/ml DNase I (Roche) and incubated for 30 minutes 37C, 5% CO<sub>2</sub>. Next, the DNase I aspirated, and wells were washed twice more with PBS containing calcium and magnesium. The matrix is then prepared for cell seeding or stored at 4°C.

Prior to plating cells on the prepared matrix, it was washed twice with growth medium. Cells were then plated at the required density ( $5 \times 10^3$  / ml) and allowed approximately four hours to spread and begin migration on the cell-derived matrix. Treated and controlled plates will then be leaved for 16 hours for imaging. The resultant images will show how each cell migrate through time. Images is then opened using FIJI application > Plugins > Tracking > Manual Tracking and each cell were tracked and analysed. Figure 2.7 illustrate the summarised steps for the migration assay.



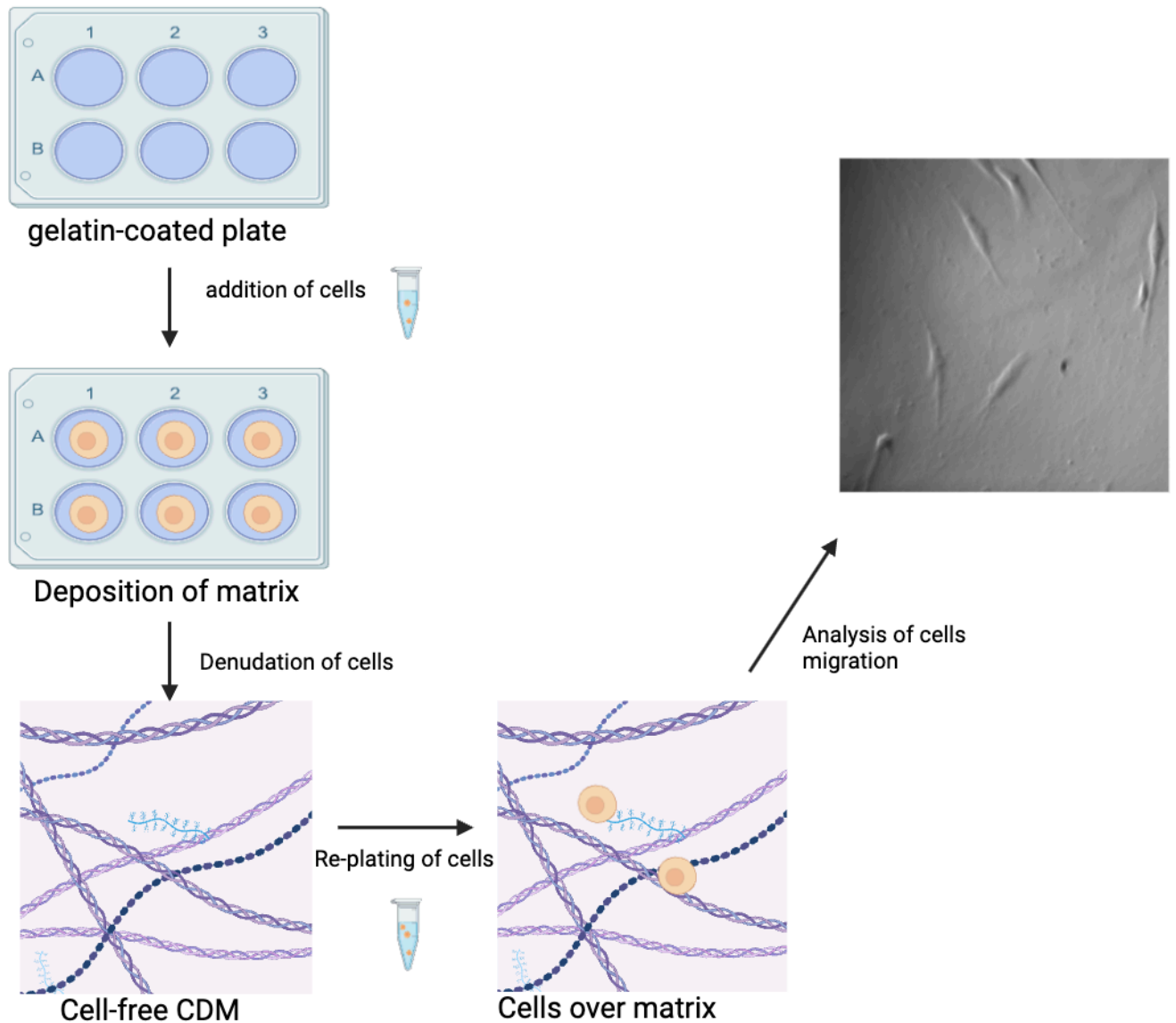


Figure 2.7 A summary of the protocol for the generation of CDMs (image created using Biorender).

## 2.11 Traction Force Microscopy

TFM elastic substrates, like the commonly used polyacrylamide (PAA) hydrogels, can be used with a wide range of elasticities, from less than 1 kPa to several hundred kPa. This flexibility allows TFM measurements of the beads movement to mimic a variety of cell surface stiffnesses and tissue environments, accommodating diverse experimental conditions (Sabass et al., 2008). Typically, the beads embedded inside PAA hydrogels positions are captured with the cell attached to the surface and then again after the cell is detached, often using trypsin (a serine

protease that degrades cell adhesions). Comparing these two images allows for the determination of the displacement field (Lekka et al., 2021). Living cells do not grow directly on PAA surfaces; therefore, ECM proteins must be covalently crosslinked to the PAA surface to create favourable conditions for cell growth. The selection of ECM proteins that can be attached is virtually limitless, with fibronectin being the most commonly used, followed by collagen, laminin, and other proteins in experiments with individual cells (Lekka et al., 2021). EasyCoat hydrogel dishes (35 mm, 20 mm glass bottom) embedded with 1  $\mu\text{m}$  red fluorescent beads, provided by Softwell®, were used in this experiment. These dishes were pre-prepared for fibronectin coating. To coat the dishes, a fibronectin solution (10  $\mu\text{g/mL}$  in PBS-) was prepared, and 200  $\mu\text{L}$  of the solution was added to each dish. The dishes were then incubated at room temperature for 1 hour. After incubation, the excess fibronectin solution was aspirated, and the dishes were gently washed with sterile PBS to remove any unbound fibronectin.

TIF cells were seeded at a density of 5,000 cells per mL and incubated in culture medium for 2 hours before being either treated with LIPUS or left as sham-treated controls (Table 2.7). The cells were then grown for 5 days before being taken to the microscope for imaging.

On the fifth day, following the final LIPUS stimulation, the culture medium was aspirated, and the dishes were washed with PBS. The samples were placed in an environmental control chamber and imaged using the Nikon Wide-field Live-Cell system equipped with a Plan Apo 10x (NA 0.45) lens. This system includes an Inverted Ti Eclipse microscope, an Andor Zyla sCMOS camera (offering a resolution of 2560 x 2160 pixels with a 6.5  $\mu\text{m}$  pixel size), and NIS-Elements software for data acquisition. To locate the cells, the eyepiece was used, and imaging was performed using Brightfield and mCherry channels with a 5 ms exposure time and 16-bit (no binning). The initial imaging was performed, immediately after 100  $\mu\text{L}$  of trypsin was added and imaging continued for an additional 10 minutes. Upon completion of imaging, the collected images were analysed using Fiji using two macros for analysis, Particle

Image Velocimetry (PIV) (Tsang et al., 2012) and Fourier transform traction cytometry (FTTC) (Sabass et al., 2008). Bead displacements were measured using PIV, a technique implemented through a plugin in ImageJ that calculate the displacement of embedded fluorescent beads before and after cellular deformation. These displacement maps were then used as input for the FTTC plugin, which converts the displacement field into a traction stress map representing the forces exerted by cells on the substrate. For the FTTC analysis, a Poisson's ratio of 0.5 and a substrate stiffness of 8 kPa were used as parameters to model the mechanical properties of the gel.

Table 2.7 Traction Force Microscopy procedure timeline.

Day1	Day2	Day3	Day4	Day5
<ul style="list-style-type: none"> <li>• TIF cells Seeding</li> <li>• LIPUS treatment (20 minutes)</li> </ul>	<ul style="list-style-type: none"> <li>• LIPUS treatment (20 minutes)</li> </ul>	<ul style="list-style-type: none"> <li>• LIPUS treatment (20 minutes).</li> </ul>	<ul style="list-style-type: none"> <li>• LIPUS treatment (20 minutes).</li> </ul>	<ul style="list-style-type: none"> <li>• LIPUS treatment (20 minutes).</li> <li>• Imaging</li> </ul>

## 2.12 Statistical Analysis

Statistical analyses were performed using GraphPad Prism software (version 9, GraphPad Software, Inc., San Diego, CA, USA). For normally distributed data, comparisons between two groups were performed using the unpaired Student's t-test.

Throughout the thesis, all figure legends provide detailed statistical information, specifying whether data are presented as mean or median values, along with standard deviation (SD) or standard error of the mean (SEM), as appropriate. Each figure legend explicitly states the statistical tests applied, the number of biological replicates and the number of technical replicates per biological replicate. Technical replicates are clearly defined in each context.

# Chapter 3

Identification of matrix proteins involved  
in wound healing by data mining

## Chapter 3 Identification of matrix proteins involved in wound healing by data mining

### 3.1 Introduction to the role of Extracellular Matrix in wound healing

The ECM is a component of all mammalian tissues, offering a bioactive environment that regulates cell behaviour through chemical and mechanical signals. With the growth of data from numerous studies, it became evident that the components of the ECM are the primary elements of the cellular microenvironment and actively participate in wound healing by affecting cell behavior, including proliferation, adhesion, and migration (Potekae et al., 2021).

When a wound occurs, various mechanisms immediately activate to prevent foreign bodies from penetrating the skin and causing infections. These mechanisms are broadly divided into four phases: first, the hemostasis phase, where a fibrin clot forms; second, the inflammatory phase, which eliminates invading microbes; third, the proliferative phase, where a new ECM is synthesized; and finally, the remodeling phase, which restores the tissue's function and integrity to their original state (Tsirogianni et al., 2006). The phased nature of the healing process is crucial, as it demonstrates that skin does not only exist in 'wounded' and 'unwounded' states. Instead, cellular signalling, behaviour, and protein expression vary throughout the healing timeline. Specific proteins may be upregulated in some phases and downregulated in others. Recognising these temporal variations is essential for accurately interpreting wound bed analyses and potentially the design of therapeutic approaches. A treatment that activates a particular signal may advance one phase of healing while hindering another. Therefore, it is vital to understand the dynamic changes in wounded skin and how they vary over time. Furthermore, the migration of inflammatory cells, chemokines, cytokines, matrix molecules, and nutrients to the wound site is essential, given the increased metabolic demands during healing (Han and Ceilly, 2017). Cutaneous wound healing reflects many biological processes seen in other tissues and provides an excellent model for studying the

stages of tissue repair. These stages are finely regulated by signalling molecules produced by a wide variety of cells within the ECM (Gonzalez et al., 2016). The interplay between these dynamic cellular and molecular changes highlights the complexity of wound healing and features the importance of understanding these processes to optimise therapeutic approaches.

The aim of this chapter is to scrutinise the existing literature to investigate the variations in protein expression within the ECM at different stages of wound healing to determine which protein is mostly involved in healing process and therefore might be susceptible to manipulation by LIPUS. This investigation was conducted through several stage. Firstly, by analysis of experimental data from Nuutile et al. (2012), to identify the changes in the expression levels of various ECM proteins during the different phases of wound healing, including the inflammatory, proliferative, and remodelling stages. This analysis was crucial to determine specific proteins that exhibited significant changes in their expression patterns and to understand their roles in the healing process. Secondly, a careful review of existing literature was performed to gather insights from previous studies on ECM protein dynamics during wound healing. This review helped to validate our findings and provided a broader context for the observed protein expression changes. By combining data analysis and literature review, we aimed to identify candidate proteins whose expression was significantly changed during wound healing through different stages of wound healing. This provided a deeper understanding of the regulatory roles of these proteins to play in wound repair and how they contributed to the structural and functional restoration of the ECM.

## 3.2 Results

### 3.2.1 Matrix metalloproteinases

Candidates were sought, initially, by interrogation of published data sets. A genome-wide microarray of 25 biopsies for split-thickness skin graft (SSG) was done by Nuutile et al. (2012). I have analysed microarray data for groups of related proteins and trends in changes over time

that could be used to select candidate proteins that might be regulated by LIPUS. The process of selecting candidate proteins was done using the Database for Annotation, Visualization, and Integrated Discovery (DAVID) v 6.8. This tool provides a comprehensive functional annotation to understand the biological meaning of a large list of genes. DAVID was used to select genes that are annotated as being part of the ECM. The filtered genes were sorted based on fold change (>2-fold change) to identify the changes between conditions. The microarray data from Nuutila et al. (2012) presented in this thesis include genes with expression changes that were statistically significant ( $p < 0.05$ ) in the original published study from which the data were derived.

The microarray data were assigned biopsies for four phases: healthy intact skin (Intact), immediately after SSG to represent acute wounds (Acute), on the third Postoperative Day (3POD) representing the inflammatory phase and on the seventh Postoperative Day (7POD) to represent the remodelling phase (Figure 3.1).

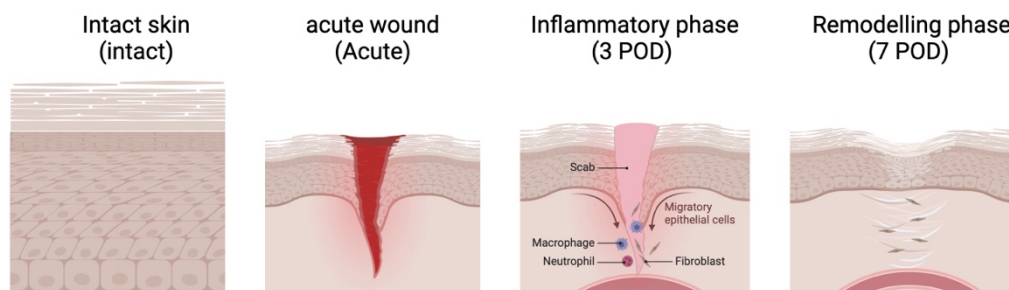


Figure 3.1 the different biopsy stages.

A. illustration mimicking each biopsy phase from Nuutile et al. (2012) : Intact = intact skin, Acute = acute wound, 3POD: the inflammatory phase, and 7POD: the remodelling phase. B. Histological sections of the phases (Image Created in BioRender.com).

MMP1, MMP3 and MMP10 were among the proteins with the highest fold change upregulated and downregulated in the acute, 3 POD and 7 POD phases, compared to intact skin (*Table 3.1* and

Table 3.2).

Table 3.1 List of ECM proteins in order from highest to lowest fold change for up-regulation in different phases of wound healing.

3 POD vs. Intact skin (Up)		7 POD vs. Intact skin (UP)		3 POD vs. Acute wound (UP)		7 POD vs. Acute wound (UP)		7 POD vs. 3POD (UP)	
Gene	Fold change	Gene	Fold change	Gene	Fold change	Gene	Fold change	Gene	Fold change
MMP1	912.8	MMP1	593.9	MMP1	892.2	MMP1	580.6	COL10A1	6.9
MMP3	84.6	MMP10	36.6	MMP10	45.8	MMP10	33.2	MMP13	6.1
MMP10	50.4	MMP3	29.2	S100A9	26.3	MMP12	19.3	POSTN	4
MMP12	9.1	MMP12	25.6	SERPINE 1	10.9	MMP3	14.3	WNT5A	3.9
LAMC2	8.3	COL10A 1	9.1	SERPINE 2	7.7	RPTN	12.3	COL11A1	3.3
TIMP1	7.7	MMP13	8.5	TFPI2	6.2	MMP13	9.6	COL5A1	3.2
SERPINA 1	7.4	COL4A1	7.1	CYR61	3.9	COL10A1	7.4	HMCN1	2.9
COL4A1	4.4	NID2	6.1	COL6A5	3.7	COL4A1	4.9	MMP12	2.8
TNC	4.3	COL11A 1	5.3	THBS1	3.7	WNT5A	4.3	LUM	2.5
PXDN	3.7	PXDN	5.3	SLPI	3.5	WNT4	3.7	NID2	2.5
COL4A2	3.1	SERPIN A1	4.7	COL4A1	3	NID2	3.5	COL5A3	2.4
VCAN	3.1	WNT5A	4.2	TNC	2.8	LAMC2	2.9	ASPN	2.3
LAMA1	3	COL5A2	4.1	F3	2.7	PXDN	2.9	SPON2	2.3
LAMB3	3	COL4A2	3.9	PLSCR1	2.6	SERPINA 1	2.9	OMD	2.2
COL15A 1	2.8	VCAN	3.7	CFP	2.5	COL5A1	2.8	DPT	2.1
SPON1	2.8	ADAMT S1	3.5	TGFB1	2.5	COL5A2	2.8		



3 POD vs. Intact skin (Up)		7 POD vs. Intact skin (UP)		3 POD vs. Acute wound (UP)		7 POD vs. Acute wound (UP)		7 POD vs. 3POD (UP)	
Gene	Fold change	Gene	Fold change	Gene	Fold change	Gene	Fold change	Gene	Fold change
ADAMT S5	2.7	COL5A1	3.5	MMP19	2.4	COL5A3	2.8		
MMP19	2.6	COL5A3	3.3	CCT2	2.3	ADAMTS 1	2.7		
ADAMT S3	2.5	ADAMT S12	3.1	LAMA1	2.3	POSTN	2.7		
TGFB1	2.5	TNC	3	SPON1	2.3	VCAN	2.7		
EMILIN2	2.5	COL6A3	2.9	VCAN	2.3	TGFB1	2.6		
COL15A 1	2.5	COL15A 1	2.9	CALR	2.1	ADAMTS 12	2.4		
NID2	2.4	LAMC2	2.7	EMILIN2	2.1	COL4A2	2.3		
COL5A2	2.3	ADAMT S2	2.6	EIF4A1	2	COL11A1	2.2		
COL6A3	2.2	TGFB1	2.6	PXDN	2	COL17A1	2.2		
ADAMT S9	2.1	EMILIN1	2.5			COL6A5	2.1		
EMILIN1	2.1	LAMA1	2.5			LAD1	2.1		
ADAMT S12	2	NID1	2.5			LAMB1	2.1		
MMP25	2	LAMB1	2.4						
NID1	2	LUM	2.4						
		ADAMT S3	2.3						
		HMCN1	2.3						
		SPON1	2.3						
		ADAMT S5	2.2						
		ANGPTL 4	2.2						
		FN1	2.2						
		BGN	2.1						
		EMILIN2	2						
		FBN2	2						
		LGALS1	2						

Table 3.2 List of ECM proteins in order from highest to lowest fold change for down-regulation in different phases of wound healing.

3 POD vs. Intact skin (Down)		7 POD vs. Intact skin (Down)		7 POD vs. Acute wound (down)		3 POD vs. Acute wound (down)		7 POD vs. 3POD (DOWN)	
Gene	Fold change	Gene	Fold change	Gene	Fold change	Gene	Fold change	Gene	Fold change
KRT1	52.2	OMD	6.7	OMD	12.1	OMD	26.4	MMP3	2.9
OGN	8.6	OGN	5.1	OGN	9.5	OGN	16.2	CTSL1	2.5
CILP	7.5	CILP	4.7	CILP	8.2	CILP	13.1	COCH	2.1
DSG1	5.5	MAMDC2	4.3	MAMDC2	6.3	ECM2	6	LAMC2	3.0
DCD	5.4	WNT3	4.2	VIT	4.5	ASPN	5.5	SEPRINE2	3.0
ASPN	4.2	LAMB4	3.4	COMP	4.4	MFAP4	4.7	CFP	2.2
POSTN	3.6	WNT16	3.1	MYOC	4.3	VIT	4.4	PTGER2	2.3
SBSN	3.6	WNT2B	3	TNN	4.2	TNN	4.3		
MFAP4	2.9	MYOC	2.9	ECM2	3.6	MYOC	4.2		
MYOC	2.8	COMP	2.7	TIMP3	3.4	DPT	3.3		
WNT2	2.7	VIT	2.7	MFAP4	3.3	MFAP5	3.2		
FGFR2	2.6	WNT4	2.6	PRELP	3.2	TIMP3	3.1		
COL21A1	2.5	CHL1	2.5	COL28A1	3	CCDC80	3		
JUP	2.5	SFTPD	2.4	FBLN1	2.8	FBLN2	2.9		
NOV	2.5	COL28A1	2.3	THBS4	2.7	COMP	2.8		
DPT	2.4	ECM2	2.3	EMILIN3	2.6	COL28A1	2.7		
RPS15A	2.4	MMP28	2.3	TFF3	2.6	FBLN1	2.7		
FGFBP3	2.3	COL9A3	2.2	FBLN5	2.5	NTN4	2.6		
MGP	2.3	PRELP	2.2	ASPN	2.4	PRELP	2.6		
APOE	2.2	BMP4	2.1	BMP4	2.4	SPON2	2.6		
CASP14	2.2	MFAP4	2.1	NTN4	2.4	FBLN5	2.4		
HSPB1	2.2	TFF3	2	SPOCK1	2.3	LAMB2	2.4		
MMP27	2.2			CCDC80	2.3	SPOCK1	2.3		
BMP7	2.1			COL8A2	2.3	EMILIN3	2.3		
SFRP2	2.1			MFAP5	2.3	LAMA2	2.3		
DSP	2			FBLN2	2.2	SPARC	2.3		
MATN2	2			LAMB2	2.2	THBS4	2.3		

		COCH	2.1	COL21A1	2.2	
		LTBP4	2.1	LOX	2.1	
		COL9A3	2	COL8A2	2	
				HMCN1	2	

MMP1 shows a significant upregulation during the early inflammatory phase, with a fold change of 912.8 at 3 POD compared to intact skin. Its expression decreases to 593.9 by 7 POD compared to intact, though it remains elevated, indicating MMP1's involvement in both ECM breakdown and modulation of inflammation throughout the wound healing process. This pattern suggests that MMP1 plays a critical role in facilitating the transition from inflammation to tissue repair, particularly in the early stages of healing.

MMP3 also exhibits increased activity early in wound healing, with a fold change of 84.6 at 3 POD compared to intact, indicating its role in the inflammatory response. However, by 7 POD, its expression drops to 29.2, highlighting MMP3's primary involvement in the early stages of healing rather than in tissue remodelling. Interestingly, no significant upregulation of MMP3 is observed between 3 POD and acute wounds, suggesting a relatively stable expression during inflammation.

MMP10 follows a similar trend, with moderate upregulation during the inflammatory phase. At 3 POD, it shows a fold change of 50.4 compared to intact, which decreases to 36.6 by 7 POD compared to intact. Like MMP3, MMP10 is more active in the early stages of wound repair, primarily contributing to ECM regulation and tissue restructuring.

Overall, MMP1 and MMP10 show significant changes from acute to 3 POD, with delayed responses compared to MMP3. This highlights their critical roles in both inflammation and remodelling phases of wound healing. MMP3 peaks earlier, playing a vital role during the

initial inflammatory phase, while MMP1 and MMP10 have sustained activity into the remodelling phase.

### 3.2.2 Extracellular Matrix

#### 3.2.2.1 *Collagens*

The data from Table 1 reveals that many collagens were reported in this microarray data (table1), including COL4A1, COL4A2, COL5A1, COL5A2, COL6A3, COL10A1, and COL11A1. They were significantly involved in the upregulation across different phases of wound healing. This emphasises the critical role of collagen in extracellular matrix remodelling and tissue repair during the wound healing process. Specifically, COL 4, 5 and 6 have shown upregulated the fold change. The COL4 family, particularly COL4A1 and COL4A2, plays a critical role in both the early inflammatory phase and the later remodelling phase of wound healing. Their increasing expression at 7 POD compared to intact highlights their importance in the stabilisation and restructuring of the basement membrane during tissue repair. The persistent upregulation of COL5A1, COL5A2, and COL5A3 throughout the wound healing process highlights their critical roles in collagen fibril formation and ECM stabilisation. These collagens contribute to both the early inflammatory phase and later stages of tissue repair and remodelling. The COL6 family, particularly COL6A5, is actively involved in the early stages of wound healing and continues to play a significant role during the remodeling phase. This consistent upregulation illustrates the importance of COL6 in maintaining the structural integrity of the ECM and promoting tissue repair.

The data reveals that collagen expression, especially for COL4, COL5, and COL6, exhibits a more pronounced fold increase at 7 POD compared to intact skin, when contrasted with the expression at 3 POD. This pattern stands in contrast to the behavior of MMPs, which show peak activity in the early stages of wound healing and experience a decline by 7 POD. This indicates that while both collagens and MMPs are activated quickly in response to injury,

collagen expression continues to increase and plays a constant role throughout the healing process, whereas MMPs are shown to be involved in early, transient events.

#### *3.2.2.2 Transforming growth factor-beta*

TGFB1 consistent upregulation (*Table 3.1*) throughout the healing process suggests that it is involved in modulating inflammatory responses, promoting ECM synthesis, and driving the transition from inflammation to tissue regeneration. TGFB1's presence in the later stages also indicates its role in wound closure.

#### *3.2.2.3 Lysyl Oxidase*

In a study done by Lambert et al., (2001) where they used human dermal fibroblasts, a model of mechanical tension release which was achieved by disrupting the cytoskeleton or through integrin-mediated stress reduction, showed a decrease in mRNA levels for LOX, procollagen types I and III, and N- and C-procollagenases. This suggests that mechanical tension regulates ECM stiffness by coordinating the expression of its structural components and the enzymes involved in their processing and stabilisation. This aligns to what is reported in (*table1*), where decrease in LOX expression observed in the comparison of 3 POD (inflammatory phase) to acute wounds. This suggests that LOX plays a mechanosensitive part in wound healing, responding to changes in tissue tension by modulating ECM stiffness through crosslinking collagen fibres. Both the Lambert et al., (2001) study and the wound healing data by Nuutila et al. (2012), demonstrate that mechanical tension influences LOX expression, which, in turn, regulates the stabilisation and remodelling of the extracellular matrix.

#### *3.2.2.4 Fibronectin*

Unlike collagen, which exhibits progressively increasing expression throughout the healing process, fibronectin emerges as a crucial ECM component that is predominantly induced later, particularly at 7 POD. This delayed and substantial upregulation of fibronectin at 7 POD, in

contrast to collagens, emphasises its pivotal role as a late-stage matrix element in the healing process. The timing of its expression suggests that fibronectin could be a promising therapeutic target for interventions designed to enhance tissue regeneration during the remodeling phase

### 3.2.2.5 Time-course visualisation of ECM-related gene expression

Figure 3.2 presents line graphs showing expression over time for MMPs, collagens, and TGFB1. These plots highlight the different temporal patterns of gene activity: MMPs peak early and decline, while collagens and TGFB1 maintain or increase their expression during later healing phases. To reconstructs relative gene expression over time, intact skin was set as the reference baseline (value = 1). The expression level for the acute wound phase was calculated by dividing (the fold-change of 3 POD vs. intact) by (the fold-change of 3 POD vs. acute). The 3 POD value was taken directly from the fold-change versus intact, while the expression at 7 POD was calculated by multiplying the acute wound value by the fold-change of 7 POD versus acute. This approach enabled the derivation of continuous expression profiles across the four key stages: intact, acute, 3 POD, and 7 POD. An example of how the calculation were done are in Table 3.3.

Table 3.3 Relative expression levels at each time point (Intact, Acute, 3 POD, and 7 POD) were calculated using fold-change values from pairwise comparisons.

Time point	Fold-change	How we it was calculated
Intact	1.0	Baseline
Acute wound	0.96	2.5/2.6 (3d vs intact / 3d vs acute)
3 days	2.5	Directly from the table
7 days	2.5	0.96 * 2.6 (Acute wounds * 7 d vs acute)

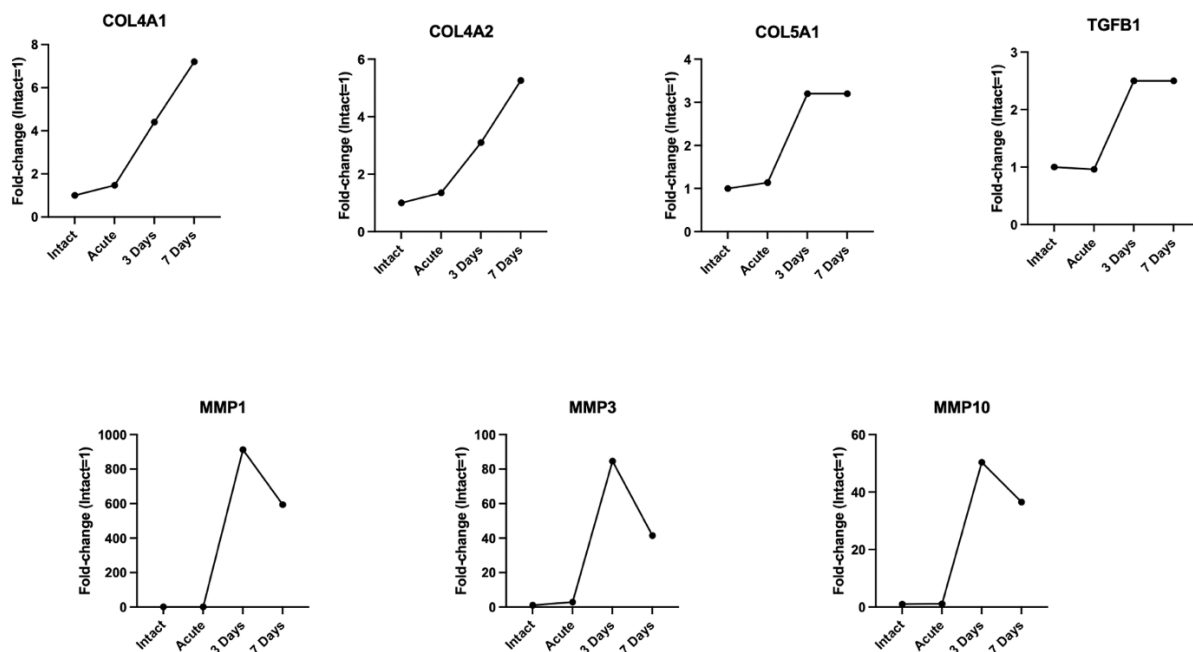


Figure 3.2 Time-course expression of key ECM-related genes during wound healing.

### 3.3 Discussion

#### 3.3.1 Why Collagens as a Target for Ultrasound Therapy But not MMPs?

MMPs and related enzymes such as astacins, serralysins, reprotlysins, and adamalysins (ADAMs) were thought to break down parts of the ECM and basement membrane and are primarily involved in tissue remodelling and maintenance of the ECM (Page-McCaw et al., 2007). MMPs also play a role in the release or activation of chemokines. This involvement extends to physiological processes such as innate and adaptive immunity, inflammation, angiogenesis, bone remodelling, and neurite growth (Löffek et al., 2011). For instance, (*Table 3.1*) illustrates that C-X-C motif chemokine ligand 5 (CXCL5) exhibited a significant increase in expression at 3 POD, showing a 47-fold upregulation compared to intact skin. Similarly, CXCL1 was also notably upregulated at 3 POD, with a 27.3-fold change. By 7 POD, CXCL5 remained elevated but at a reduced level, showing a 13.6-fold increase compared to intact skin, while CXCL1 maintained its elevated expression, with a 25.1-fold upregulation at this time point.

In skin, the basement membrane contains a variety of ECM components that help keratinocytes physically attach to it. Main components of the basement membrane include collagen types-4, 7, 17, laminin-5, -6, and -10, nidogen, and fibronectin (Almine et al., 2012; McMillan et al., 2003). The skin's structural integrity is maintained by various components of the ECM like collagens, fibronectin, and elastin. Specifically, the dermis tensile strength and elasticity are determined by the properties of its ECM, which includes type I and III collagen fibrils, microfibrils, and elastic fibers, all surrounded by a proteoglycan substance (Krieg et al., 2011). During fetal development, the ECM composition differs with higher collagen type III relative to collagen type I and increased levels of GAGs, such as hyaluronic acid (Almine et al., 2012; Larson et al., 2010).

For achieving this project aims and objectives, the choice to focus on ECM components rather than MMPs was guided by the different expression patterns and roles these molecules play throughout the wound healing process. MMPs, such as MMP1, MMP3, and MMP10, exhibit a high fold change early in wound healing, especially in the inflammatory phase, but their expression declines significantly by the time where the wound enters the remodeling phase. While MMPs are critical in the initial breakdown of damaged tissue and ECM reorganisation, their activity is transient. This transient nature makes them not the ideal targets for therapeutic interventions, such as LIPUS therapy, which is typically used later in the healing process. Therefore, although MMPs play important early roles, their diminished activity in the later stages limits their relevance as key targets for sustained healing therapies. In contrast, the ECM components, particularly collagens, show a more sustained and increasing expression as the wound progresses from inflammation to remodeling. Collagens such as COL4, COL5, and COL6 exhibit higher fold changes at 7 POD than at 3 POD when compared to intact, indicating that their expression continues to rise throughout the healing process. This prolonged activity makes them more relevant candidates for therapies aimed at promoting tissue repair over a



longer period. Collagens are integral to the structural integrity of the ECM and play a crucial role in tissue regeneration and remodeling, making them ideal targets for US therapy, which is applied during the later stages of wound healing.

Given our objective to study the effects of LIPUS on skin, investigating collagen types provides an excellent starting point. Our initial focus included COL4, COL5, and COL6 since there where a significant change as observed from Nuuttila et al. (2012) study (table 1).

Collagen types 1–3 are predominantly found in elastic soft tissues like the dermis and blood vessels, playing essential roles in tissue structure and function. In healthy dermal tissue, approximately 80% of the collagen is type 1, providing tensile strength, while about 20% is type 3, which offers flexibility and support. However, during the formation of acute wound granulation tissue, the proportion of type 3 collagen dramatically increases to 30–40%, reflecting its role in the early stages of wound repair (Velnar et al., 2009). The delicate balance between type I and type III collagen is crucial for normal tissue repair, as an imbalance can lead to dysfunctional healing processes, such as pathological scarring or abnormal tissue remodelling (Slemp and Kirschner, 2006).

Given the significance of COL1 and COL3 in wound healing and ECM stability, their inclusion in this study, despite not being represented in the provided dataset, is based on their well-established functions. COL1 and COL3 are integral in providing structural support and strengthening tissue, especially in the later stages of healing when organised collagen fibres are necessary for proper wound closure and durability. Their roles are essential for examining how external stimuli, like LIPUS, influence matrix deposition, cross-linking, and collagen fibre organisation. Thus, the study's second aim, which focuses on understanding LIPUS's impact on matrix deposition, cross linking and organisation, directly ties to the critical functions of COL1 and COL3 in supporting the wound healing process.

### 3.3.2 The Importance of Fibronectin in Wound Healing

Fibronectin (FN) is a substantial glycoprotein that can be found in various tissue types and plays a crucial role in numerous cell-matrix interactions. FN binds to cell surfaces through integrins, which connects the FN outside the cell to the actin filaments inside the cell thereby forming fibrils (Kular et al., 2014). FN can be found in two forms: plasma-FN, which is synthesised in a soluble form by hepatocytes and released into the blood plasma, and cellular or tissue FN which is produced by various cells such as fibroblasts and keratinocytes (Lenselink, 2015).

FN is involved throughout all stages of wound healing. Plasma FN primarily functions in the initial phase, aiding in clot formation and the creation of a cell-ECM matrix. Platelets enable the integration of plasma-derived FN into fibrillar matrices by increasing platelet binding sites. In contrast, cellular-derived FN plays a crucial role in the later stages of tissue remodeling through local FN assembly (Lenselink, 2015). Although FN is associated in health improvement, however, different studies have demonstrated adverse effect of excessive amount of FN such as in abnormal wound healing and fibrosis (Stoffels et al., 2013; Kubow et al., 2015). Therefore, it is Important to maintain the normal level of FN during the wound healing.

FN was included in the study due to its importance in ECM formation and re-epithelialisation. This observation positions fibronectin as a potential key matrix component that aligns with the timing of feasible LIPUS therapy application. The absence of fibronectin upregulation at 3 POD compared to its significant upregulation expression at 7 POD highlights its unique role in the later stages of wound healing, making it a promising candidate for therapeutic targeting. This finding justifies FN's importance as a key molecule in the study, suggesting that its later induction may be critical for supporting sustained wound repair, and thus, fibronectin becomes a prime focus for further investigation.

### 3.3.3 Lysyl Oxidase as a Cross Linker for Collagen

Lysyl oxidases (LOX) are pivotal in the maturation of collagen by oxidizing lysine or hydroxylysine to allysine residues (Hiebert et al., 2024). Following injury, the complicated and organised series of wound healing process is crucial for preserving integrity to the tissue's structure and function (Hiebert et al., 2024). An essential element of this mechanism involves the dynamic reformation of the ECM, including the fibrillar collagens' maturation and deposition, which create the main structural element of the ECM (Hiebert et al., 2024). Maintaining an appropriate balance between the formation and remodelling of collagen is critical for effective wound healing. Pathological conditions can arise from both insufficient and excessive collagen formation and maturation, leading to issues such as chronic non-healing wounds or hypertrophic scars, respectively (Xue and Jackson, 2015). Accurate control of LOX activity is crucial for the effective development of tissue repair during wound healing. Abnormal LOX activity has been linked to a range of conditions, such as fibrotic and malignant diseases (Hiebert et al., 2024; Cox et al., 2013).

From the data analysis the decrease in LOX expression on day 3 POD reflects its expression in an early stage in wound healing (inflammatory phase). This can be explained by that in the acute phase, wounds are likely subject to mechanical stress due to the contraction of surrounding tissues and the need for rapid ECM remodeling. As the wound progresses to 3 POD, some of this tension may be reduced as the early wound repair begins. This could explain why LOX expression drops in this stage — there is less mechanical stress, and thus less need for LOX-mediated crosslinking of collagen and elastin to increase ECM stiffness. The study by Lambert et al., (2001) indicates that a release of mechanical tension results in decreased expression of LOX and other ECM-related components. Also, Liu et al., (2016) demonstrated that chronic TNF- $\alpha$ -induced inflammation in lung diseases like asthma and fibrosis leads to copper deficiency, which downregulates LOX. This mirrors the trend observed with LOX in

Table 2, where at 3 POD (inflammatory phase) which is characterised by less mechanical tension, has lower LOX expression when compared to the acute wound phase which is characterised by higher mechanical tension. This, in addition to what has already mentioned earlier in the introduction chapter (in section 1.6.7) indicate the importance of LOX to be investigated by LIPUS.

### 3.3.4 Transforming Growth Factor-Beta: A Key Growth Factor Target for Ultrasound Therapy

The TGF- $\beta$  superfamily regulates cellular processes like proliferation, differentiation, adhesion, and collagen deposition (Gumucio et al., 2015). Also, has been demonstrated to be significant in various physiological and pathological processes, encompassing immune regulation, atherosclerosis, and the development of tumors (David and Massague, 2018). Mechanical stress and TGF- $\beta$  can induce myofibroblast formation, emphasizing fibroblasts' crucial role in wound healing. Various cell types and soluble factors also contribute to creating a conducive environment for proper wound healing (Almine et al., 2012). TGF- $\beta$  has been shown to elevate the levels of tissue inhibitor matrix metalloproteinase 1 (TIMP1),  $\alpha$ -SMA, collagen I - II, which facilitates the transition of fibroblasts to myofibroblasts and plays a key role in regulating ECM formation and remodeling during fibrosis (Ren et al., 2023).

TGF- $\beta$  is crucial in regulating various cellular responses throughout all three phases of wound healing. For example, in Inflammation phase which lasts about 2–4 days is marked by the recruitment of immune cells like neutrophils and macrophages to the injury site in response to chemotactic cytokines, including TGF- $\beta$  (Finnson et al., 2013; Wang et al., 2006). In response to TGF- $\beta$ , two important actions occur; firstly, monocytes infiltrate the wound site, and then differentiate into activated macrophages. The functions of these macrophages are to digest foreign particles and necrotic debris, releasing TGF- $\beta$  and other growth factors to promote capillary growth and start the formation of granulation tissue. Once the immune cells are

activated, TGF- $\beta$ 1-driven suppression can counteract and reduce the inflammatory response (Gonzalez-Junca et al., 2019). Thus, TGF- $\beta$  plays a crucial role in the inflammation phase of wound healing by initially enhancing pro-inflammatory responses and later facilitating the reduction of inflammation (Finsson et al., 2013).

During the proliferative phase, TGF- $\beta$  is involved in various cellular responses, including re-epithelialisation, angiogenesis, fibroblast proliferation, and production of ECM components. These processes lead to granulation tissue formation and wound contraction (Midwood et al., 2004).

The findings indicate that TGFB1 plays a pivotal role in both the inflammatory and remodelling phases of wound healing. Its continued upregulation as shown in Table 1, implies that TGFB1 is actively involved in regulating inflammatory responses, enhancing ECM production, and facilitating the shift from inflammation to tissue regeneration. Additionally, its continued presence in the later stages of healing highlights its significance in promoting wound closure. Also, the activation of TGF- $\beta$  and fibroblast differentiation are crucial components of the wound healing process. In a study by Roper et al., (2015) involved experiments on mice, where ultrasound was used to observe its effects on wound healing. Their findings demonstrated that US promoted the recruitment of fibroblasts to the wound site. However, it did not result in the formation of myofibroblasts. This suggests a potential role of US in facilitating cell migration without inducing differentiation (Figure 3.3). Given that TGF- $\beta$  signalling and fibroblast differentiation are essential to typical healing, it is crucial to further explore the specific impact of TGF- $\beta$  following ultrasound therapy to better understand how US modulates the healing process.

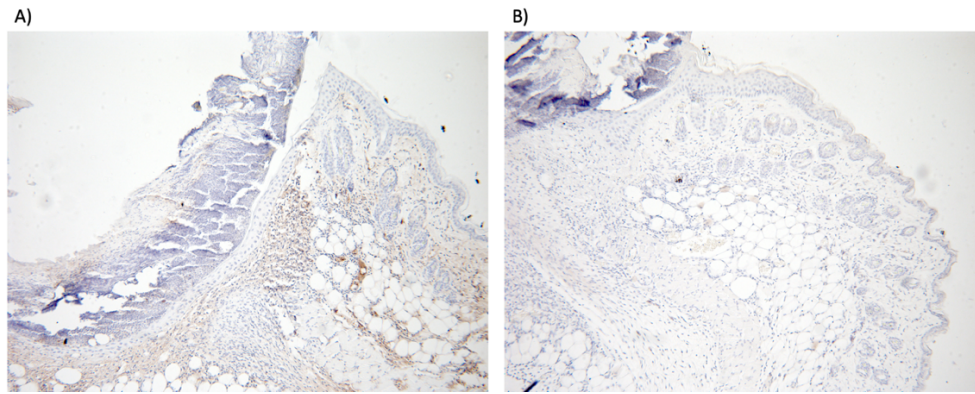


Figure 3.3 Skin sections at 72 hours post-wounding.

Skin sections stained for fibroblast-specific protein (FSP). Both images show similarities at the wound edge. However, the control image displays brown cells in the shoulder region (A), while this is absent in ultrasound-treated image (B). (Image taken from Roper et al., (2015).

### 3.3.5 Limitations of Microarray Data and Alternative Approaches

Although Nuutila et al. (2012) study provided valuable insights about changes in protein expression within the ECM during different stages of wound healing, however, alternative approaches such as RNA sequencing (RNA-Seq) or proteomics could complement or provide additional insights beyond microarray analysis. Combining RNA-Seq and proteomics with microarray analysis can enhance deep insights into gene regulation. RNA-Seq enables sensitive detection of novel transcripts and splice variants (Stark et al., 2019), while proteomics directly measures protein expression and modifications (Alharbi, 2020). Integrating these approaches provides a more comprehensive understanding of gene regulation and biological processes in wound healing.

## 3.4 Conclusion

The decision to focus this research on ECM components (specifically collagen types 1, 3, 4, and 6, fibronectin, TGF- $\beta$ , and LOX) was guided by their sustained expression and critical roles throughout the wound healing process. In contrast to MMPs, which are primarily involved in

the early stages by promoting tissue breakdown and regulating inflammation, these ECM components are key to the later phases of tissue repair and remodelling.

Collagens and fibronectin provide essential structural proteins that form the scaffolding for new tissue development. TGF- $\beta$  plays a central role in regulating cellular processes such as proliferation, differentiation, and contractility, ensuring the smooth transition from inflammation to tissue regeneration. LOX contributes to the stabilisation and maturation of the ECM by facilitating collagen cross-linking, which enhances the mechanical strength of the repaired tissue.

By concentrating on these sustained and influential components, we aim to develop more effective therapeutic strategies that not only accelerate wound closure but also improve the quality of tissue repair. Targeting collagens, fibronectin, TGF- $\beta$ , and LOX presents a promising approach for enhancing the remodelling phase of wound healing, leading to improved functional and aesthetic outcomes. This focus supports the goal of promoting long-term tissue integrity and functionality, making these ECM components ideal targets for interventions designed to optimise the wound healing process.

# Chapter 4

## Effect of LIPUS on Matrix Deposition



## Chapter 4 Effect of LIPUS on Matrix Deposition

### 4.1 Introduction

Collagen is a vital component of connective tissues, including cartilage, tendons, ligaments, and various organs such as the skin, heart, liver, kidneys, lungs, blood vessels, and bones. It belongs to the fibrous protein family that constitutes the ECM (Koskinas et al., 2013; Kisling et al., 2019). In flexible connective tissues like the skin, type I collagen is commonly found alongside type III collagen, which are the primary types present in the ECM (Katsuda et al., 1992). Variations in collagen levels, particularly collagen I and collagen III, can significantly impact disease prognosis and progression. For instance, elevated collagen I protein levels can increase myocardial stiffness, impairing both diastolic and systolic heart functions (Ricard-Blum, 2011). Collagen enhances the mechanical strength and flexibility of tissues while also serving as a natural substrate supporting cellular adhesion, proliferation, and differentiation. Also, during wound healing and ECM remodelling after an injury, changes in collagen distribution occur. For example, collagen III increases during the healing phase, while collagen I levels rise in the healed wound (Singh et al., 2023). Changes in the type, amount, and organization of collagen are crucial in wound healing, affecting the tensile strength of healed skin. Initially, collagen III is synthesized in the early stages of wound healing and is later replaced by collagen I, the primary collagen in the skin (Singh et al., 2023).

Fibronectin is crucial for wound healing as it contributes to the formation of a platelet plug and stabilises fibrin clots. It can opsonise ECM debris, prompting macrophages to engage in phagocytosis, and is observed in areas of active bleeding after severe trauma (Lenselink, 2015). Also, Fibronectin is recognised for facilitating cell migration-related processes, such as wound healing (Longstreth et al., 2024). Deficiency in the fibronectin has been observed in trauma cases such as shock, sepsis, and burns. In aged skeletal muscle stem cells (MuSCs), reduced fibronectin levels result in decreased cell number, function and maintenance, similar to the

effects seen in young FN knockout MuSCs. Restoring fibronectin levels in aged mice restores the youthful phenotype, cell levels, muscle maintenance and function of MuSCs (Patten and Wang, 2020).

LIPUS has been shown to affect wound size during the early stages of wound healing. Therefore, our hypothesis is that LIPUS would increase fibronectin and collagen III and decrease collagen I expression, reducing skin stiffness and potential scar formation. This chapter aims to investigate how LIPUS alter the expression of fibronectin, collagen types I and III, thereby clarifying its specific impact on the wound healing process.

## 4.2 Results

At the beginning, it is worth mentioning that qPCR was initially attempted during the early stages of data collection. However, the results were inconsistent across repeats (see appendices Figure 7.4 – Figure 7.6). Subsequently, previous work in our lab attempted to solubilise the ECM and perform Western blot analysis, but this approach proved ineffective. As a result, we decided to focus on using conditioned medium and cell lysates for each individual protein.

### 4.2.1 Period of LIPUS stimulation

The determination of the LIPUS stimulation effect was based on a collaborative experiment in our lab that measured the fold change from Day 2 to Day 5 after the initial LIPUS stimulation using qPCR (with Day 1 being the start of LIPUS stimulation) (Figure 4.1). The data showed a slight reduction in fold change on Day 4. However, after the fifth stimulation, there was a significant increase in fold change. Therefore, the decision to choose 20 minutes/day for 5 days of treatment was determined.

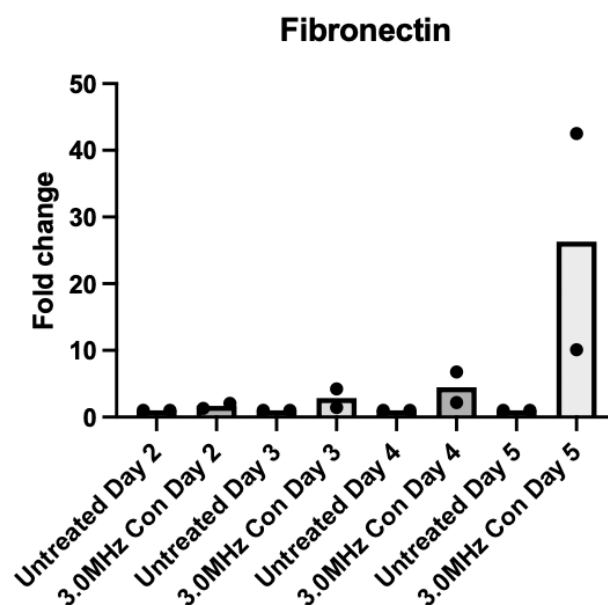


Figure 4.1 Time scale of LIPUS stimulation.

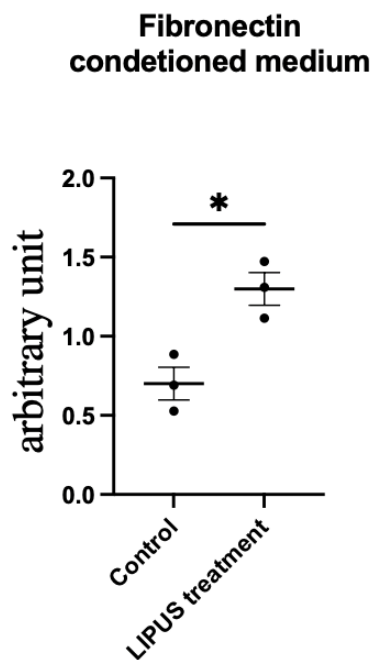
Fibronectin fold change using qPCR. Data used to determine timing for subsequent experiments, presented as two independent replicates conducted by [Lab Postdoc Dr Aimee Paskins] with my direct involvement. Due to the limited number of replicates, only the values and mean is shown. The consistency of the results supports the chosen timing parameters.

#### 4.2.2 Fibronectin

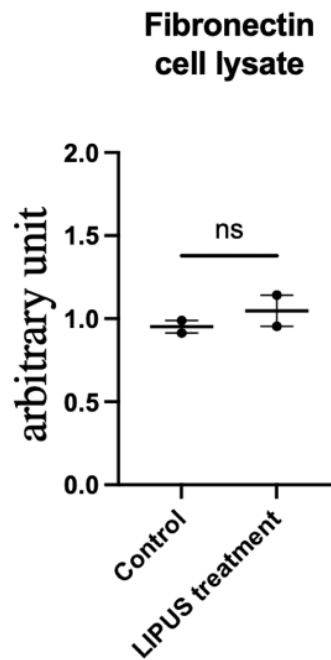
Fibronectin expression of conditioned medium and cell lysate were analysed using western blot to investigate the role of LIPUS. The cells were cultured and treated with for five days and on the fourth day the medium was replaced with serum-free medium and left for 24 hours. The medium was then collected for western blot analysis.

The analysis revealed that an increase in the fibronectin expression on the conditioned medium was observed after the LIPUS stimulation, whereas there was no significant difference at the cell lysate level (Figure 4.2), suggesting that LIPUS stimulation may primarily influence the secretion or release of fibronectin into the conditioned medium, rather than affecting the intracellular levels.

A).



B)



C)

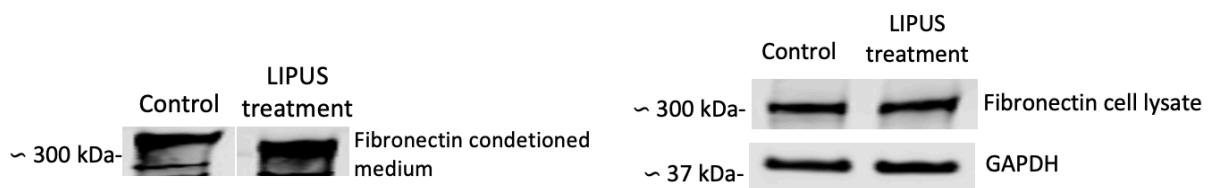


Figure 4.2 Protein expression of fibronectin conditioned medium and cell lysate

Sham-treated and LIPUS-stimulation using TIF cell line. A) The graph shows an increase in the protein expression of fibronectin in the conditioned medium. C) The western blot bands for fibronectin conditioned medium and cell lysate. All results are normalised to GAPDH band. (n=3 replication). Error bars represent SEM. Statistical significance was calculated using a t-test.

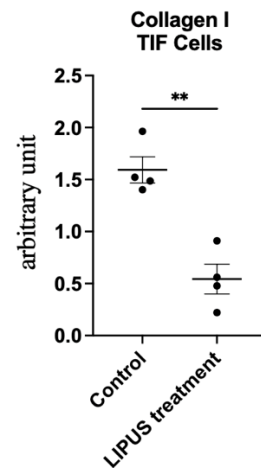
### 4.2.3 Collagens

To investigate the effect of LIPUS on collagen expression levels, two cell lines were utilised: TIF (immortalised) and HFF (primary fibroblasts). TIFs were chosen to avoid changes in cellular properties over time, ensuring consistent results. In contrast, HFFs, being a primary cell line, provided insights into the effects of LIPUS on non-transformed cells. Both cell lines, being fibroblasts, allowed for a comprehensive analysis of LIPUS-induced collagen

expression. Since collagen I and III are secreted protein, so the protein expression level of collagens I and III on the conditioned medium were compared between LIPUS-stimulated and sham treated cells.

Figure 4.3 and Figure 4.4 shows that collagen I expression has decreased in the conditioned medium after the LIPUS stimulation by 65.42% and 24.90% for the TIF and HFF, respectively. To further assess collagen I levels, immunofluorescence staining was performed. Cells were seeded at a density of  $6 \times 10^4$  cells/ml onto glass coverslips and cultured for five days, with daily LIPUS or sham treatments. On the fifth day, cells were fixed and stained for collagen I. The specificity of the collagen I antibody was supported by the manufacturer's validation data. While this provides confidence in the staining results, the experiment did not include additional negative controls, such as omission of the primary antibody to assess non-specific secondary antibody binding or the use of collagen I knockdown samples to confirm signal specificity. Incorporating such controls in future studies would strengthen the findings. Verification of ECM retention after washing was not directly performed; future experiments could benefit from including ECM-preserving protocols or additional markers for matrix components. Images were acquired using a Nikon A1 confocal microscope under consistent settings for laser power, gain, and exposure across all samples to ensure comparability. Image analysis was performed using ImageJ, where mean fluorescence intensity was measured for each image. "Mean intensity" refers to the average pixel intensity within the selected area of the image, representing the overall level of collagen I staining. A higher mean intensity indicates stronger collagen I signal, while a lower mean intensity reflects reduced collagen I presence. Three independent biological replicates were used, and within each replicate, images were randomly selected to reduce selection bias. (Figure 4.5). This result aligned with reduction in protein expression from the western blot.

A)



B)

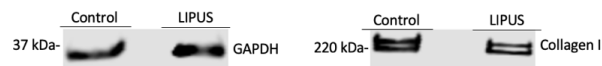


Figure 4.3 Protein expression of collagen I conditioned medium.

Sham treated and LIPUS-stimulated cells using TIF cell line. A) The graph shows a reduction in the protein expression of collagen I after the LIPUS stimulation by almost three folds. B) The western blot bands for Collagen I normalised to GAPDH band from the cell lysate (n=4). Error bars represent SEM. Statistical significance was calculated using a t-test.

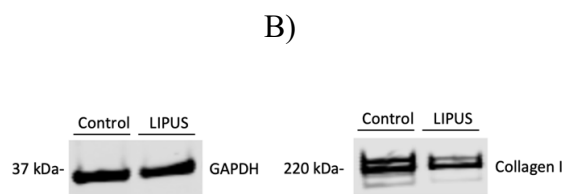
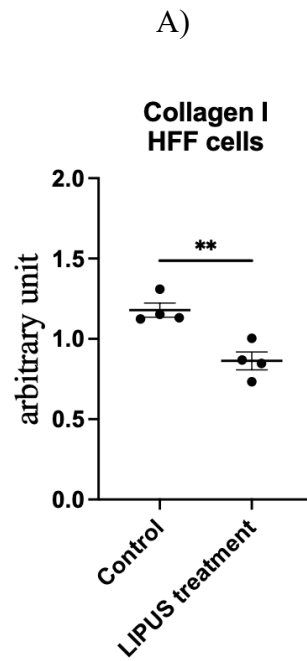


Figure 4.4 Protein expression of collagen I conditioned medium.

Sham treated and LIPUS-stimulated cells using HFF cell line. The graph shows a reduction in the protein expression of collagen I. (n=4). Error bars represent SEM. Statistical significance was calculated using a t-test.

A)

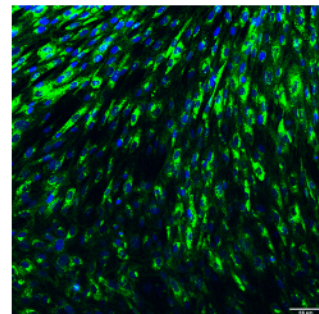
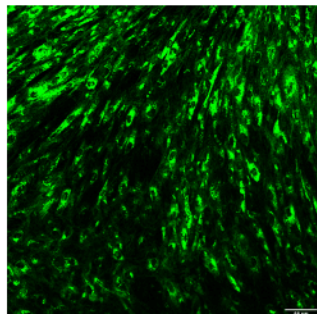
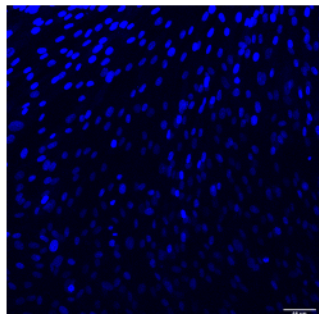
Control

DAPI

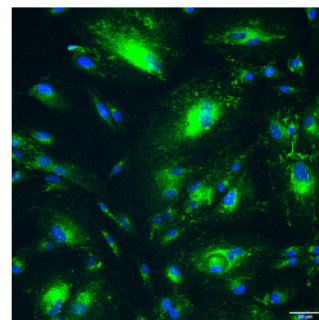
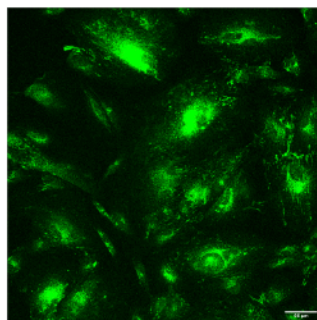
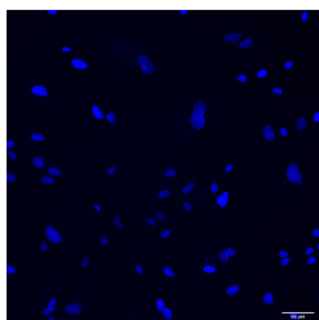
Collagen I

Merged

Exp 1



Exp 2



B)

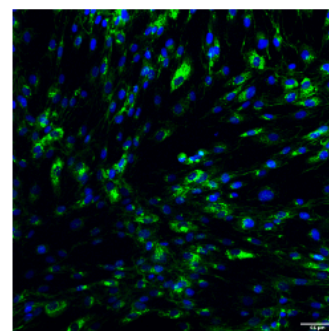
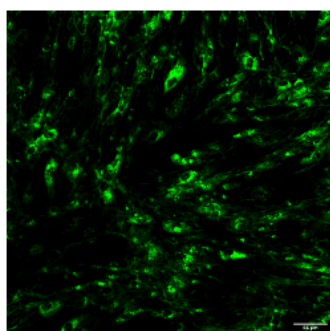
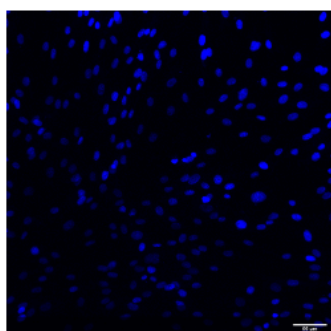
LIPUS

DAPI

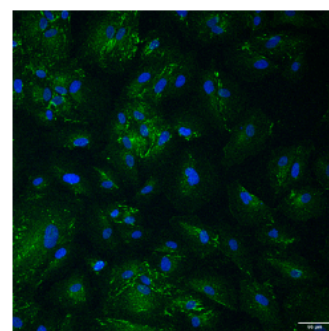
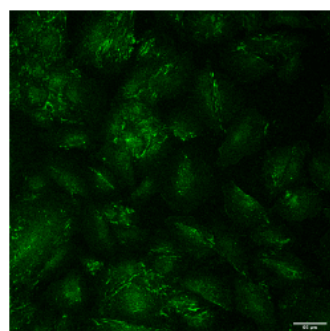
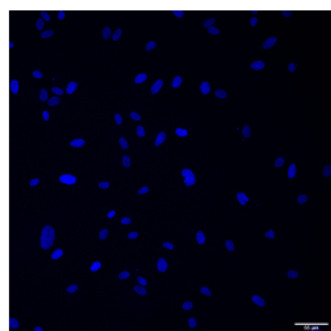
Collagen I

Merged

Exp 1

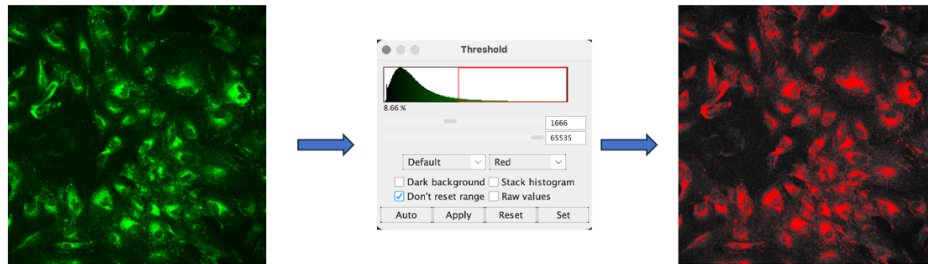


Exp 2





C)



D)

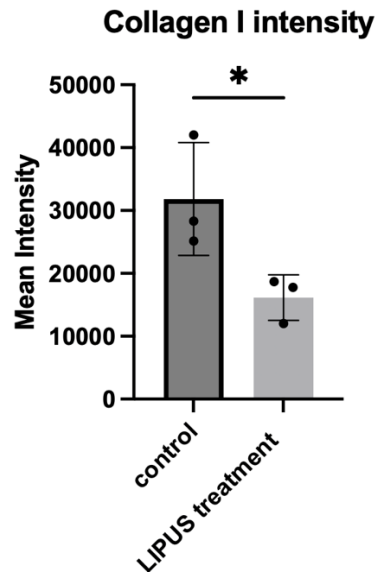


Figure 4.5 Immunofluorescence analysis of collagen I showing the mean intensity.

A) Sham-treated and B) LIPUS treated HFF cells. C) The process of calculating the intensity using ImageJ. D) The figure exhibit decreased collagen I expression in the LIPUS treated compared to the control. Scale bar: 66  $\mu$ m. (images are representative of 5 separate fields within a single experiment and the experiment was repeated on 3 separate experiments). Scale bar: 66  $\mu$ m. Error bars represent SEM. Statistical significance was calculated using a t-test.

When the effect of LIPUS stimulation on collagen III was examined, the opposite effect was observed. Western blot analysis showed an 111.1% increase in the expression of collagen III in the treated samples compared to the control group (Figure 4.6). This upregulation of collagen III indicates that the collagen synthesis is effectively enhanced by the LIPUS stimulation while an opposite effect was observed in collagen I. This observation provides an insight on how LIPUS affect differently on the collagen for the sake of wound healing because as collagen I reduced after the stimulation, an increase occurred in collagen III. Additionally, collagens IV were amongst the proteins of interest, however, the western blotting was not successful as bands were not clear throughout different repeats (See appendices Figure 7.2)

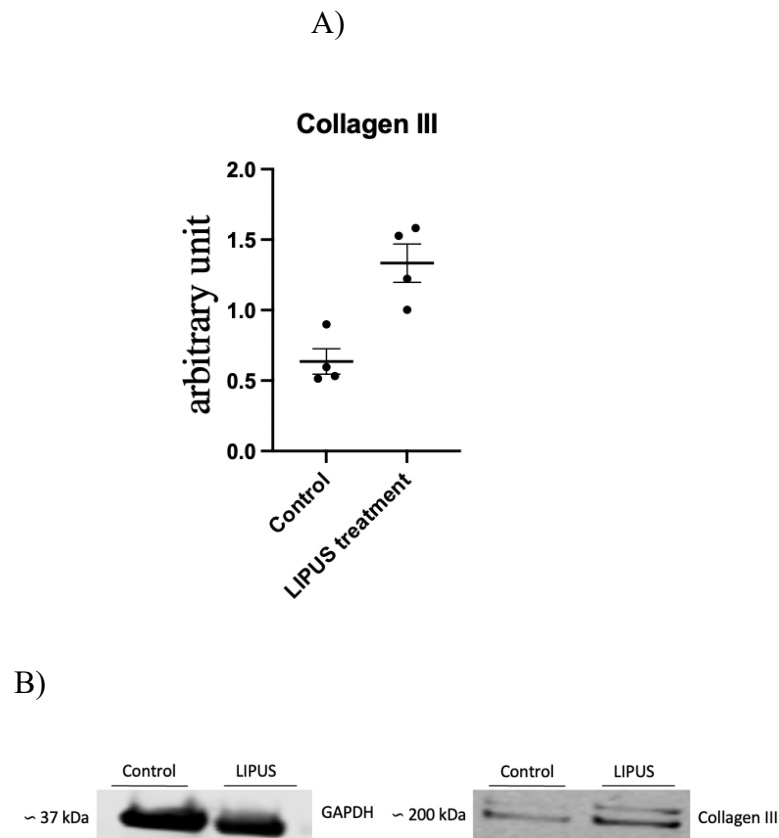


Figure 4.6 Protein expression of Collagen III conditioned medium.

Sham-treated and LIPUS-stimulated cells using TIF cell line. A) The graph shows an increase in the protein expression of collagen III. B) The western blot bands for Collagen III normalised to GAPDH band (n=4 replication). Error bars represent SEM. Statistical significance was calculated using a t-test.

#### 4.2.4 Matrix alignment

To investigate the role of LIPUS in matrix alignment, HFF cells were cultured on glass coverslips, stained for fibronectin, and imaged using a Nikon A1 confocal microscope. A FIJI macro for quantifying pattern in extracellular matrix was used. TWOMBLI, which is used to quantify matrix patterns in an ECM image by deriving a range of metrics. To measure curvature using TWOMBLI, Ridge Detection was first run on all Test Set images, creating masks that highlighted the matrix fibers. Using the Straight-Line tool in Fiji, typical lengths of the curves on these masks were measured, avoiding any branching or significant changes in direction. Given the subjectivity in selecting the right window size, a range of curvature windows was evaluated (40, 50 and 60). Smaller windows captured the waviness of individual fibers, while larger windows measured curvature on a more global scale. The results revealed that in the sham-treated samples fibronectin was aligned more parallelly, whereas in the treated samples, the alignment appeared more random and forming a mesh-like structure (Figure 4.7 and Figure 4.8). Two non-overlapping fields of view were imaged per experiment across four independent biological replicates. The two images were averaged per experiment to account for intra-sample variation. Image selection was randomised, and analysis was performed in a blinded manner. The average curvature values for the sham-treated samples were 45.87 for the 40-curvature window, 45.23 for the 50-curvature window, and 47.08 for the 60-curvature window. In comparison, the LIPUS treated samples exhibited curvature values of 66.12 for the 40-curvature window, 68.75 for the 50-curvature window, and 72.85 for the 60-curvature window. The increasing curvature values at different window sizes indicate that LIPUS affects both small and large-scale structural organisation, potentially leading changes in matrix structure. A  $p\text{-value} < 0.05$  was considered statistically significant.

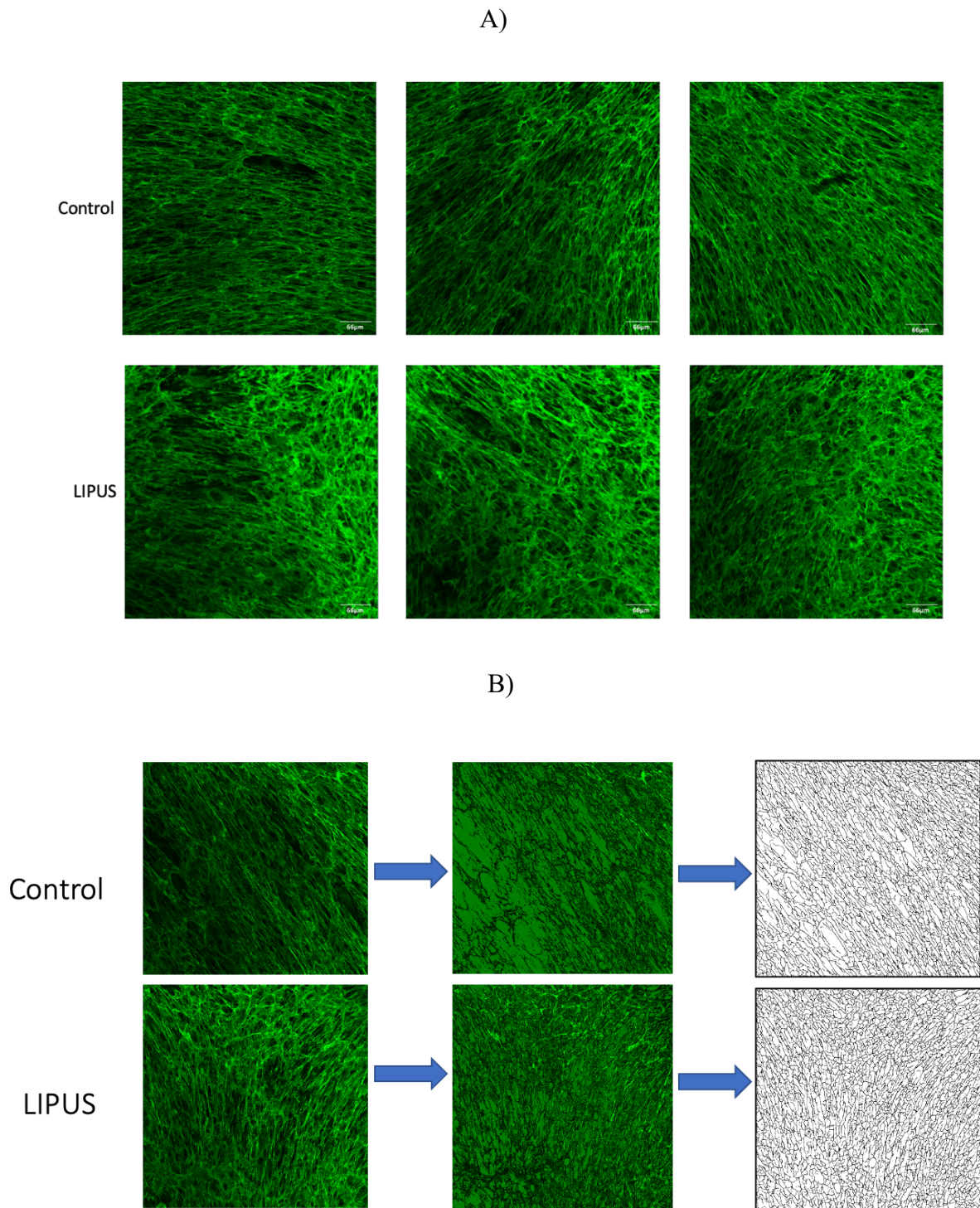


Figure 4.7 Immunofluorescence analysis of fibronectin.

A) Images representing fibronectin fibers and the process of analysing the fibers alignment using TOWMBLI macro. B) The process of how the fibres analysed. Image selected to analyse (left), ridge detection will trace a mask looking for matrix fibre bundles (Middle) resultant image for calculating the degree of curvature (right). Two non-overlapping fields of

view per condition were analysed per experiment, with four independent experiments performed ( $n = 4$ ). Image selection and analysis were performed in a blinded manner.

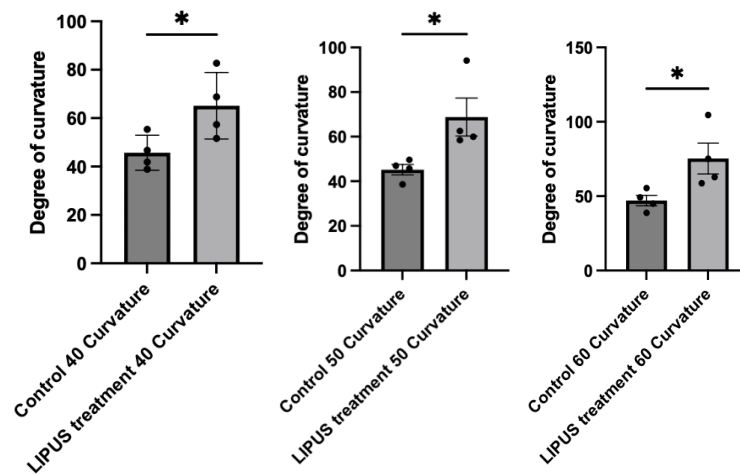


Figure 4.8 The result of different curvature windows used.

Quantification of matrix fiber curvature at different analysis window sizes. Curvature values calculated using TWOMBLI at window sizes of 40, 50, and 60 for sham and LIPUS-treated samples. Data represent mean values from two fields per experiment across four independent experiments ( $n=4$ ). Error bars represent SEM. Statistical significance was assessed using t-test. Scale bar: 66  $\mu\text{m}$ .

### 4.3 Discussion

Most previous studies have investigated the use of LIPUS for bone regeneration and muscles therapy, only limited studies have investigated its potential use for the promotion of wound healing. Roper et al., (2015) concluded their results that LIPUS has restored healing to diabetic mice through activating fibroblast. In the present study I have shown that LIPUS significantly reduced collagen I and increased fibronectin and collagen III expression in the conditioned medium.

Collagen provides mechanical strength and elasticity to tissues, serving as a natural scaffold for cell attachment, growth, and differentiation (Soroushanova et al., 2019). During wound healing, fibroblasts are the primary producers of new collagen (Sinha et al., 2018). Collagen III is predominantly synthesised during the early stages of healing, providing flexibility and

promoting a regenerative environment. Over time, collagen III is gradually replaced by collagen I, which is the dominant collagen in healthy, undamaged skin (Singh et al., 2023). Our results suggest that LIPUS promotes early healing by driving the expression changes associated with these early stages, particularly by enhancing collagen III production. This shift toward early-stage collagen expression may explain how LIPUS accelerates the wound healing process. A more detailed understanding of the roles of collagen III and I is crucial here; collagen III supports initial tissue formation and flexibility, while collagen I reinforces strength and stability in the later stages of healing. By promoting collagen III expression, LIPUS may promote a more efficient transition through the early reparative phase, setting the foundation for improved tissue regeneration.

During the formation of granulation tissue, collagen is randomly deposited, and this process is further strengthened by covalent cross-linking induced by the enzyme lysyl oxidase (Mathew-Steiner et al., 2021). Collagen I is known for its rigidity, while collagen III is more elastic and the alteration of the expression level of the collagen can be an important factor that can pause normal wound healing (Singh et al., 2023). For example, elevated level of collagen I was associated with diabetic foot ulcer fibroblasts (DFUFs) compared to normal foot fibroblasts (NFFs) (Maione et al., 2016). A controlled increase in collagen III also suggests a more organised healing process, potentially leading to less scarring (Singh et al., 2023). This balance between the two types of collagens is essential for healthy tissue regeneration, and these changes are positive signs that the chronic wound is progressing towards successful healing, moving from inflammation to tissue repair and remodeling.

Aged skin exhibits lower collagen density, increased collagen cross-linking, and increased collagen fragmentation. Along with fibroblast senescence, collagen fiber remodelling results in increased stiffness (Blair et al., 2020; Marcos-Garcés et al., 2014). Also, as skin ages, collagen fibers become fragmented, clustered, and thicker, aligning parallel to the skin's

surface. These changes contribute to wrinkles and loss of skin elasticity (Blair et al., 2020). LIPUS may promote rapid, scar-free healing by shifting the balance towards increased collagen III expression, a crucial factor in early tissue repair. Supporting this, the work of Roper et al. (2015) demonstrates that Rac1 activation is essential for ultrasound-stimulated healing, which accelerates the process but can also potentially contribute to scarring. However, our data suggests that LIPUS might mitigate this issue by promoting a more regenerative environment that favours collagen III over collagen I, potentially reducing the risk of fibrosis. This interpretation opens promising avenues for LIPUS as a therapeutic tool in improving wound healing outcomes.

It is worth mentioning that permeabilisation step was included during immunofluorescence staining to allow the antibody to access both intracellular and extracellular pools of collagen I. Collagen is synthesised intracellularly in fibroblasts, particularly within the endoplasmic reticulum and Golgi apparatus, before being secreted into the extracellular space where it assembles into fibrillar structures (Yue, 2014). Without permeabilisation, antibodies are generally unable to penetrate intact cell membranes and would only bind to collagen present on the cell surface or within accessible extracellular matrix components. Permeabilisation disrupts the plasma membrane using detergents such as Triton X-100, enabling antibodies to enter the cells and bind to intracellular targets (Jamur and Oliver, 2009). In this study, the use of permeabilisation ensured that early-stage, intracellular collagen I, as well as any extracellular collagen loosely associated with the cell layer, could be detected. However, it is important to acknowledge that this approach does not allow discrimination between intracellular collagen, newly secreted collagen, and mature extracellular collagen deposited into the ECM. Therefore, permeabilisation allowed a more complete visualisation of total collagen I content associated with the cells, but interpretation requires careful consideration of this limitation.

Fibronectin is the primary ECM protein present in the provisional matrix during the initial stages of wound healing, serving as a scaffold for later collagen deposition (Maione et al., 2016). Fibronectin's role is evident in the early stages of wound healing, such as during haemostasis. After a wound occurs, platelets are released from the blood to form a platelet plug. This plug is established through interplatelet binding via integrins and fibrinogen. Factor XIII then stabilises the fibrin clot by linking fibrins to fibronectin, creating a fibrin-fibronectin clot. Fibronectin has also been detected in actively bleeding areas in humans following fatal trauma (Lenselink, 2013). Earlier studies have indicated that increasing fibronectin levels in the matrix accelerates wound healing. For example, fibronectin nanofiber dressings significantly accelerate wound healing and improve tissue restoration by mimicking fetal skin's regenerative properties (Chantre et al., 2018). Additionally, Topical application of pure soluble fibronectins enhances wound healing in both normal and diabetic animals (Qiu et al., 2007). Our results showed a significant increase in fibronectin expression in the conditioned medium. This finding provides further insight into how LIPUS accelerates the healing process, as increased fibronectin likely supports ECM remodelling and cell migration, both critical for effective tissue repair.

Numerous studies have been instigating the cancer-associated fibroblasts (CAF) ECM alignment, however, there has been limited investigation into fibroblast remodelling in common fibrotic conditions such as different wound scars. In a study conducted by Verhaegen et al. (2009) investigating keloid scars, a fibrotic skin disorder of unknown origin, the disease pathogenesis was explored. They found that keloid tissue exhibited a highly bundled ECM fibre organisation, in contrast to the randomly distribution pattern of normal dermis. Also, a recent study by Kenny et al. (2023) illustrated the differences between keloid dermal fibroblasts (KDF) and normal dermal fibroblasts (NDF). They found that KDF fibronectin fibers are aligned in a parallel pattern, unlike the random alignment seen in NDF. The fibronectin



immunofluorescence results indicate that LIPUS influences matrix alignment by reorganising the fibers. This suggests that LIPUS treatment actively contributes to the structural rearrangement of fibronectin within the extracellular matrix, promoting a more randomly organised fiber pattern.

# Chapter 5

Chapter 5 (Effect of LIPUS on matrix cross-linking and cell contractility)

# Chapter 5 Effect of LIPUS on matrix cross-linking and cell contractility

## 5.1 Introduction

The ECM plays a key role in regulating extracellular functions. In addition to maintaining tissue mechanical strength and stiffness, it influences cellular behavior and directs cell migration (Al Ameri et al., 2019). Amongst many components found in the ECM, fibrous proteins and proteoglycans are the two primary constituents. Since these proteins have a fibrous structure, proper crosslinking between these macromolecules is essential for appropriate tissue formation (Wei et al., 2020). Secretory reticular fibroblasts in the reticular dermis display a prominent ECM gene expression profile, including collagen type 1A1, Fibronectin, and LOX, indicating that this subpopulation is crucial for ECM assembly, fiber organisation, wound healing, and angiogenesis (Bensa et al., 2023). Moreover, ECM metabolic processes and remodelling are critical to the formation of the complex extracellular network, with LOX as cross-linking enzyme playing a central role in catalyzing these processes (Gartland et al., 2016).

The organisation of the ECM is just as critical as its composition, and it is influenced by factors such as the tension exerted by cells and modifications like crosslinking. These structural dynamics are key to ensuring proper tissue function and stability. This chapter seeks to explore the hypothesis that LIPUS will alter ECM organisation, cross-linking and contractility potentially reducing wound scarring, focusing on the expression of key proteins (LOX and TGF- $\beta$ ). By investigating these specific markers, the goal is to understand how LIPUS influences the structural and functional remodelling of the ECM during tissue repair and wound healing.

### 5.1.1 Cell-Derived Matrix (CDM)

The ECM's role in cell migration is particularly well-known. Tissue-resident cells continually interact with the ECM, relying on its anchor points for migration, proliferation, and differentiation. Glycoproteins like fibronectin and laminin provide these anchor points by serving as ligands for cell surface receptors (Bonnans et al., 2014; Pfisterer et al., 2021). Dynamic interactions between the ECM and integrins enable cycles of cell adhesion and detachment from the substrate. Combined with the traction forces generated by a contractile cytoskeleton, these cycles facilitate cell movement (Rozario and DeSimone, 2010). The cell-derived matrix (CDM) produced by fibroblasts forms a diverse fibrous network, predominantly consisting of linear fibronectin fibrils. These fibrils can be arranged in parallel or in a more random organisation (Kutys et al., 2013).

### 5.1.2 The role of Lysyl Oxidase (LOX) in matrix cross-linking

LOX plays a key role in forming cross-links in collagen fibrils and elastin within the ECM, which is essential for ECM formation and repair. This cross-linking is crucial for ECM stabilisation, development, maturation and remodeling, making LOX vital for tissue repair and regeneration. Collagens produced by fibroblasts are deposited following a cross-linking reaction catalysed by LOX, which accelerates the reparative process in tissues like the cardiovascular system, skin, and bone, promoting the healing cascade (Cai et al., 2017). During embryogenesis and organ development, LOXs play a vital role in promoting structural integration, while also ensuring the appropriate cell stiffness and rigidity needed for organogenesis and the long-term maintenance of tissue morphology (Wei et al., 2020). This enables the cells to be properly anchored within the matrix, ensuring they maintain their functional polarity and stability. As LOXs secreted locally, their expression levels and activity have been linked to the modulation and transformation of cells. In this way, cells are able to

sense changes in their microenvironment and act as both responders and regulators in adapting to these changes (Wei et al., 2020).

### 5.1.3 Transforming growth factor-beta (TGF- $\beta$ )

In the proliferative phase of wound healing, collagen, proteoglycans, and fibronectin are produced to procedure a new ECM, resume epithelialisation, and promote angiogenesis. Fibroblasts, the main cells responsible for producing both the matrix and collagen, dominate this stage of healing (Deonarine et al., 2007). TGF- $\beta$  is a potent stimulant for fibroblasts and plays a crucial role in this process. Angiogenesis begins with endothelial cells migrating into the fibrin matrix and degrading the interstitial matrix to procedure new capillaries. In addition to TGF- $\beta$ , vascular endothelial growth factor (VEGF) and other fibroblast growth factors also promote angiogenesis (Deonarine et al., 200; Gharee-Kermani and Pham, 2001).

It has been reported that TGF- $\beta$ 1 triggers the differentiation of fibroblasts into myofibroblasts, which exhibit greater activity in collagen production compared to fibroblasts (Guler and Roovers, 2022). Additionally, it inhibits various MMPs, leading to the accumulation of collagen fibers (White et al., 2000). During wound repair, fibroblasts also differentiated into myofibroblasts and express  $\alpha$ SMA, which is induced by mechanical tension and TGF- $\beta$  (Werner et al., 2007).

### 5.1.4 Traction Force microscopy

Cells generate traction forces through the actomyosin cytoskeleton, transmitting these forces to the ECM and adjacent cells via cell-cell and cell-matrix interactions (Wang and Li, 2010). The forces produced by individual cells are typically very small, ranging from pico-newtons to nano-newtons and are applied over small distances, usually between nanometres to micrometres. These traction forces are essential for various biological processes, including wound healing (Wang and Li, 2010). Cell traction forces (CTFs) are created by the interaction between actin filaments with myosin-II, as well as through the process of actin polymerisation

(Wang and Lin, 2007). CTFs are conveyed to the ECM or substrate via focal adhesions (FAs), which consists of structural and signalling proteins, such as kinases and integrins, forming physical connections between the actin cytoskeleton and the ECM (Figure 5.1). Determining CTFs not only aids in characterising cell migration, as well as for identifying changes in cell phenotype resulting from biochemical and biomechanical treatments (Wang and Li, 2010).

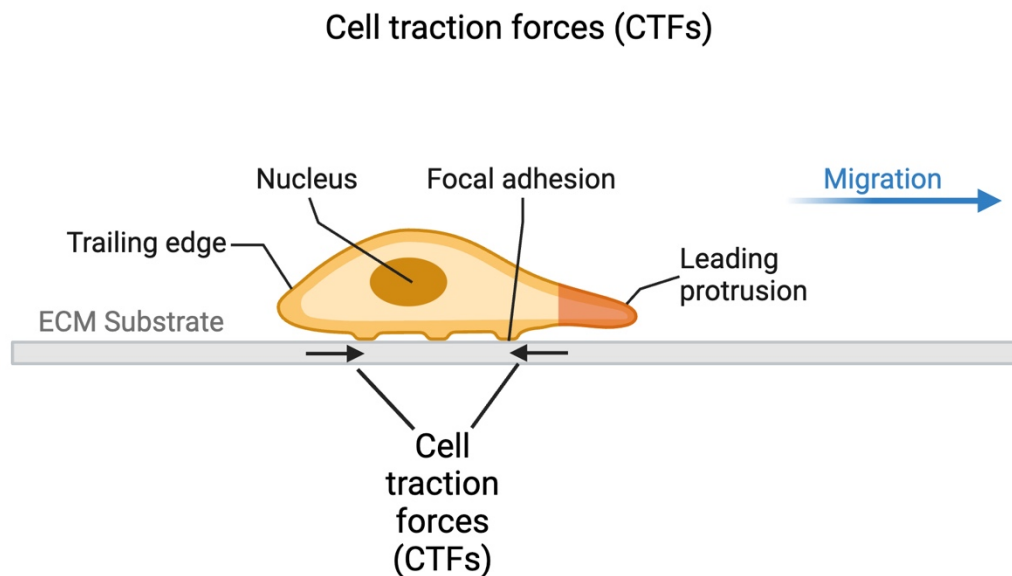


Figure 5.1 A depiction of cell migration and CTFs (Image Created in BioRender.com).

Various techniques have been developed to measure CTFs both qualitatively and quantitatively. Traction Force Microscopy (TFM), which can quantitatively, efficiently, and reliably determine the traction forces of both individual cells and groups of cells (Style et al., 2014; Wang and Li, 2010). In TFM, elastic hydrogels embedded with fluorescent microbeads, such as polyacrylamide gel (PAG) or gelatin gel, serve as the substrate for cell culture. The substrate used in TFM, PAG, exhibits linear elasticity in response to a wide range of forces and completely recovers its original shape upon force removal (Style et al., 2014). After coating with an appropriate ECM protein, like type I collagen or fibronectin, cells adhere to the gel and spread across its surface. As the cells generate traction forces, they deform the gel, causing the embedded beads to shift positions. During TFM measurement, two images are captured: a

'force-loaded' image, taken while the cells are still attached to the gel, and a 'null-force' image, taken after the cells have been removed. These images are used in a two-step process to calculate the CTFs (Li and Wang, 2011).

In summary, in addition to the role of LOX in stabilising ECM components, TGF- $\beta$  plays a crucial role in modulating the production and organisation of the matrix, particularly by when fibroblast activated. TGF- $\beta$  also promotes the differentiation of fibroblasts into myofibroblasts leading to matrix remodelling. This process not only affects ECM composition but also drives the alignment of fibres, influencing tissue repair and scar formation. In CDMs, this results in enhanced deposition of fibronectin fibrils, which can influence the matrix's structure and organisation.

## 5.2 Result

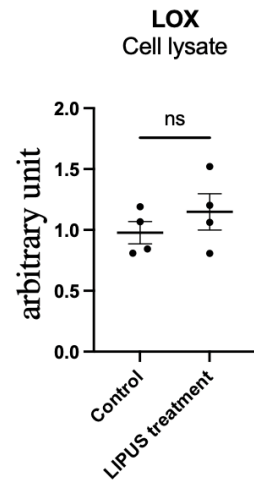
### 5.2.1 LIPUS-stimulation increase abundance of secreted Lysyl Oxidase.

Western blot analysis was performed to investigate the effect of LIPUS stimulation on LOX expression. The medium was replaced with serum-free medium 24 hours before it was collected for analysis (Table 5.1). LOX expression levels analysed in both cell lysate and conditioned medium for the LIPUS-stimulated and sham treated cells (Figure 5.2). In the cell lysate, the western blot shows no significant difference between the sham treated cells and LIPUS-treated groups (Figure 5.2 A and Figure 5.2C, indicated by "ns"), indicating that LIPUS stimulation does not affect LOX expression within the cells. However, the result of serum-free conditioned medium shows increased LOX expression in the LIPUS-stimulated compared to the sham-treated cells, confirming that LIPUS stimulation raises the amount of LOX release in the extracellular environment (Figure 5.2 B indicated by "\*\*",  $p < 0.05$ ). This indicates that LIPUS stimulation enhances LOX expression in the extracellular environment. Therefore, while LIPUS treatment does not impact intracellular LOX levels, it significantly promotes the release of LOX expression in conditioned medium.

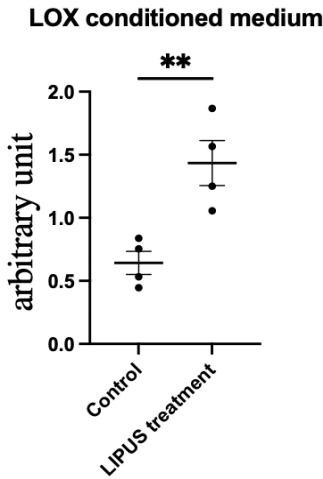
Table 5.1 The period of LIPUS treatment.

Day1	Day2	Day3	Day4	Day5
<ul style="list-style-type: none"><li>• TIF cells Seeding</li><li>• LIPUS treatment (20 minutes)</li></ul>	<ul style="list-style-type: none"><li>• LIPUS treatment (20 minutes)</li></ul>	<ul style="list-style-type: none"><li>• LIPUS treatment (20 minutes).</li></ul>	<ul style="list-style-type: none"><li>• Change medium to serum free medium.</li><li>• LIPUS treatment (20 minutes).</li></ul>	<ul style="list-style-type: none"><li>• LIPUS treatment (20 minutes).</li><li>• Cellular lysate</li><li>• Serum free medium concentration.</li></ul>

A)



B)



C)

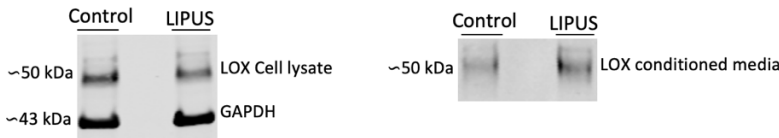


Figure 5.2 Protein expression of LOX cell lysate and conditioned medium.

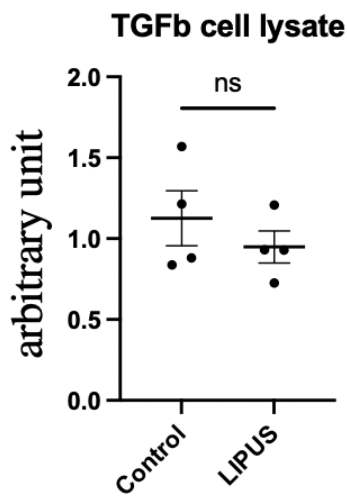


Sham-treated and LIPUS-stimulated using TIF cell line. A) There was no significant change in the cell lysate protein expression of LOX. B) Increase in LOX protein expression in the conditioned medium in LIPUS-stimulated samples compared to sham-treated C) The western blot bands for LOX. (n=4). Error bars represent SEM. Statistical significance was calculated using a t-test.

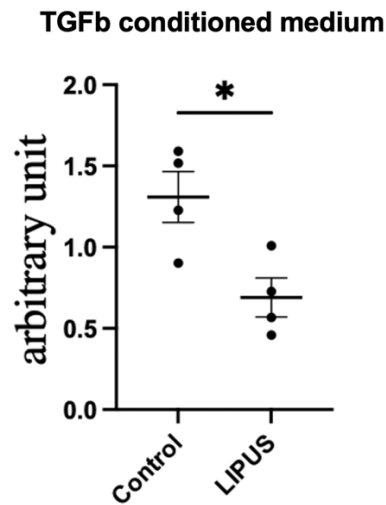
### 5.2.2 Effects of LIPUS on TGF- $\beta$ Expression

Western blot analysis was conducted to evaluate the effect of LIPUS stimulation on TGF- $\beta$  expression. The analysis included both cell lysate and serum-free conditioned medium, similar to the previous examination of LOX. Figure 5.3 presents the TGF- $\beta$  levels in conditioned medium and cell lysates after LIPUS stimulation and sham treatment. The analysis of serum-free conditioned medium revealed a significant decrease in TGF- $\beta$  levels following LIPUS stimulation compared to the sham-treated cells (Figure 5.3 B, indicated by "\*",  $p < 0.05$ ). In contrast, the western blot of the cell lysate showed no significant difference in TGF- $\beta$  expression between the LIPUS-treated and sham-treated groups (Figure 5.3 A, indicated by "ns"). This suggests that the changes in TGF- $\beta$  expression induced by LIPUS are primarily reflected in the secreted pool, rather than being retained within the cells' cytoplasm. This result indicates that, contrary to the observed increase in LOX expression in the extracellular environment, LIPUS-stimulation leads to a reduction in TGF- $\beta$  expression in conditioned medium. Therefore, while LIPUS-stimulation does not alter intracellular TGF- $\beta$  levels, it significantly decreases its presence in the extracellular environment, contrasting with the effects seen on LOX.

A)



B)



C)

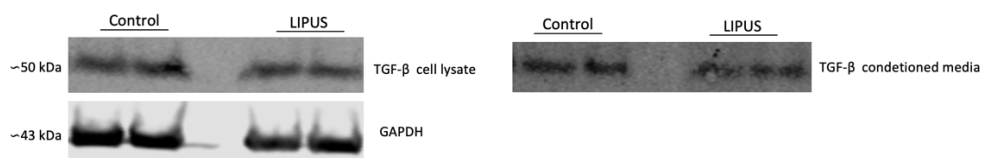


Figure 5.3 Protein expression of TGF- $\beta$ .

Sham-treated and LIPUS-stimulated using TIF cell line. A) There was no significant change in the cell lysate protein expression of TGF- $\beta$ . B) Decrease in the TGF- $\beta$  protein expression in conditioned medium compared to sham-treated sample C) The western blot bands for TGF- $\beta$ . (n=4). Error bars represent SEM. Statistical significance was calculated using a t-test.

### 5.2.3 Cell-derived matrix

In order to investigate how cells interact with LIPUS-treated matrix and how this can affect the migrating behaviour, A CDM experiment was conducted. In this experiment, HFF cells were seeded into two 6-wells plate and divided into LIPUS-stimulated (for 20 mins/day for 5 days) and sham treated matrix. They were then left to grow until confluency to produce a rich matrix. To verify that the ECM remained intact after decellularization before TIF reseeding, the CDM-coated surfaces were examined under phase-contrast microscopy. This step was carried out in consultation with my supervisor to ensure that the ECM layer was visibly present prior to

reseeding. This visual inspection served as a qualitative control to confirm ECM retention throughout the experimental process. At the day of imaging, TIF cells were seeded over the matrix and left for about 4 hours to spread and start migrating on the CDM. After that, cells were taken to the microscope and left for live imaging for 16 hours.

In order to investigate the cells migration, Figure 5.4 presents a sequence of images taken from a video showing cell migration over a 16-hour period under a microscope. The images were captured at 0 hours, 8 hours, and 16 hours.

The result revealed that cells traveled longer and in a straight line on the LIPUS treated matrix, compared to the sham treated matrix as they seemed to travel shorter distance and in a more random way (Figure 5.6 and Figure 5.7). A total of 16 cells were measured for each condition and the persistence was calculated as follows: Directional Persistence=
$$\frac{\text{Net Displacement}}{\text{Total Path Length}}.$$

#### 5.2.4 Collagen III knockdown CDM

##### Persistence and total distance

To gain a deeper understanding of LIPUS's effects on the extracellular matrix, collagen III was specifically knocked down in the HFF used to generate the matrix. This approach ensured that the reduction of collagen III occurred in the matrix itself, rather than in the migrating cells, allowing us to isolate and examine the role of LIPUS in ECM remodelling without influencing the behaviour of the migrating cells. Collagen III plays a critical role in the early stages of wound healing by promoting tissue flexibility and reducing scar formation. Our previous findings (chapter 4) have shown that LIPUS increases collagen III deposition, which suggests that LIPUS may enhance the healing process by fostering a regenerative environment. Therefore, by knocking down collagen III, we aimed to investigate how this alteration affects

the role of LIPUS in ECM remodelling and healing, allowing us to better understand the mechanism behind LIPUS's impact on collagen dynamics and tissue repair.

In this knockdown experiment, two different conditions were applied: one matrix was exposed to LIPUS stimulation, while the other served as a control and received no treatment. In the matrix stimulated with LIPUS, cells migrated a longer distance, but they did not move in a completely straight line, often changing or reversing direction. In contrast, cells in the sham treated matrix migrated shorter distances and followed a random path, frequently oscillating back and forth (Figure 5.5).

The directional persistence and total distance of all tracked cells under the four conditions: the sham-treated matrix, the LIPUS-treated matrix, and the LIPUS and sham-treated collagen III knockdown matrix (Col III KD) (Figure 5.8).

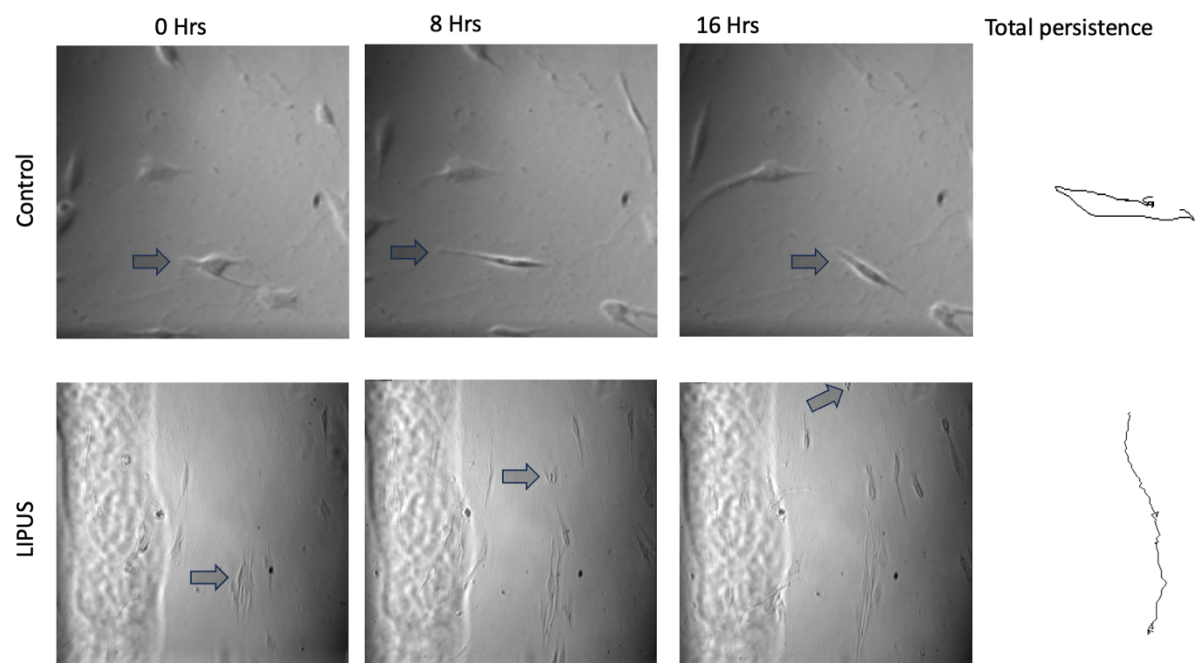
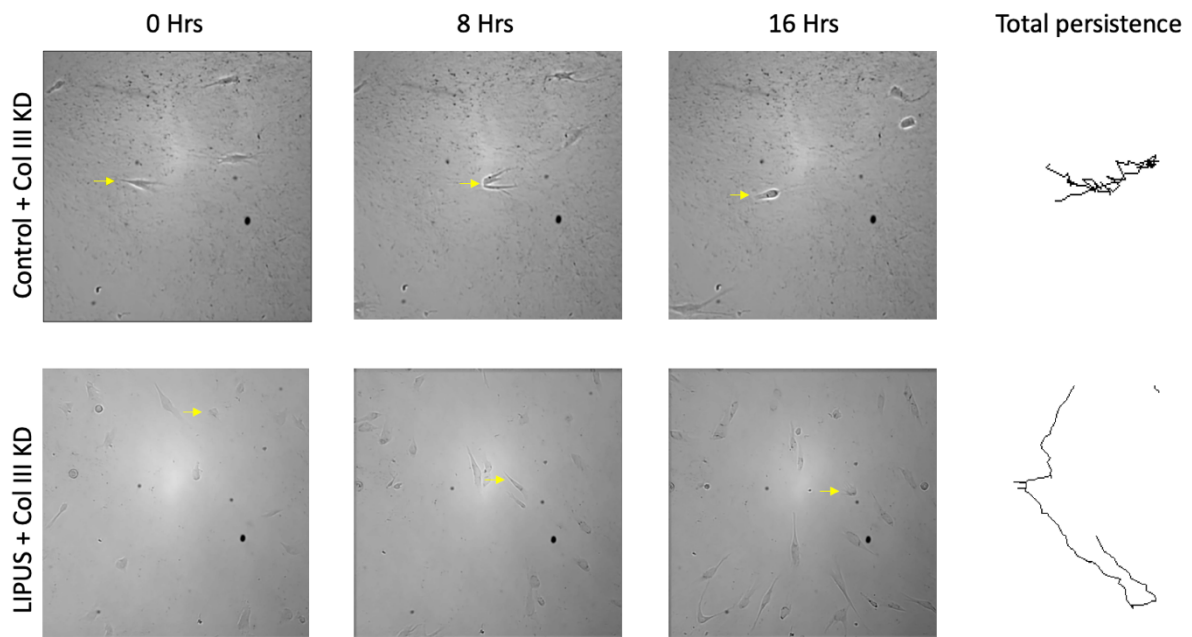


Figure 5.4 Cells migrating over the sham-treated and LIPUS-stimulated matrix

A live illustration of cells migrating throughout 16 hours. Arrows indicate the movement of individual cells. Scale bar = 256  $\mu\text{m}$ .

A)



B)

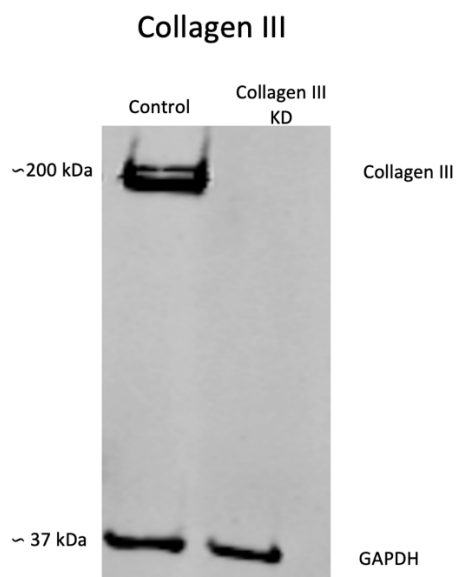


Figure 5.5 Cells migration over 16 hours with and without Collagen III knockdown.

A) a live illustration of collagen III knockdown matrix for the sham-treated and LIPUS-stimulated matrix. Arrows indicate the movement of individual cells. Scale bar = 256  $\mu\text{m}$ .

B) Western blot analysis of collagen III expression following knockdown. Protein from cells transfected with either control siRNA (Control) or collagen III-targeting siRNA (Collagen III KD)

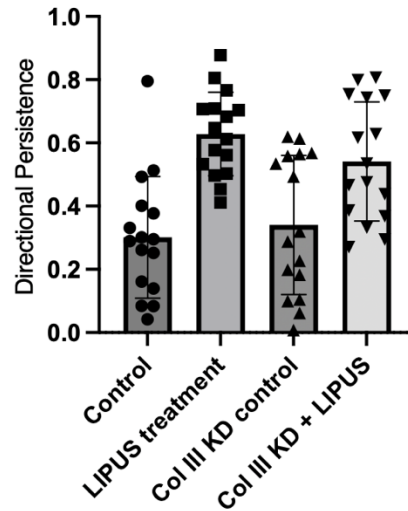


Figure 5.6 Bar chart of the total cells' directional persistence.

Total cells' directional persistence on Sham-treated and LIPUS-stimulated matrix with and without collagen III knockdown. (cells counted for each condition= 16). Data are from a single biological replicate. Statistical significance was not calculated due to the limited sample size.

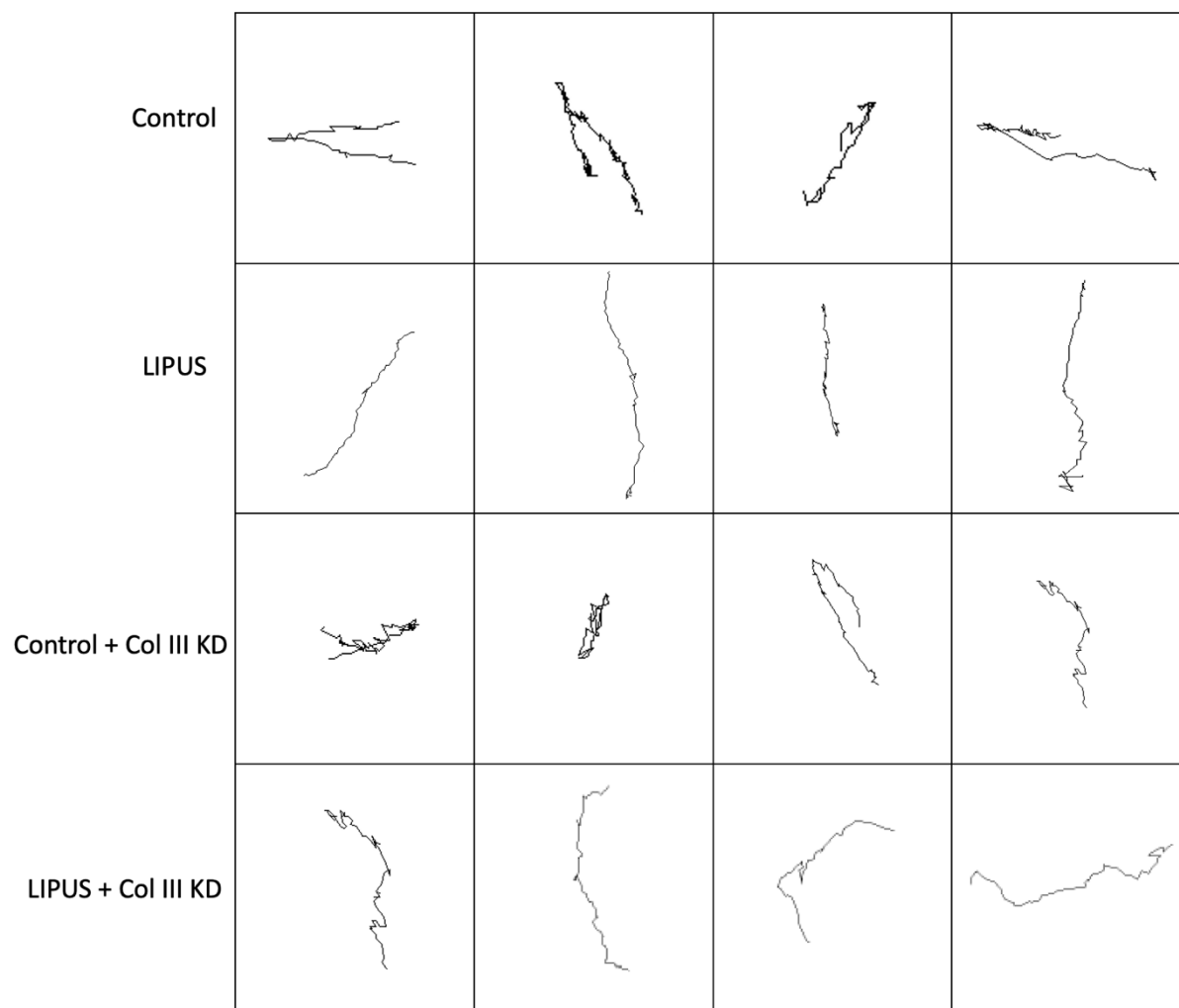


Figure 5.7 Cells migrating on matrix.

Cells movement over 16 hours on sham-treated and LIPUS-stimulated matrix with and without collagen III knockdown.

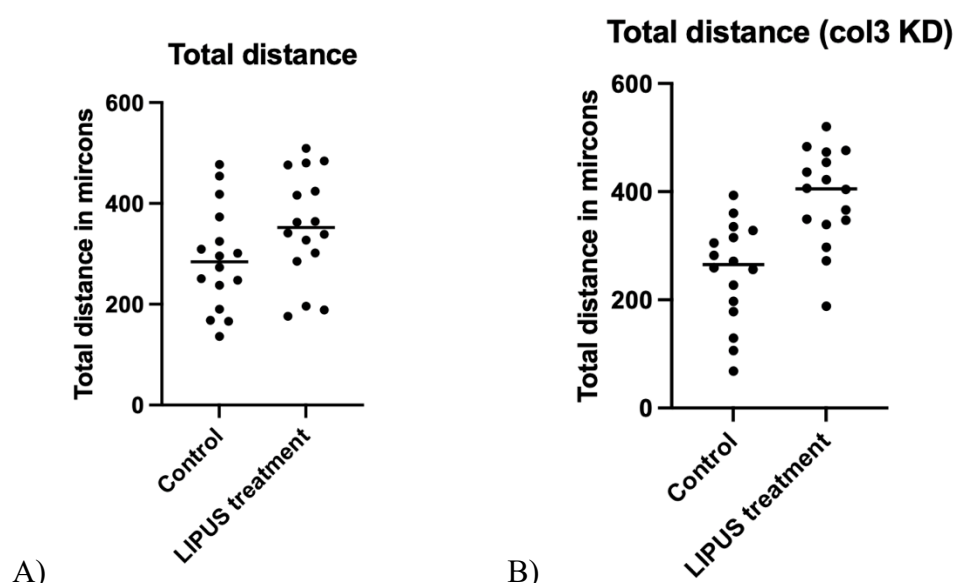


Figure 5.8 Cells total distance.

Total distance for cells migration on sham-treated and LIPUS-stimulated matrix without collagen III knockdown (cells counted for each condition=16) and B) with collagen III knockdown (Col III KD) (cells counted for each condition=16). Data are from a single biological replicate. Statistical significance was not calculated due to the limited sample size.

### 5.2.5 Traction Force Microscopy

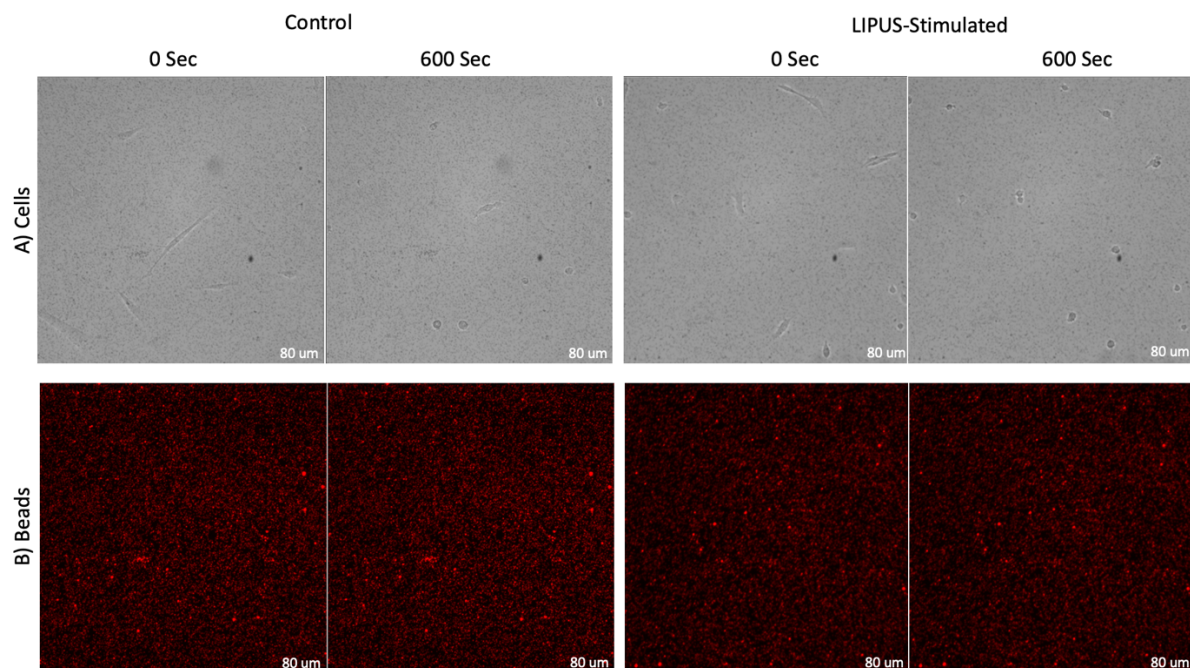
To investigate the impact of LIPUS stimulation on cellular mechanics, we employed TFM to quantify the traction stresses exerted by cells on a soft substrate. In the previous chapter, we reported changes in matrix organisation following LIPUS treatment, which are likely influenced not only by matrix composition but also by the application of tension by cells. Given that our data showed a reduction in TGF- $\beta$  levels with LIPUS, and considering TGF- $\beta$ 's role in promoting cell contractility, we hypothesised that LIPUS would reduce cellular contractility. This hypothesis aligns with our observation of increased matrix curvature in LIPUS-treated samples, suggesting a decrease in cellular tension. Thus, this section aims to explore whether the reduction in TGF- $\beta$  correlates with decreased contractility, tying together the result of reduced TGF- $\beta$  expression and the production of altered matrix architecture, with traction force measurements providing crucial insight into the mechanics driving these changes.



In this experiment, cells were seeded on PAA gels, which were coated with fibronectin to facilitate cell adhesion. The cells were allowed to adhere and spread and left to be either stimulated with LIPUS or sham treated. Then, on the fifth day, cells were subsequently trypsinised to remove them from the substrate under live imaging microscope. The experiments included both sham-treated cells, which served as a control group, and LIPUS-stimulated to examine the effects of the specific intervention.

Bead displacements were calculated using particle image velocimetry (PIV) implemented in ImageJ. The resulting displacement fields were input into the Fourier Transform Traction Cytometry (FTTC) plugin assuming a Poisson's ratio of 0.5 and known gel stiffness of 8 kPa.

The analysis revealed a non-significant difference in the traction stresses between the sham-treated and LIPUS-stimulated cells. Specifically, sham-treated cells exerted an average traction stress of 962 Pa. In contrast, LIPUS-Stimulated cells exhibited a lower traction stress, with an average value of 619 Pa (Figure 5.9).



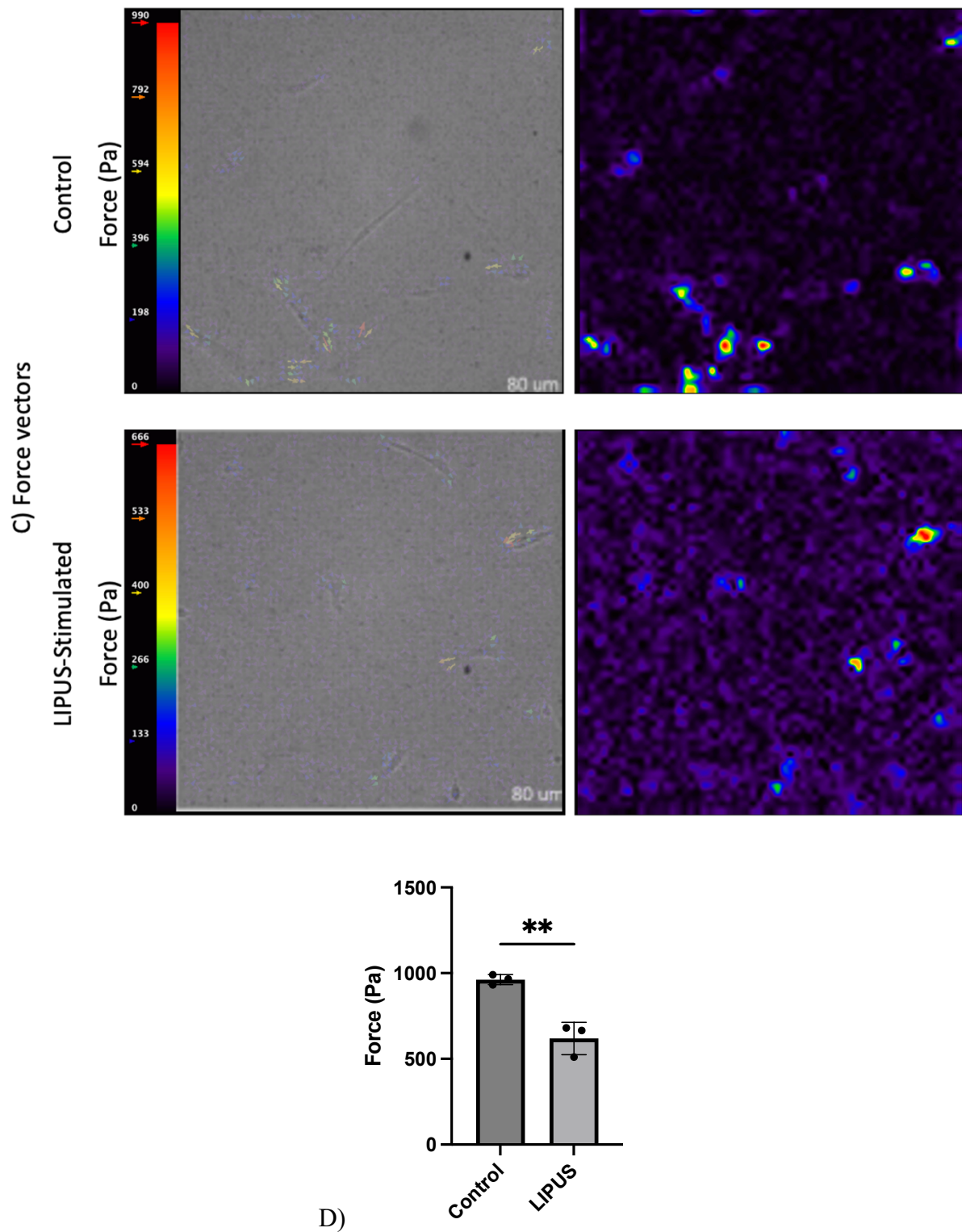


Figure 5.9 TFM experiment.

A) Cells seeded on the plate covered with fibronectin. B) the beads embedded within the PAA gel. C) Includes a merged panel overlaying traction force vectors and cell outlines to show the spatial relationship between force application and cell position determined using the PIV plug-in (left). Then, the FTTC plug-in was used to calculate the traction force exerted by the cell, which causes gel deformation and bead movement (right). D) 'Force' represents the total traction stress integrated over the entire image field, calculated from bead displacement

caused by cellular traction. (n=3 independent biological replicates with one representative image analysed per replicate. Each image contains multiple cells (approx. 5–10 per field). Error bars represent SEM. Statistical significance was calculated using a t-test.

## 5.3 Discussion

### 5.3.1 Alternative mechanisms for regulating matrix organisation

Matrix organisation can be significantly influenced by mechanical forces applied through cellular contractility or by the biochemical cross-linking between matrix fibres. Cellular contractility, driven by actin-myosin interactions within cells such as fibroblasts or myofibroblasts, generates tension that can reorganise and align ECM fibres (Muntz et al., 2022). Additionally, cross-linking enzymes like LOX play a crucial role in stabilising the ECM by creating covalent bonds between collagen and elastin fibres, enhancing the matrix's mechanical strength and resistance to deformation (Yue, 2014). Together, these processes ensure that the ECM maintains both flexibility and durability, enabling it to respond to mechanical and biochemical signals during tissue development, repair, and remodelling.

### 5.3.2 The role of Lysyl Oxidase (LOX) in matrix cross-linking

Fibroblasts are essential for responding to injury, driving key processes such as tissue contraction, remodeling, and maturation during wound healing, fibrosis, and abnormal scarring. In cases of skin wounds, excessive fibroblast activity can result in tissue contracture, as fibroblasts are primary producers of collagen, ECM components, and LOX (Szauter et al., 2005). LOX facilitates collagen fiber cross-linking, which is essential for ECM stabilisation and maturation (Kim et al., 2011). Collagen, rich in lysine and hydroxylysine residues, undergoes covalent cross-linking through LOX activity, forming a stable, interwoven fibrillar network that enhances tissue strength and resilience (Kong et al., 2021).

In fibroblast-mediated collagen gel contraction models, inhibiting LOX with BAPN did not impact the immediate contraction forces driven by cells but significantly reduced delayed contraction, which relies on collagen cross-linking. Moreover, during later contraction phases,

LOX-mediated collagen cross-linking was independent of fibroblast density, demonstrating the enzyme's critical role in ECM remodeling (Redden and Doolin, 2003). Additionally, during collagen synthesis, LOX showed a similar expression pattern to collagen type III, activating the collagen 3A1 promoter—a process completely blocked by BAPN inhibition (Szauter et al., 2005; Giampuzzi et al., 2000).

Following tissue injury, the upregulation of LOX coincides with increased collagen cross-linking, which helps mature the ECM into complex, organised structures to restore tensile strength (Nuthakki et al., 2004). Collagen remodelling continues for months after wound closure, ultimately restoring tensile strength to about 80-85% of normal tissue if the healing process is uninterrupted (Mathew-Steiner et al., 2021). Our findings suggest that LIPUS stimulation enhances LOX levels in conditioned medium, indicating a boost in ECM remodeling stage, as observed in earlier figures. This increase in LOX expression may support more efficient tissue repair through enhanced cross-linking and ECM stabilisation.

### 5.3.3 Transforming growth factor-beta (TGF- $\beta$ ) affects scarring

Studies have shown that fibroblasts from hypertrophic scars display a distinct phenotype compared to those from normal scars or uninjured skin. Wang et al. (2000) demonstrated that fibroblasts from hypertrophic scar tissue produced significantly higher levels of TGF- $\beta$ 1 mRNA and protein than fibroblasts from normal skin or those derived from it. This indicates that TGF- $\beta$ 1 may contribute to the development of hypertrophic scars. Moreover, a study by Shah et al. (1995) demonstrated that treating wounds in animal models with antibodies against TGF- $\beta$ 1 and TGF- $\beta$ 2 led to a significant reduction in immune cell infiltration, particularly monocytes and macrophages. Based on our data, this is a crucial insight as LIPUS has been shown to lower TGF- $\beta$  expression, potentially shifting the wound healing process away from the hypertrophic scar phenotype, which is typically driven by excessive TGF- $\beta$  activity. By

reducing TGF- $\beta$ , LIPUS may encourage a more balanced healing response, promoting proper ECM remodelling and reducing the risk of excessive scarring.

In a study by Atsawasuwan et al. (2008), it was shown that LOX directly interacts with mature TGF- $\beta$ 1 *in vitro*, forming a binding complex present in the mineralized bone matrix. Furthermore, the study revealed that LOX can inhibit TGF- $\beta$ 1 signaling through its amine oxidase activity. This interaction between LOX and TGF- $\beta$ 1 is particularly important in the context of wound healing and tissue repair, as excessive TGF- $\beta$ 1 activity is often associated with fibrosis and hypertrophic scarring. Given that LIPUS has been shown to increase LOX levels in conditioned medium, it suggests that LIPUS may enhance the beneficial effects of LOX in modulating TGF- $\beta$ 1 activity, thereby reducing fibrosis and promoting a more controlled wound healing response.

By reducing TGF- $\beta$ 1 signalling, LIPUS could help create a more favourable healing environment, preventing the excessive collagen deposition and fibrosis typically associated with hypertrophic scars. This could explain why LIPUS not only accelerates healing but also potentially shifts the process away from a scar-heavy outcome. Thus, LIPUS fits into the therapeutic process by its effects on both LOX and TGF- $\beta$  pathways, offering a dual benefit of faster and less scar-prone healing. Our results showed a reduction in the expression of TGF- $\beta$ , which can be beneficial toward wound healing and reduce the effect of scarring. This reduction can be explained by the increase in the LOX expression which we demonstrated earlier. However, several questions remain, particularly regarding the specific mechanisms by which LIPUS influences the TGF- $\beta$  pathway and its downstream effects on fibroblast activity and collagen synthesis. Next steps should focus on further exploring these connections. For Instance, to test whether blocking LOX activity in the context of LIPUS treatment would reverse the observed reduction in TGF- $\beta$ 1 expression, reinforcing the link between LOX and TGF- $\beta$ 1 regulation.

#### 5.3.4 CDM migration

Cells anchor themselves to the extracellular matrix (ECM) through transmembrane adhesion receptors like integrins, which link the cytoskeleton to matrix components such as fibronectin. Intracellular adhesion structures, such as focal adhesions (FAs) and podosomes, create these connections. However, if adhesion to the matrix is excessive, cell movement is restricted, causing immobility. On the other hand, weak adhesion or insufficient mechanical resistance leads to uncontrolled sliding on the matrix, hindering or stopping cell migration (Pfisterer et al., 2021). Before moving, migratory cells use filopodia or lamellipodia at their leading edge to explore the ECM, allowing them to assess the matrix's topography, stiffness, and anchoring points. Once these assessments are complete, the cells retract their filopodia and switch to a migration mode that does not rely on them. A key signalling mechanism in this process involves the generation of forces between the cells and the matrix. Cells detect forces on the ECM, triggering Rho GTPase signalling and myosin contractility, which aids in migration (Pfisterer et al., 2021).

Collagen and fibronectin are arranged into aligned fibres that guide fibroblast migration in a linear direction within the dermis. This structure can be replicated *in vitro* by lysing fibroblasts from a cultured monolayer, leaving behind a cell-derived matrix. This model enables detailed study of how migrating cells move along the fibres, with migration persistence assessed by calculating the ratio of the cell's straight-line displacement to the total distance travelled (Roper et al., 2015). Wild-type cells exhibit persistent migration over the cell-derived matrix, while in knocked down Syndecan-4 fibroblasts migrate randomly due to dysregulated Rac1 signalling (Bass et al., 2007). To enable effective cell migration, it is crucial to establish a rear-front Rac1 gradient. When syndecan-4 is knocked down, it leads to a uniform distribution of Tiam1, which can subsequently result in the improper activation of Rac1 (Becsky et al., 2020).

To elaborate, Roper et al. (2015) demonstrated that ultrasound can activate Rac1 independently of the typical fibronectin pathway seen in healthy fibroblasts (Figure 5.10).

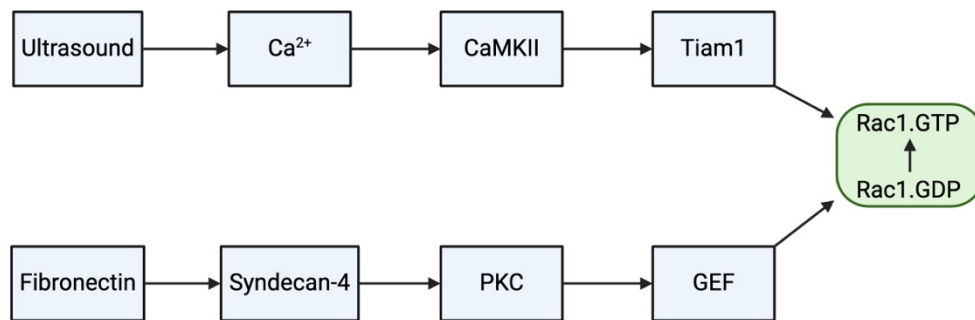


Figure 5.10 Mechanical (ultrasound) and chemical (fibronectin) stimuli activate Rac1.

The activation of Rac1 through different pathways (Created in BioRender.com with adaption from Roper et al., 2015).

While our result is preliminary data, we found matrix deposited by LIPUS-stimulated cells led to a longer and more directed cell migration distance compared to the control group. Unlike in previous studies where the ultrasound was applied directly to the cells, our approach involved modifying the extracellular matrix itself. LIPUS-stimulated matrix appears to have enhanced the alignment and guidance properties of the fibres, promoting a persistent and linear migration pattern in the cells. This suggests that altering the matrix can influence cell behaviour in a manner similar to the modulation of Rac1 signalling within cells, as highlighted by Roper et al. (2015), but through an external modification of the cell environment rather than a direct cellular intervention.

### 5.3.5 Traction Force Microscopy

Wound healing typically involves three distinct phases: inflammation, proliferation, and remodelling. During the proliferative phase, contraction occurs as a cell-rich granulation tissue form. Contraction plays a crucial role in wound healing by facilitating wound closure. While it is beneficial in narrowing the wound margins and promoting closure, excessive contraction can have negative consequences. It may lead to the formation of undesirable contractures and

scarring, which can result in both cosmetic and functional issues (Li and Wang, 2011). Biochemical signalling and mechanical characteristics are fundamental to cell proliferation, differentiation, and metabolism (Yue, 2014).

Focusing specifically on how cells respond to mechanical properties, there is a clear correlation between fibroblast activity and the mechanical attributes of the substrate. This relationship highlights the critical role of fibroblasts in wound healing, matrix deposition, and the associated positive feedback loop that contributes to fibrosis. During healing processes, fibroblasts are essential for generating forces and depositing the matrix, both of which are crucial for effective tissue repair (Li and Wang, 2011; Chen et al., 2007). A suitable amount of force is required to allow cells to maintain adequate tissue function and deposit new matrix (Li and Wang, 2011).

It has been demonstrated that a reduction in wound contraction leads to minimized scar formation and enhances the process of epithelialization (Penn et al., 2014). By investigating the effects of LIPUS-stimulation on cellular properties, we gain a deeper understanding of its influence on cellular contractility. The traction force microscopy results demonstrated a significant reduction in cellular traction forces following LIPUS stimulation (962 Pa and 629 Pa) for the sham-treated cells and LIPUS-stimulation, respectively. This indicates that the treatment profoundly impacts the mechanical properties of the cells and reduce contractility. Also, this observation is consistent with the observed decrease in TGF- $\beta$  levels we presented earlier, suggesting that LIPUS affects cellular contractility.

In summary, the results presented in Chapters 4 and 5 demonstrate that LIPUS influences molecular composition and organisation through the expression of key proteins. Specifically, the following changes were observed: a reduction in the expression of Collagen I and TGF- $\beta$ , alongside an increase in LOX, Collagen III, and Fibronectin. The matrix also showed a more disorganised and random alignment compared to that of the sham-treated cells. Additionally,



the traction force microscopy results suggest a potential reduction in substrate deformation in LIPUS-stimulated cells compared to sham-treated controls. Summary of the LIPUS effect on ECM molecules illustrated in Figure 5.11.

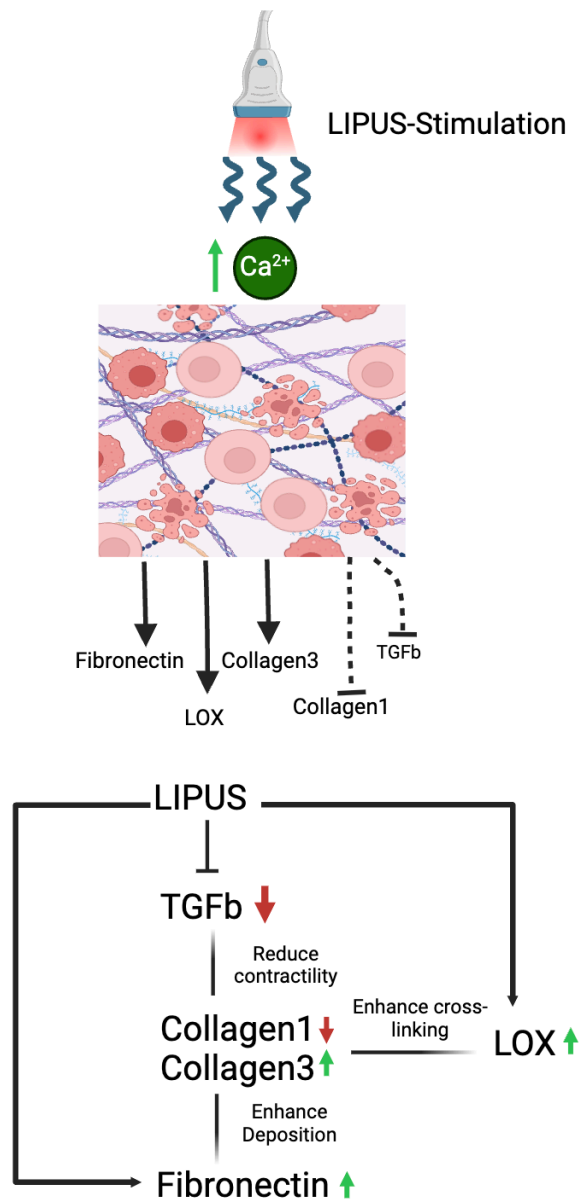


Figure 5.11 Summary of the LIPUS effect on the candidate proteins.

# **Chapter 6**

## **Discussion**

## Chapter 6 Discussion

### 6.1 Effect of LIPUS as a therapy tool on fibroblast

Low-intensity ultrasound (LIUS) is a type of mechanical energy transmitted to tissues and cells via acoustic waves. These waves create physical forces that activate ion channels on the cell surface and modify cell membrane permeability (Hormozi-Moghaddam et al., 2021). Research has outlined an intricate network of signalling pathways activated by acoustic pulsed energy in primary fibroblasts, demonstrating that ultrasound-induced proliferation is dependent on the activation of  $\beta 1$  integrins and the Rac1, RhoA/ROCK- and Src-ERK signaling pathways (Zhou et al., 2004).

Bohari et al. (2015) conducted a study where LIPUS stimulation was administered for 5 minutes each day over a period of 10 days, using a frequency of 1 MHz and an intensity of 0.2 W/cm<sup>2</sup> with a 20% duty cycle. They found that for Human Dermal Fibroblast (HDF) cells, LIPUS may promote an increase in cell numbers, but this effect was observed only in the absence of TGF- $\beta 1$  and ascorbic acid. This suggests that short-term LIPUS stimulation can acutely influence fibroblast proliferation under specific conditions. However, it is essential to also consider how long-term LIPUS treatments may influence broader fibroblast behaviour, particularly in relation to matrix remodelling and extracellular signalling.

In another study, Mostafa et al. (2009) applied LIPUS treatment (1.5 MHz, 30 mW/cm<sup>2</sup>) to human gingival fibroblasts (HGF) for either 5 or 10 minutes per day over a 28-day period. They found no significant changes in cell viability, proliferation, or in the expression of PCNA and collagen I, however, the absence of immediate changes in cell proliferation does not rule out the possibility of long-term ECM remodelling, as evidenced by my results. Also, as previously reported that acute responses to LIPUS were observed. Also, acute responses to LIPUS were observed at earlier stages of Rac1 activation with a single stimulation (Mahoney et al., 2009).

Cárdenas-Sandoval et al. (2023) used LIPUS at 1 MHz with a 1:1 ratio (1 ms on, 1 ms off), corresponding to a 50% duty cycle, applied every 24 hours for 5 days, to two treatment groups: low dose (1.0 W/cm<sup>2</sup>) and high dose (2.0 W/cm<sup>2</sup>). Atomic force microscopy (AFM) revealed that the median elastic modulus of the treated ligament fibroblasts decreased by 22% at the low dose (1.0 W/cm<sup>2</sup>) and by 31% at the high dose (2.0 W/cm<sup>2</sup>) relative to the control group. The scratch assay showed that after 5 days of ultrasound stimulation, the mean migration length of ligament fibroblasts increased by 4% in the low-dose group and decreased by 11% in the high-dose group compared to the control. However, by the sixth day after treatment, none of the groups, including the control, expressed sufficient type I or type III collagen protein, making the results of this study inconclusive.

In a study by Zhang et al. (2003), a single 20-minute LIPUS stimulation at 30 mW/cm<sup>2</sup> was applied to assess the viability and gene expression of chondrocytes. The results showed no change in cell viability, but there was an increase in type II collagen production and inhibition of type X collagen. Also, a study by Saito et al. (2004) applied LIPUS for 17 days at two different intensities (30-120 mW/cm<sup>2</sup>) on MC3T3-E1 cells. They observed an upregulation of LOX mRNA specifically at the 30 mW/cm<sup>2</sup> intensity.

The previous studies showed promising results of LIPUS as a therapy. However, variations existed in regards the intensities, stimulation time and the targeted area. In the current study, I showed when LIPUS was applied to fibroblasts for 5 days, 20-minutes treatment each day, notable alterations in key ECM components were observed, which may hint at a longer-lasting signal generated by short bursts of LIPUS stimulation. These cumulative changes suggest that short, daily LIPUS treatments can shift fibroblast behaviour towards an adaptive, long-term remodelling response. Specifically, collagen I and TGF- $\beta$  expression, alongside an increase in collagen III, fibronectin, and LOX. These findings suggest that even relatively short-term LIPUS treatments may induce significant shifts in fibroblast ECM organisation, moving

towards a matrix profile that supports tissue remodelling rather than stable fibrosis. The decrease in collagen I and increase in collagen III, combined with the reduction in TGF- $\beta$ , align with a less fibrotic and more regenerative ECM environment. The upregulation of fibronectin and LOX further supports this remodelling hypothesis, indicating alterations in matrix assembly and cross-linking over time.

Building on this foundation, this PhD thesis focused on exploring the potential of LIPUS-stimulation to modulate ECM, cross-linking and organisation, with the aim of understanding its subsequent effects on wound healing and scar formation by using a frequency of 1.5 MHz, an intensity of 30 mW/cm<sup>2</sup> (SATA), a 20% duty cycle pulse, and a treatment duration of 20 minutes per day for 5 consecutive days. These parameters were chosen based on a careful consideration of existing literature to balance efficacy in stimulating ECM deposition and organisation. The following sections will delve into the results, providing insights of how LIPUS-stimulation specifically impacts the candidate ECM proteins which can contribute to improved wound healing outcomes by altering these molecules expression.

## 6.2 Exploring the Impact of LIPUS on Extracellular Matrix Composition and Alignment

### 6.2.1 Regulation of fibronectin expression highlights changes in ECM structure and function

Wound healing is a complex and dynamic process that involves the coordinated interaction of various cells and molecules, progressing through distinct phases: haemostasis, inflammation, proliferation, and remodelling. Fibronectin, an essential adhesive molecule, plays a pivotal role throughout these stages, primarily by facilitating cellular adhesion (Lenselink, 2015). It serves as a foundational scaffold for collagen deposition, which is critical for proper wound healing. The absence of a functional fibronectin matrix at the wound site can lead to impaired or unsuccessful healing (Maione et al., 2016). Moreover, a study by Serezani et al. (2017) revealed

that IL-4 stimulation significantly suppresses fibronectin expression, critically impairing wound healing in human keratinocytes. This finding emphasises the essential role of fibronectin, as the suppression delays re-epithelialisation in mouse models of Atopic Dermatitis. Topical application of fibronectin was found to effectively restore the epidermal repair process, in a study by Qiu et al., (2007) their findings suggest that Plasma Fibronectin (pFn) enhances the healing of full-thickness skin wounds in rats. Initially, pFn appears to enhance the migration of macrophages, myofibroblasts, and fibroblasts. Migrating fibroblasts start producing collagen, which plays a crucial role in the healing process. Furthermore, the release of TGF- $\beta$  from activated fibroblasts and keratinocytes may enhance the beneficial effects of fibronectin on wound repair.

However, excessively high levels of fibronectin have been associated with negative outcomes, including poor wound healing and fibrosis (Stoffels et al., 2013; Kubow et al., 2015). Interestingly, in aged MuSCs, reduced levels of fibronectin contribute to decreased cell numbers, impaired functionality, and compromised maintenance, similar to what is observed in young fibronectin knockout MuSCs. Restoration of fibronectin levels in aged mice has been shown to rejuvenate the young MuSC phenotype. This leads to an increase in cell numbers, improved muscle maintenance, and enhanced functionality (Patten and Wang, 2021; Lukjanenko et al., 2016).

Fibronectin is a component of the fibrin clot and is later linked with the newly formed collagen fibrils (Hoffmann and Smith, 2019). The importance of fibronectin is further indicated by its close association with the collagen III matrix during the proliferation phase of wound healing. The deposition of fibronectin into the ECM controls the deposition of type I collagen (Grinnell et al., 1981; Shi et al., 2010), which highlights the importance of fibronectin when damage occur to the skin and maintain a proper wound healing.

Our finding that LIPUS stimulation increases fibronectin expression offers new insights into wound healing, highlighting fibronectin's essential role in cellular adhesion and collagen deposition. By stimulating fibronectin production within the wound, rather than just applying it externally, we may improve the healing process and enhance the formation of a proper collagen matrix. This could be especially impactful in cases where low fibronectin levels contribute to impaired healing. However, questions remain to answer, for instance, do wounds with low fibronectin levels respond more effectively to LIPUS? Additionally, does the absence of fibronectin, such as in fibronectin knockout models, block the healing response to LIPUS because fibronectin is no longer available to be expressed? These questions could deepen our understanding of fibronectin's role and LIPUS's potential in wound therapy.

### 6.2.2 Differential Regulation of Collagen I and III Reflects ECM Composition Changes

Collagen I, classified as a coarse fibre, is typically considered a structural scaffold that helps maintain the mechanical strength of the skin. It also plays a crucial role as a key component of the reticular fibres within the skin's interstitial tissue. On the other hand, Collagen III, a finer fibre, usually coexists alongside Collagen I, contributing to the skin's elasticity (Gao et al., 2023).

The balance and interaction between these collagens are essential, as highlighted by various studies. In this context, a study conducted by Cheng et al. (2011) illustrated age-related differences in the collagen type I/III ratio. They found that the overall collagen levels in healthy skin decline with age, with a noticeable reduction in type III collagen specifically. This leads to a gradual rise in the type I/III ratio, potentially linked to increased stiffness and the formation of permanent scar tissue. When analysing hypertrophic scar tissue, they found that overall collagen content, especially type I, was significantly higher than in uninjured skin. This finding aligns with a study by Gao et al. (2023), which noted an increase in the collagen I to collagen

III (COL-I/COL-III) ratio as age advanced, followed by stabilisation. At week 0, the COL-I/COL-III ratio was 1.3:1, but by weeks 9 to 18, it had risen to 4.5–4.9:1. The total amount of collagen I and III increased from week 0 to week 9, then began to decrease with age. This shift occurred because the relative content of collagen I continued to rise from week 0 to week 18, while collagen III steadily declined, reflecting the reduced elasticity and increased wrinkling associated with aging. This supports the observation that skin becomes less elastic, and wrinkles become more prominent as we age (Lovell et al., 1987).

Further evidence from Volk et al. (2011) supports the importance of collagen III in regulating collagen I synthesis, as mice lacking collagen III due to a genetic deficiency showed increased myofibroblast differentiation and significant wound contraction. This supports the idea that a higher ratio of collagen III to collagen I is linked to scarless foetal wound healing, as observed in several mammal models (Merkel et al., 1988), underscoring the critical balance of collagen types in skin integrity and repair.

LIPUS stimulation exhibits a unique modulatory effect on the ECM by selectively enhancing the expression of collagen III while simultaneously reducing collagen I levels. This shift in collagen composition alters the structural and functional properties of the ECM, as collagen III is associated with a more flexible, less dense matrix, in contrast to the more rigid, tightly packed structure formed by collagen I. This regenerative shift not only promotes tissue elasticity but also mirrors the collagen profile of younger, healthier skin, highlighting the potential value of LIPUS in accelerating wound repair and improving outcomes by reducing susceptibility to fibrosis and long-term scarring.

### 6.2.3 LIPUS Effect on Matrix Alignment

Fibronectin fibrils create linear and branched networks around cells, linking neighbouring cells together. In vivo, fibronectin is present in developing tissues before collagen is deposited. Since collagen can bind to fibronectin, the timing and spatial relationship between fibronectin and



collagen indicates that fibronectin may serve as a scaffold leading to align collagen fibrils (Singh et al., 2010). Fibronectin matrix organises cells in a way that ensures collagen fibrils are aligned, thereby aiding the formation of parallel collagen fibres. Additionally, the fibronectin matrix might direct the contraction of the actomyosin contractile apparatus that would affect cellular tension to ensure collagen fibrils are deposited in parallel alignment (Singh et al., 2010; Plotnikov et al., 2012). A study by Das et al., (2021) where they used bioengineered model system, they have illustrated that there was a correlation between ECM alignment and provisional matrix growth during gap closure. However, the slower growth of the provisional matrix along highly aligned edges in rectangular microtissues could be due to ECM fibres guiding cell migration along these aligned fibres, preventing them from moving into the gap. In less aligned ECMs, cells migrate more randomly, which might help them move into the gap more easily.

Our findings revealed that LIPUS significantly alters matrix organisation by enhancing the curvature of ECM fibres, resulting in a more randomly meshed structure rather than a highly aligned one. This observation suggests that LIPUS may disrupt the typical alignment of ECM components, such as fibronectin fibrils, which are known to create linear and branched networks that link neighbouring cells and guide collagen fibril alignment (Singh et al., 2010). The shift toward a more randomly organised ECM could influence cellular behaviour by allowing cells to migrate in a less constrained manner, potentially facilitating their movement into gaps within the tissue. This outcome contrasts with the effects seen in highly aligned ECMs, where cells tend to migrate along the aligned fibres, potentially slowing gap closure as observed in the study by Das et al. (2021).

## 6.3 Impact of LIPUS on matrix cross-linking and cellular mechanics: insights into LOX activity, TGF- $\beta$ signaling, and cell-matrix interactions

### 6.3.1 Altered LOX Expression Reflects Changes in ECM Remodeling Dynamics

LOX initiates the cross-linking process of collagen and elastin, a critical step for establishing the mechanical properties of the ECM and tissues (Avery and Bailey, 2008). Typically, collagen type I is the primary component of the ECM, with other types of collagens making up only a small fraction, for example, collagen type III comprises just 10% in the skin. However, this balance shifts after an injury. Collagen I levels decrease, while collagen III levels significantly rise. The early surge in collagen type III mRNA is a characteristic response to wounding (Cai et al., 2007). This increase in collagen type III expression is closely linked with the rise in LOX following skin injury, where the peak in LOX mRNA occurs several days before that of collagen type III. These findings suggest that LOX is produced in advance of collagen synthesis to prepare for cross-linking during the early stages of wound healing (Cai et al., 2007).

The increase in collagen cross-linking aligns with the upregulation of LOXs following tissue injury (Nuthakki et al., 2004). Several studies have explored methods to accelerate tissue healing by enhancing LOX expression during the acute phase post-injury. Pathi et al. (2012) demonstrated that following the injection of mesenchymal stem cells at the injury site, there was a significant increase in LOX expression, which linked to increased collagen deposition. Additionally, Olaso et al., (2011) reported that mice deficient in discoidin domain receptor-2, which exhibited lower LOX levels, had impaired dermal wound healing responses. These findings suggest that LOX could be a promising target for improving healing outcomes.

Our findings revealed that LIPUS selectively increases LOX expression in the conditioned medium, but not within the cell lysate. This can be attributed to the fact that synthesised LOX is secreted rather than retained inside the cell, explaining its elevated levels outside the cellular

environment. The increased LOX in conditioned medium could potentially accelerate the cross-linking of collagen and elastin, supporting tissue integrity and recovery, similar to the effects observed with mesenchymal stem cell injections (Pathi et al., 2012). When combined with the earlier findings of LIPUS increasing collagen III expression, the increased LOX-driven cross-linking contribute to a more regenerative ECM environment. These changes collectively steer the wound healing process toward an optimal outcome, accelerating recovery while reducing fibrosis and enhancing tissue strength. This connection highlights that the various effects observed are not isolated but work together to promote more efficient and effective tissue repair.

### 6.3.2. LIPUS modulates cell migration dynamics on cell-derived matrices, highlighting ECM influence on cellular behaviour

ECM and cells are two primary components of the tissues. When a cell migrates into a tissue, it encounters various physical cues within the ECM, which can influence and alter its migration strategy accordingly (Le and Mayor, 2023).

Cell migration is more efficient and directional on aligned matrices, whereas random alignment disrupts orientation and slows migration. In a study by Wang et al., (2018) they explored the impact of ECM alignment on cell migration speed and persistence, comparing highly aligned ( $\pm 5^\circ$ ) and non-aligned ( $\pm 90^\circ$ ) patterns. It was observed that cells on aligned patterns maintained an elongated shape and demonstrated more persistent and faster migration compared to cells on non-aligned patterns. Also, Riching et al., (2014) demonstrates that aligned collagen restricts protrusion formation, leading to more persistent cell migration.

Roper et al., (2015) illustrated in their study that ultrasound stimulation had no impact on the speed of wild-type fibroblasts and did not significantly enhance their persistence, as these fibroblasts already demonstrate linear migration (Figure 6.1 ).

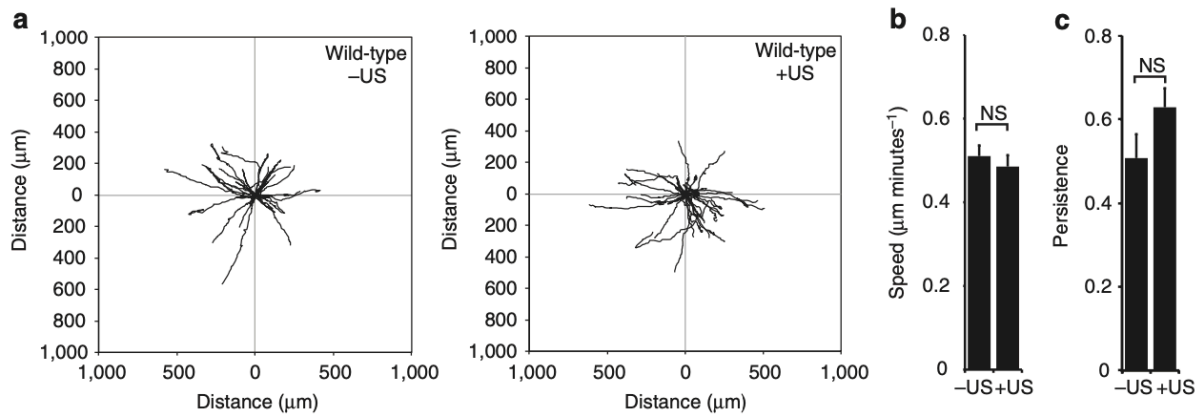


Figure 6.1 Sham- or ultrasound (US)-treated wild-type (a–c). (Images are from Roper et al., 2015)

My new findings are complementing those of Roper et al., (2015). LIPUS migration assays demonstrated that cells travelled greater distances and followed straighter paths when the cells themselves stimulated with LIPUS. This thesis now shows when cells are stimulated with LIPUS during matrix deposition, the resultant matrix also induces migration that is faster and follows a straight path. This new finding suggests that LIPUS-induced ECM modifications promote more directed cell movement. While Roper's study did not achieve statistical significance, our results align with the same trend, reinforcing the idea that LIPUS exerts a directional effect. This effect seems to operate in two ways: first, by stimulating cells during the creation of the matrix, and second, by enhancing cell migration across the modified ECM. The enhanced migration on LIPUS-treated matrices could potentially improve tissue repair dynamics by guiding cells more effectively to the wound site. Notably, even when collagen III was knocked down in the cells used to synthesise the matrix, LIPUS-treatment of those cells still resulted in increased migration distances in the subsequent migration analysis. This finding demonstrates that the effect of LIPUS is not mediated by collagen III alone and underscores the robust impact of LIPUS-modified ECM on cellular behaviour.

### 6.3.3 Modulation of TGF- $\beta$ expression highlights changes in fibrotic signalling pathways

LOX is regulated by TGF- $\beta$ 1 and several other factors throughout the repair process, including during the remodelling phase (Cai et al., 2017). Fibrosis and impaired wound healing are widespread issues with limited treatment options. Scars are characterised by the excessive deposition of dysfunctional ECM, which hinder tissue regeneration during wound healing. TGF- $\beta$  signalling plays a pivotal role in these processes, indicating that targeting this pathway could improve wound healing outcomes and reduce scarring (Lichtman et al., 2016; Finnson et al., 2013).

In a study conducted by (Noble et al., 1992) researchers observed that targeting TGF- $\beta$  with inhibitors in injured glomeruli led to normal healing. This suggests that blocking TGF- $\beta$ , which typically leads to excessive matrix deposition in injured tissue, is not detrimental but rather beneficial to tissue repair, as it helps prevent the damaging effects of scarring.

Also, it is likely that excessive TGF- $\beta$  levels restricted to the epidermal layer at the ulcer's edge could play a role in the wound's chronic nature (Liarte et al., 2020). Also, a study by Lee et al., (2012), where they used keloids fibroblast as a model, they found a strong correlation between the increased cells rigidity and TGF- $\beta$  and SMA. In chronic wounds the dysregulation of TGF- $\beta$  which characterised by raised levels in the epidermis and reduced levels in the dermis, contributes to the chronicity of wounds by maintaining an inflammatory environment and disrupting the normal wound healing processes, highlighting the complexity of TGF- $\beta$ 's role in wound healing (Liarte et al., 2023) (Figure 6.2).

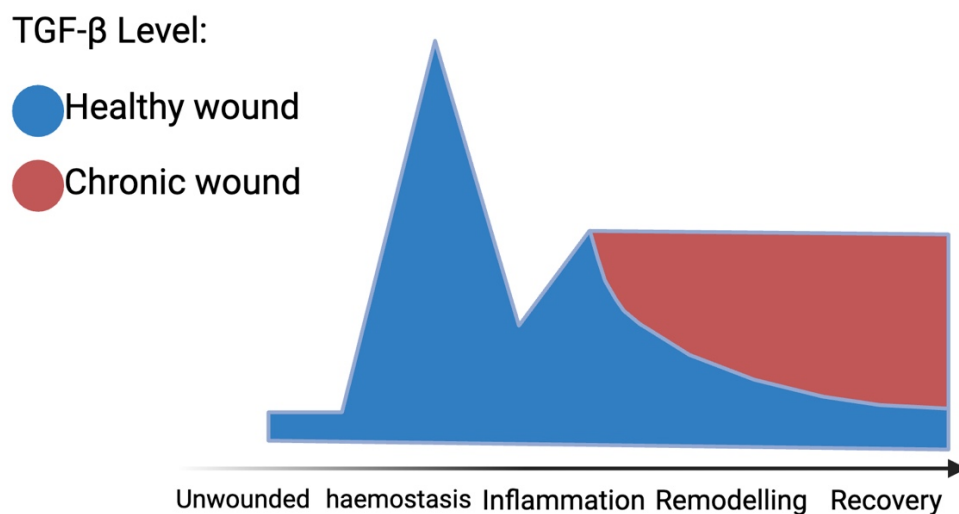


Figure 6.2 The amount of TGF- $\beta$  in the epidermis

Fluctuates of the TGF- $\beta$  throughout the different stages of wound healing (Created in BioRender.com with adaption from Liarte et al., 2023).

Our findings demonstrated that TGF- $\beta$  levels were reduced in the conditioned medium but remained unchanged in the cell lysate after the LIPUS-stimulation. This reduction of TGF- $\beta$  in the extracellular environment suggests that LIPUS may modulate the TGF- $\beta$  signalling pathway in a way that could potentially mitigate excessive ECM deposition and fibrosis, a common issue in impaired wound healing. By lowering TGF- $\beta$  levels in the conditioned medium, LIPUS could help balance the pro-inflammatory and reparative phases of wound healing, thereby promoting a more favourable healing environment and reducing the risk of chronic wounds or excessive scarring. This aligns with the potential therapeutic benefits of targeting TGF- $\beta$  pathways, as suggested by studies using decorin to block TGF- $\beta$ , which showed normal healing without the adverse effects of fibrosis (Noble et al., 1992). Since TGF- $\beta$  plays a crucial role in promoting fibroblast differentiation into myofibroblasts—marked by the expression of  $\alpha$ -SMA and the development of contractile properties (Marconi et al., 2021)—we sought to evaluate  $\alpha$ -SMA expression after LIPUS treatment to further understand

broader effects of modified TGF- $\beta$  activity. However, our measurements of  $\alpha$ -SMA expression were inconsistent, making it difficult to draw firm conclusions from the data (See appendices, Figure 7.1).

#### 6.3.4 Traction force analysis reveals altered force generation following LIPUS stimulation

It is widely understood that mechanical forces surrounding cells are closely connected to cellular functions, affecting each other in both physiological and pathological contexts (Ingber et al., 2003; Hahn et al., 2009). These cellular forces can either be generated within the cells, known as endogenous forces, conveyed through actin stress fibres, or be exerted on the cells from external sources, referred to as external forces (Hur et al., 2020). Research on mechanical forces has focused on the role of integrin-mediated FAs as key mechanotransducers, connecting actomyosin stress fibres to cell culture substrates of different stiffness, whether based on the extracellular matrix ECM or polymers (Hur et al., 2020).

Adherent cells use actomyosin-generated forces transmitted through focal adhesions to the ECM. TGF- $\beta$ 1 promotes fibroblast differentiation into myofibroblasts and increases  $\alpha$ -SMA expression (Vallée and Lecarpentier, 2019). Myofibroblast traction force has been shown to increase by the expression of  $\alpha$ -SMA (Hinz et al. 2001). Also, Chen et al. (2007) found that  $\alpha$ -SMA expression greatly enhances these forces in myofibroblasts. Using TFM to measure the cell traction force is crucial, as it can indicate different pathological condition, such as wound healing and fibrosis. For instance, fibrosis results from increased traction forces generated by the excessive myofibroblast (Wang and Lin, 2007).

Our results from TFM, using 8 kPa stiffness PAA gel to simulate soft tissue (skin) rigidity, revealed that cells stimulated with LIPUS exhibited lower traction stress compared to sham-treated cells, suggesting a potential decrease in cellular contractility. This finding suggests that LIPUS-induced ECM remodelling, likely mediated by increased LOX expression, may

decrease the mechanical forces exerted by cells, which could influence the fibroblast-to-myofibroblast transition, which is a process heavily regulated by TGF- $\beta$  signalling (Desmoulière et al., 1993). This reduction in traction stress aligns with our observation of reduced TGF- $\beta$  expression in the conditioned medium, pointing to a shift that may mitigate fibrotic signalling pathways. These results are consistent with previous studies showing that elevated TGF- $\beta$  levels enhance  $\alpha$ -SMA expression and myofibroblast traction forces (Campbell et al., 2004; Hinz et al., 2001). By modulating these mechanical forces and ECM interactions, LIPUS may not only improve tissue repair by enhancing cell migration on aligned matrices, as observed previously in our experiments, but also potentially reduce pathological ECM deposition and fibrosis.

TFM was performed using fibronectin-coated PAA gels with a stiffness of 8 kPa, selected to mimic the mechanical properties of soft biological tissues. Imaging was conducted at 10x magnification to balance resolution and field of view to enable the detection of traction forces while maintaining spatial context across multiple cells. Differences between PAA and traditional glass substrates, such as deformability and surface characteristics, can affect cell behaviour, including spreading and traction generation. PAA is widely recognised as a linearly elastic material across a broad range of strains and can be tuned to specific stiffness values (ranging from ~0.2 to 150 kPa), making it a versatile choice for mechanobiology studies. Additionally, its surface can be selectively functionalised with extracellular matrix proteins, such as fibronectin, to promote cell adhesion (Denisin et al., 2024). While alternative substrates, such as silicone-based polymers or gelatine are available, PAA was chosen for its reproducible mechanical properties and established use in TFM protocols (Sigaut et al., 2021). Although fibronectin coating supported strong cell adhesion and traction generation, we cannot directly confirm whether cells produced or organised their own ECM during the experiment, as endogenous ECM components were not labelled. The TFM data allow us to assess where



and how cells exert forces on the substrate, but do not capture ECM remodelling or distinguish force contributions at the individual cell level.

## 6.4 Limitations

Identifying appropriate controls for secreted protein normalisation remains a challenge, as few stable, constitutively secreted proteins exist. Alternatives, such as total protein normalisation of conditioned medium or the use of exogenous controls, may provide more direct normalisation but come with their own technical limitations. This limitation highlights the broader issue of standardising normalisation methods in secretome analysis.

Another limitation of this study is that certain experiments, including the directional persistence and total distance analyses, were based on a single biological replicate and should therefore be considered preliminary data. Due to the limited sample size, statistical analysis was not performed for these datasets, and the observed trends require further validation through additional replicates. While the findings suggest a potential effect of LIPUS on matrix-guided cell migration, definitive conclusions cannot be drawn without a larger dataset. Future studies should aim to increase the number of biological replicates to ensure the robustness and reproducibility of the results, allowing for statistical comparisons and stronger conclusions regarding the impact of LIPUS on extracellular matrix organisation and cell behaviour.

TFM reconstructions are often affected by limited data sampling and noise during image acquisition, which can reduce the accuracy of the measured traction forces. In this study, one limitation is the assumption that the polyacrylamide gel behaves as a perfectly linear elastic material, which may not fully reflect real tissue mechanics. We did not perform single-cell segmentation, so the measured force represents the total per image rather than being normalised to individual cells. In addition, as we did not label endogenous ECM proteins, we could not assess matrix deposition or remodelling by the cells. Despite these limitations, TFM remains a powerful tool for quantifying cell–substrate interactions.

## 6.5 Future Direction

Building on our findings, several key follow-up investigations arise for future research. A critical question is whether the effects of LIPUS on wound healing, such as the modulation of collagen I and III, can be replicated by knocking down TGF- $\beta$ , or if blocking TGF- $\beta$  can prevent the effects of LIPUS. Additionally, further investigation is needed into how altered TGF- $\beta$  expression influences  $\alpha$ -SMA levels, providing deeper insight into LIPUS's role in enhancing cellular contractility. Additionally, what is the impact of this blocking on matrix alignment, cellular contractility, and migration, as this factor is essential for effective tissue repair. Also, while LIPUS has opposing effects on collagen I and III expression, TGF- $\beta$  stimulates both which raise questions about the mechanisms underlying this difference, for instance, are collagens I and III regulated independently, or do they influence each other's expression? Furthermore, it's important to investigate whether LIPUS induces the same effects on collagen expression in vivo, and if these changes result in altered tensile strength of healed skin, potentially improving the quality of repair. Addressing these questions will help clarify the broader implications of LIPUS in wound healing and provide a foundation for future therapeutic strategies.

The TFM data presented here enable the visualisation and quantification of cellular traction forces exerted on 8 kPa polyacrylamide substrates under both control and LIPUS-stimulated conditions. From these data, it can be concluded that cells generate substrate deformations indicative of traction stress, and that LIPUS treatment may influence the magnitude and spatial distribution of these forces. To strengthen and extend these findings, future experiments could incorporate live-cell TFM to capture the dynamic nature of cellular force generation. Analysing isolated cells or segmenting force maps per cell would also allow more precise quantification of individual traction profiles. Additionally, increasing the number of image fields per biological replicate would enhance the statistical robustness of the analysis.

## 6.6 Conclusion

This PhD thesis presents novel insights into how LIPUS uniquely modulates the ECM, significantly influencing tissue remodelling and organisation using frequency of 1.5 MHz, an intensity of 30 mW/cm<sup>2</sup>, a 20% duty cycle pulse and a treatment duration of 20 minutes per day for 5 consecutive days. LIPUS stimulation was found to increase collagen III and fibronectin levels while reducing collagen I, thereby reshaping the ECM's composition. Furthermore, LIPUS significantly alters matrix organisation by enhancing the curvature of ECM fibres, resulting in a more randomly meshed structure rather than a highly aligned one.

Our findings demonstrate that LIPUS increases LOX expression in the conditioned medium, which may suggest a potential role in promoting collagen cross-linking and contributing to ECM remodelling. In contrast, TGF- $\beta$  levels were reduced in the conditioned medium, suggesting an attenuation of fibrotic signalling pathways often implicated in excessive matrix deposition and fibrosis. Cell migration assays revealed that cells travelled longer distances and in straighter paths on stimulated matrices, indicating that the ECM changes induced by LIPUS promote more directed cell movement, which could improve tissue repair dynamics. Even with collagen III knockdown, cells on the LIPUS-treated matrix still migrated longer distances, highlighting the robust impact of LIPUS-modified ECM on cellular behaviour. Traction force microscopy showed a reduction in traction stresses in LIPUS-treated cells, further suggesting that the altered ECM environment reduces cellular contractility and modifies mechanotransductive feedback, potentially impacting fibroblast-myofibroblast differentiation. Collectively, these findings illustrate that LIPUS significantly modulates ECM composition, organisation, and mechanical properties, offering a novel therapeutic strategy to enhance healing, minimise scarring, and improve the quality of regenerated tissues.

## Chapter 7 Appendices

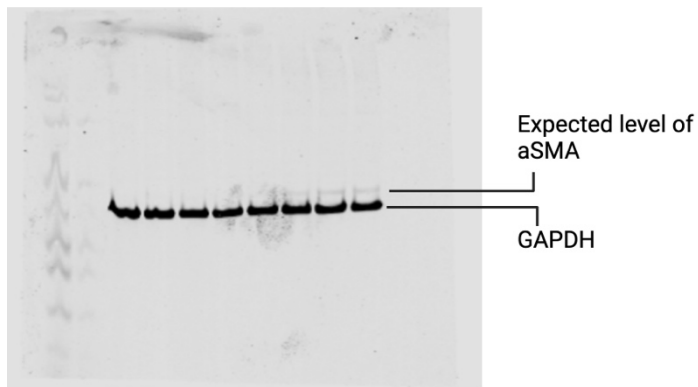


Figure 7.1 aSMA Western blot gel with GAPDH.

The aSMA bands either did not appear or showed only a very faint band.

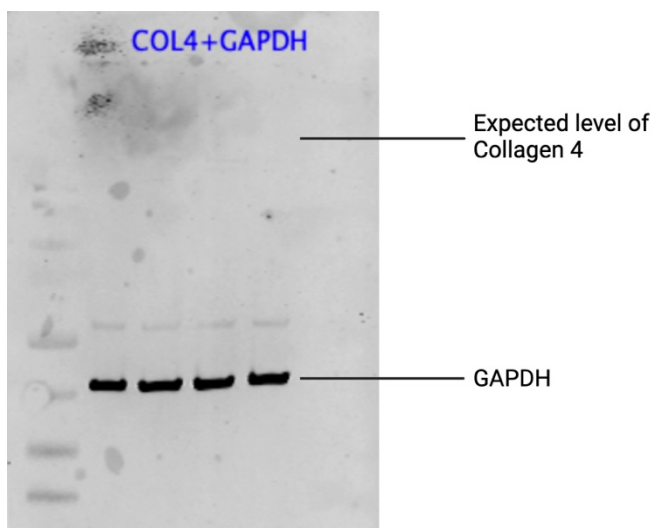


Figure 7.2 Collagen 4 Western blot gel with GAPDH.

No bands appeared for the collagen 4.

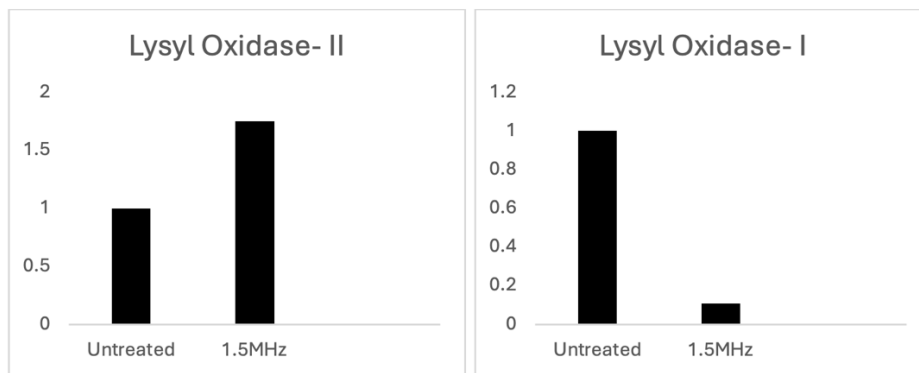


Figure 7.3 qPCR of LOX (n=2).

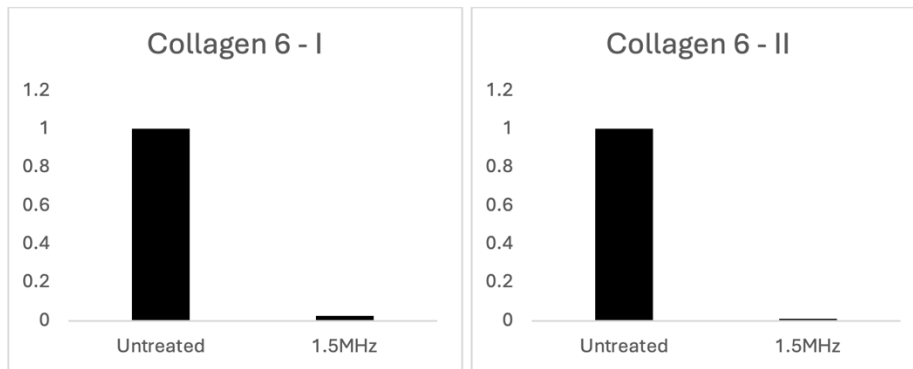


Figure 7.4 qPCR of collagen 1 (n=2).

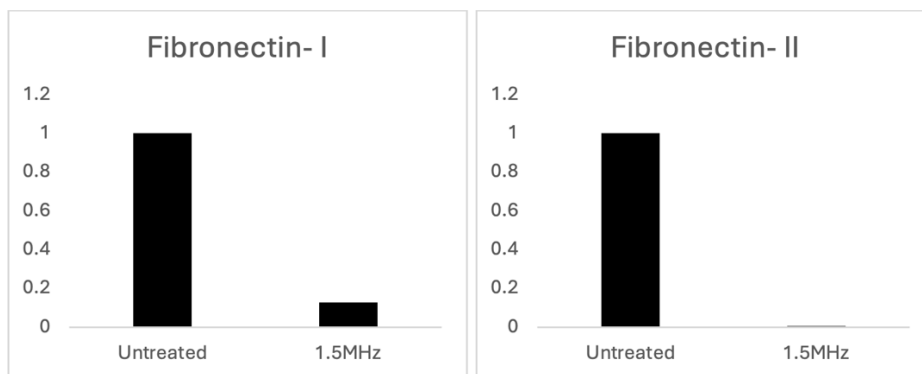


Figure 7.5 qPCR of fibronectin (n=2).

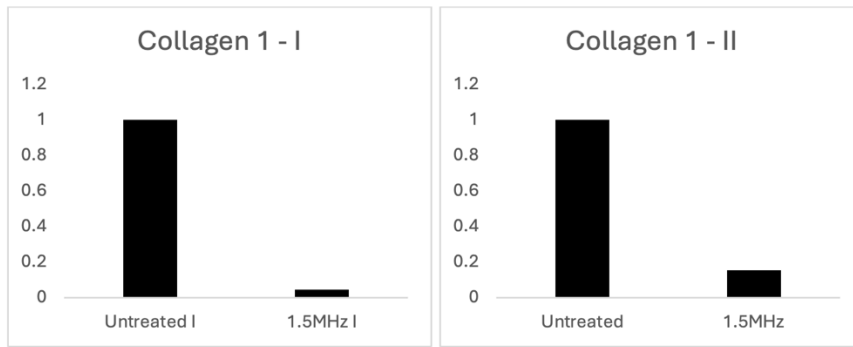


Figure 7.6 qPCR of collagen 6 (n=2).

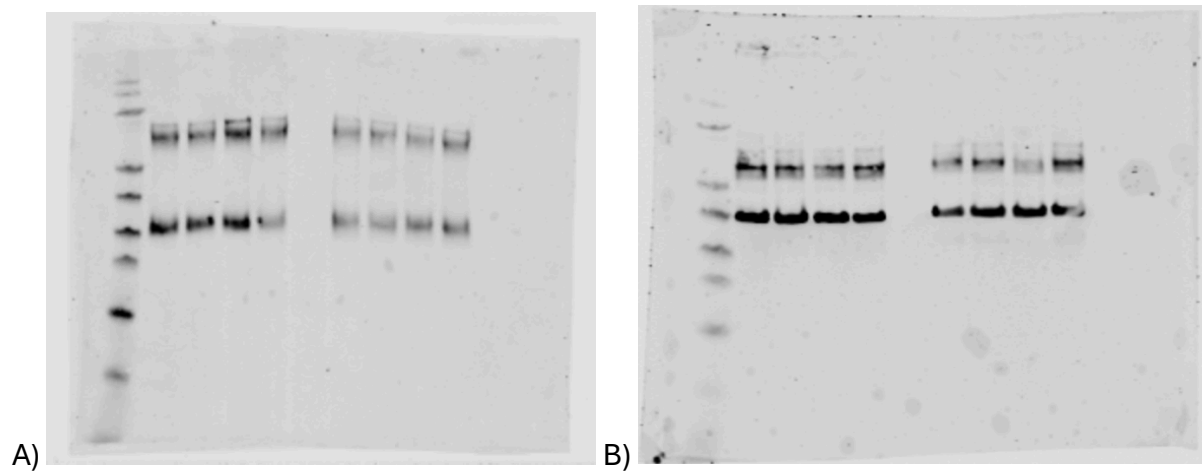


Figure 7.7 Western blot gels for A) conditioned medium and B) cell lysate LOX.

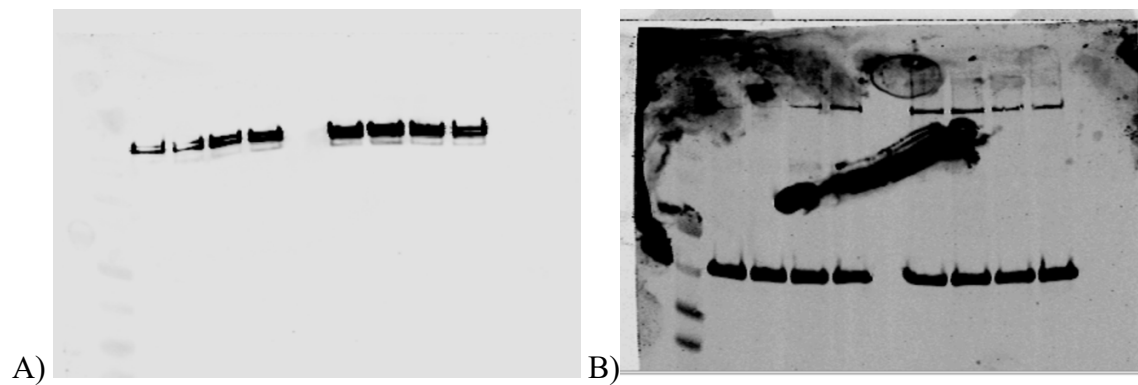


Figure 7.9 Western blot gels for A) conditioned medium Col I and B) GAPDH from cell lysate.

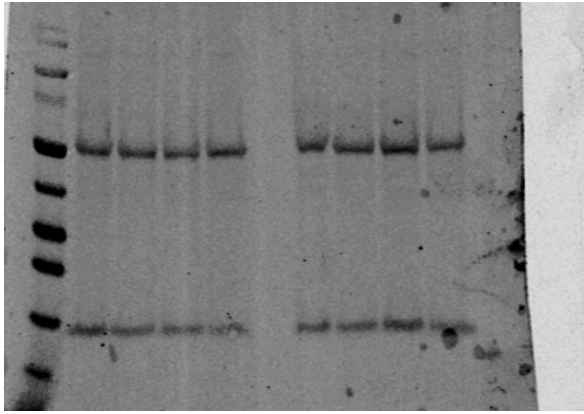


Figure 7.10 Western blot gels for conditioned medium TGFb.

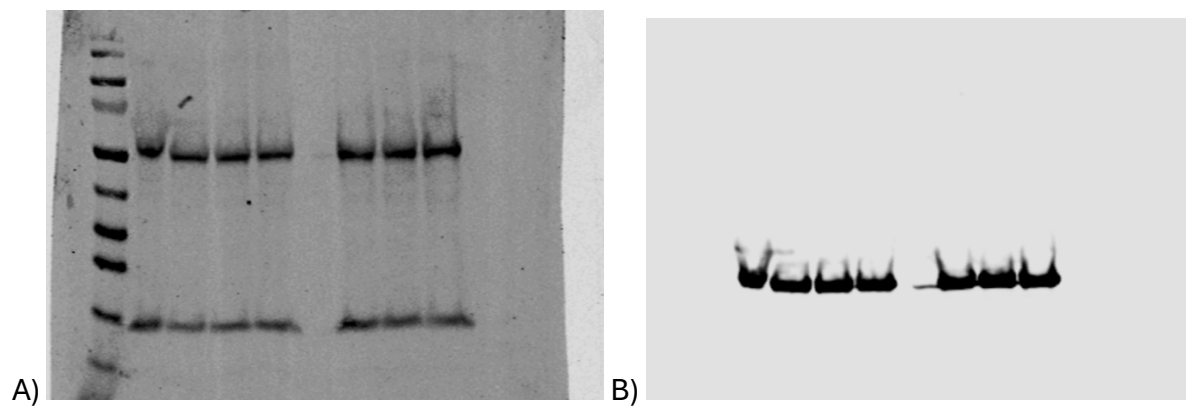


Figure 7.11 Western blot gels for A) cell lysate TGFb and B) GAPDH.

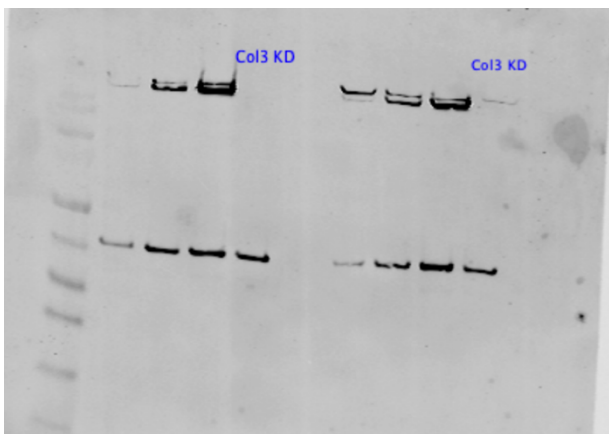


Figure 7.12 Western blot gels for Col3 KD.

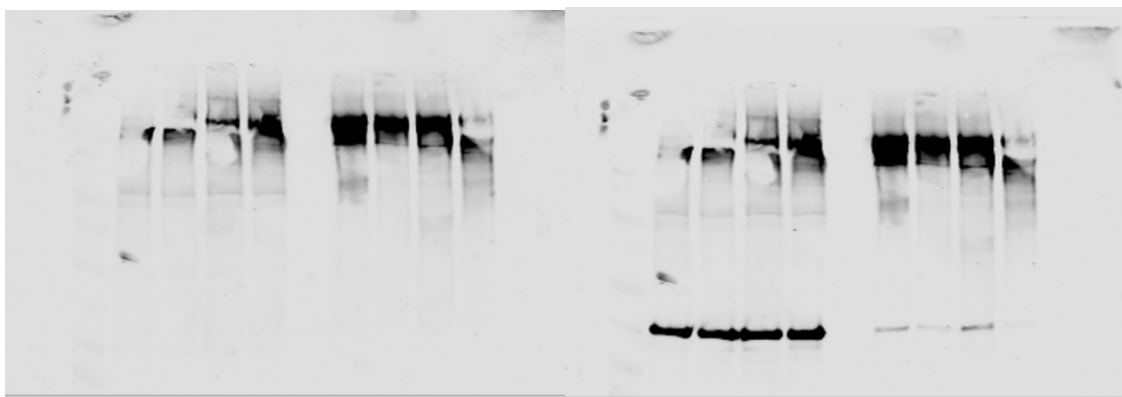


Figure 7.13 Western blot gels for A) Fibronectin Conditioned medium and B) with GAPDH.

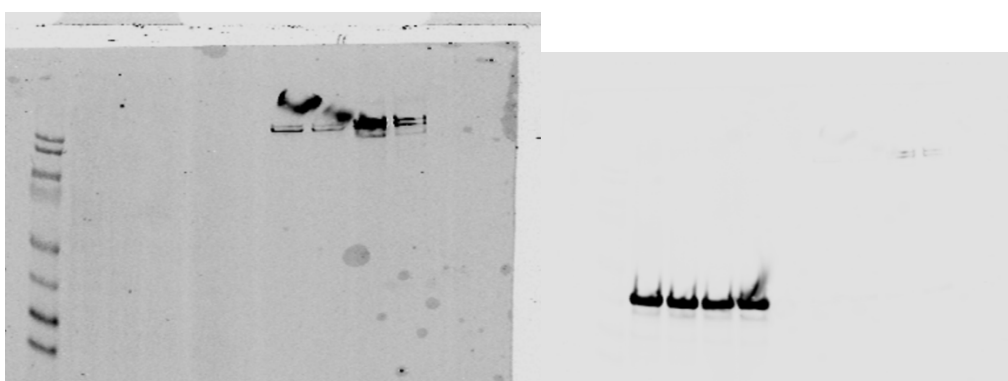


Figure 7.14 Western blot gels for A) Col III Conditioned medium and B) with GAPDH.



## References

- Abreu-Velez, A.M. and Howard, M.S., 2012. Collagen IV in normal skin and in pathological processes. *North American journal of medical sciences*, 4(1), p.1.
- Abu-Zidan, F.M., Hefny, A.F. and Corr, P., 2011. Clinical ultrasound physics. *Journal of emergencies, trauma, and shock*, 4(4), pp.501-503.
- Al Ameri, W., Ahmed, I., Al-Dasim, F.M., Ali Mohamoud, Y., Al-Azwani, I.K., Malek, J.A. and Karedath, T., 2019. Cell type-specific TGF- $\beta$  mediated EMT in 3D and 2D models and its reversal by TGF- $\beta$  receptor kinase inhibitor in ovarian cancer cell lines. *International journal of molecular sciences*, 20(14), p.3568.
- Alharbi, R.A., 2020. Proteomics approach and techniques in identification of reliable biomarkers for diseases. *Saudi Journal of Biological Sciences*, 27(3), pp.968-974.
- Almine, J.F., Wise, S.G. and Weiss, A.S., 2012. Elastin signaling in wound repair. *Birth Defects Research Part C: Embryo Today: Reviews*, 96(3), pp.248-257.
- Angelini, A., Trial, J., Ortiz-Urbina, J. and Cieslik, K.A., 2020. Mechanosensing dysregulation in the fibroblast: a hallmark of the aging heart. *Ageing research reviews*, 63, p.101150.
- Atherton, P., Lausecker, F., Harrison, A. and Ballestrem, C., 2017. Low-intensity pulsed ultrasound promotes cell motility through vinculin-controlled Rac1 GTPase activity. *Journal of Cell Science*, 130(14), pp.2277-2291.
- Atsawasuwan, P., Mochida, Y., Katafuchi, M., Kaku, M., Fong, K.S., Csiszar, K. and Yamauchi, M., 2008. Lysyl Oxidase Binds Transforming Growth Factor- $\beta$ ; and Regulates Its Signaling via Amine Oxidase Activity. *Journal of Biological Chemistry*, 283(49), pp.34229-34240.
- Avery, N.C. and Bailey, A.J., 2008. The effects of the Maillard reaction on the physical properties and cell interactions of collagen. *Pathologie Biologie*, 56(5), pp.405-413.
- Bae, Y.K., Kim, A., Kim, M.K., Choi, J.E., Kang, S.H. and Lee, S.J., 2013. Fibronectin expression in carcinoma cells correlates with tumor aggressiveness and poor clinical outcome in patients with invasive breast cancer. *Human pathology*, 44(10), pp.2028-2037.

Baker, K.G., Robertson, V.J. and Duck, F.A., 2001. A review of therapeutic ultrasound: biophysical effects. *Physical therapy*, 81(7), pp.1351-1358.

Bao, L., Cai, X., Zhang, M., Xiao, Y., Jin, J., Qin, T. and Li, Y., 2022. Bovine collagen oligopeptides accelerate wound healing by promoting fibroblast migration via PI3K/Akt/mTOR signaling pathway. *Journal of Functional Foods*, 90, p.104981.

Barrientos, S., Stojadinovic, O., Golinko, M.S., Brem, H. and Tomic-Canic, M., 2008. Growth factors and cytokines in wound healing. *Wound repair and regeneration*, 16(5), pp.585-601.

Bass, M.D., Roach, K.A., Morgan, M.R., Mostafavi-Pour, Z., Schoen, T., Muramatsu, T., Mayer, U., Ballestrem, C., Spatz, J.P. and Humphries, M.J., 2007. Syndecan-4-dependent Rac1 regulation determines directional migration in response to the extracellular matrix. *The Journal of cell biology*, 177(3), pp.527-538.

Becsky, D., Gyulai-Nagy, S., Balind, A., Horvath, P., Dux, L. and Keller-Pinter, A., 2020. Myoblast migration and directional persistence affected by syndecan-4-mediated tiam-1 expression and distribution. *International Journal of Molecular Sciences*, 21(3), p.823.

Ben-Porath, I. and Weinberg, R.A., 2005. The signals and pathways activating cellular senescence. *The international journal of biochemistry & cell biology*, 37(5), pp.961-976.

Bensa, T., Tekkela, S. and Rognoni, E., 2023. Skin fibroblast functional heterogeneity in health and disease. *The Journal of Pathology*, 260(5), pp.609-620.

Benson, H.A., 2012. Skin structure, function, and permeation. *Topical and Transdermal Drug delivery: Principles and practice*, pp.1-22.

Black, E., Vibe-Petersen, J., Jorgensen, L.N., Madsen, S.M., Ågren, M.S., Holstein, P.E., Perrild, H. and Gottrup, F., 2003. Decrease of collagen deposition in wound repair in type 1 diabetes independent of glycemic control. *Archives of surgery*, 138(1), pp.34-40.

Blair, M.J., Jones, J.D., Woessner, A.E. and Quinn, K.P., 2020. Skin structure–function relationships and the wound healing response to intrinsic aging. *Advances in wound care*, 9(3), pp.127-143.

Bohari, S.P., Grover, L.M. and Hukins, D.W., 2015. Pulsed low-intensity ultrasound increases proliferation and extracellular matrix production by human dermal fibroblasts in three-dimensional culture. *Journal of Tissue Engineering*, 6, p.2041731415615777.

Bonnans, C., Chou, J. and Werb, Z., 2014. Remodelling the extracellular matrix in development and disease. *Nature reviews Molecular cell biology*, 15(12), pp.786-801.

Boraldi, F., Lofaro, F.D., Bonacorsi, S., Mazzilli, A., Garcia-Fernandez, M. and Quaglino, D., 2024. The Role of Fibroblasts in Skin Homeostasis and Repair. *Biomedicines*, 12(7), p.1586.

Cai, L., Zhang, J., Li, X., Tong, Q., Tang, Y., Wang, Y., and Fu, X., 2017. Lysyl oxidase in remodeling of the extracellular matrix and its role in wound healing: A review. *Frontiers in Bioengineering and Biotechnology*, 5, p.58.

Campbell BH, Agarwal C, Wang JH (2004) TGF-beta1, TGFbeta3, and PGE(2) regulate contraction of human patellar tendon fibroblasts. *Biomech Model Mechanobiol* 2(4): 239–245.

Cárdenas-Sandoval, R.P., Pastrana-Rendón, H.F., Avila, A., Ramírez-Martínez, A.M., Navarrete-Jimenez, M.L., Ondo-Mendez, A.O. and Garzón-Alvarado, D.A., 2023. Effect of therapeutic ultrasound on the mechanical and biological properties of fibroblasts. *Regenerative Engineering and Translational Medicine*, 9(2), pp.263-278.

Carovac, A., Smajlovic, F. and Junuzovic, D., 2011. Application of ultrasound in medicine. *Acta Informatica Medica*, 19(3), p.168.

Chan, Y.S., Hsu, K.Y., Kuo, C.H., Lee, S.D., Chen, S.C., Chen, W.J. and Ueng, S.W.N., 2010. Using low-intensity pulsed ultrasound to improve muscle healing after laceration injury: an in vitro and in vivo study. *Ultrasound in medicine & biology*, 36(5), pp.743-751.

Chantre, C.O., Campbell, P.H., Golecki, H.M., Buganza, A.T., Capulli, A.K., Deravi, L.F., Dauth, S., Sheehy, S.P., Paten, J.A., Gledhill, K. and Doucet, Y.S., 2018. Production-scale fibronectin nanofibers promote wound closure and tissue repair in a dermal mouse model. *Biomaterials*, 166, pp.96-108.

Chattopadhyay, S. and Raines, R.T., 2014. Collagen-based biomaterials for wound healing. *Biopolymers*, 101(8), pp.821-833.

Chen, J., Li, H., SundarRaj, N. and Wang, J.H.C., 2007. Alpha-smooth muscle actin expression enhances cell traction force. *Cell motility and the cytoskeleton*, 64(4), pp.248-257.

Chen, W. and Frangogiannis, N.G., 2013. Fibroblasts in post-infarction inflammation and cardiac repair. *Biochimica et Biophysica Acta (BBA)-Molecular Cell Research*, 1833(4), pp.945-953.

Chen, W.J., 2002. Functions of hyaluronan in wound repair. *Hyaluronan*, pp.147-156.

Cheng, W., Yan-hua, R., Fang-gang, N. and Guo-an, Z., 2011. The content and ratio of type I and III collagen in skin differ with age and injury. *African Journal of Biotechnology*, 10(13), pp.2524-2529.

Cheung, V.Y., 2018. High-intensity focused ultrasound therapy. *Best practice & research Clinical obstetrics & gynaecology*, 46, pp.74-83.

Choquet, D., Felsenfeld, D.P. and Sheetz, M.P., 1997. Extracellular matrix rigidity causes strengthening of integrin-cytoskeleton linkages. *Cell*, 88(1), pp.39-48.

Claes, L. and Willie, B., 2007. The enhancement of bone regeneration by ultrasound. *Progress in biophysics and molecular biology*, 93(1-3), pp.384-398.

Cohen, B.E., Geronemus, R.G., McDaniel, D.H. and Brauer, J.A., 2017. The role of elastic fibers in scar formation and treatment. *Dermatol Surg*, 43(Suppl 1), pp.S19–S24.

Corr, D.T. and Hart, D.A., 2013. Biomechanics of scar tissue and uninjured skin. *Advances in wound care*, 2(2), pp.37-43.

Costa, A., Naranjo, J.D., Londono, R. and Badylak, S.F., 2017. Biologic scaffolds. *Cold Spring Harbor perspectives in medicine*, 7(9), p.a025676.

Cox, T.R., Bird, D., Baker, A.M., Barker, H.E., Ho, M.W., Lang, G. and Erler, J.T., 2013. LOX-mediated collagen crosslinking is responsible for fibrosis-enhanced metastasis. *Cancer research*, 73(6), pp.1721-1732.

Cramer, M.C. and Badylak, S.F., 2020. Extracellular matrix-based biomaterials and their influence upon cell behavior. *Annals of biomedical engineering*, 48(7), pp.2132-2153.

Dallon, J.C., Sherratt, J.A. and Maini, P.K., 2001. Modeling the effects of transforming growth factor- $\beta$  on extracellular matrix alignment in dermal wound repair. *Wound Repair and Regeneration*, 9(4), pp.278-286.

Dalton, C.J. and Lemmon, C.A., 2021. Fibronectin: molecular structure, fibrillar structure and mechanochemical signaling. *Cells*, 10(9), p.2443.

Das, A., Abas, M., Biswas, N., Banerjee, P., Ghosh, N., Rawat, A., Khanna, S., Roy, S. and Sen, C.K., 2019. A modified collagen dressing induces transition of inflammatory to reparative phenotype of wound macrophages. *Scientific reports*, 9(1), p.14293.

Das, L. and Levine, A.D., 2008. TGF- $\beta$  inhibits IL-2 production and promotes cell cycle arrest in TCR-activated effector/memory T cells in the presence of sustained TCR signal transduction. *The Journal of Immunology*, 180(3), pp.1490-1498.

Das, S.L., Bose, P., Lejeune, E., Reich, D.H., Chen, C. and Eyckmans, J., 2021. Extracellular matrix alignment directs provisional matrix assembly and three dimensional fibrous tissue closure. *Tissue Engineering Part A*, 27(23-24), pp.1447-1457.

David, C.J. and Massagué, J., 2018. Contextual determinants of TGF $\beta$  action in development, immunity and cancer. *Nature reviews Molecular cell biology*, 19(7), pp.419-435.

Dembo, M. and Wang, Y.L., 1999. Stresses at the cell-to-substrate interface during locomotion of fibroblasts. *Biophysical Journal*, 76(4), pp.2307-2316.

Denisin, A.K., Kim, H., Riedel-Kruse, I.H. and Pruitt, B.L., 2024. Field Guide to Traction Force Microscopy. *Cellular and Molecular Bioengineering*, 17(2), pp.87-106.

Denton, C.P., Merkel, P.A., Furst, D.E., Khanna, D., Emery, P., Hsu, V.M., Silliman, N., Streisand, J., Powell, J., Akesson, A., Coppock, J., Fv H., Herrick, A., Mayes, M.D., Veale, D., Haas, J., Ledbetter, S., Korn, J.H., Black, C.M., Seibold, J.R., Scleroderma Clinical Trials Consortium, 2007. Recombinant human anti-transforming growth factor beta1 antibody therapy in systemic sclerosis: a multicenter, randomized, placebo-controlled phase I/II trial of CAT-192. *Arthr Rheum*, 56(1), pp.323–33.

Deonaraine, K., Panelli, M.C., Stashower, M.E., Jin, P., Smith, K., Slade, H.B., Norwood, C., Wang, E., Marincola, F.M. and Stroncek, D.F., 2007. Gene expression profiling of cutaneous wound healing. *Journal of translational medicine*, 5, pp.1-11.

Desmoulière, A., Geinoz, A., Gabbiani, F. and Gabbiani, G., 1993. Transforming growth factor-beta 1 induces alpha-smooth muscle actin expression in granulation tissue myofibroblasts and in quiescent and growing cultured fibroblasts. *The Journal of cell biology*, 122(1), pp.103-111.

Drew, P., Posnett, J., Rusling, L. and Wound Care Audit Team, 2007. The cost of wound care for a local population in England. *International Wound Journal*, 4(2), pp.149-155.

Du, M., Li, Y., Zhang, Q., Zhang, J., Ouyang, S. and Chen, Z., 2022. The impact of low intensity ultrasound on cells: Underlying mechanisms and current status. *Progress in Biophysics and Molecular Biology*, 174, pp.41-49.

Duarte, L.R., 1983. The stimulation of bone growth by ultrasound. *Archives of orthopaedic and traumatic surgery*, 101, pp.153-159.

Ekstein, S.F., Wyles, S.P., Moran, S.L. and Meves, A., 2021. Keloids: a review of therapeutic management. *International journal of dermatology*, 60(6), pp.661-671.

Ellis, S., Lin, E.J. and Tartar, D., 2018. Immunology of wound healing. *Current dermatology reports*, 7, pp.350-358.

Engler, A.J., Sen, S., Sweeney, H.L. and Discher, D.E., 2006. Matrix elasticity directs stem cell lineage specification. *Cell*, 126(4), pp.677-689.

Enwemeka, C.S., Rodriguez, O. and Mendosa, S., 1990. The biomechanical effects of low-intensity ultrasound on healing tendons. *Ultrasound in medicine & biology*, 16(8), pp.801-807.

Falanga, V., Isseroff, R.R., Soulika, A.M., Romanelli, M., Margolis, D., Kapp, S., Granick, M. and Harding, K., 2022. Chronic wounds. *Nature Reviews Disease Primers*, 8(1), p.50.

Falanga, V., Zhou, L. and Yufit, T., 2002. Low oxygen tension stimulates collagen synthesis and COL1A1 transcription through the action of TGF- $\beta$ 1. *Journal of cellular physiology*, 191(1), pp.42-50.

Finney, J., Moon, H.J., Ronnebaum, T., Lantz, M. and Mure, M., 2014. Human copper-dependent amine oxidases. *Archives of biochemistry and biophysics*, 546, pp.19-32.

Finnson, K.W., McLean, S., Di Guglielmo, G.M. and Philip, A., 2013. Dynamics of transforming growth factor beta signaling in wound healing and scarring. *Advances in wound care*, 2(5), pp.195-214.

Finnson, K.W., McLean, S., Di Guglielmo, G.M., Philip, A., 2013. Dynamics of transforming growth factor beta signaling in wound healing and scarring. *Adv Wound Care*, 2, pp.195–214.

Fisher, G.J., Varani, J. and Voorhees, J.J., 2008. Looking older: fibroblast collapse and therapeutic implications. *Archives of dermatology*, 144(5), pp.666-672.

Fontana, F., et al., 2021. Development and validation of low-intensity pulsed ultrasound systems for highly controlled in vitro cell stimulation. *Journal of Cutan. Med. Surg.*, 21, pp.425–437.

Forbat, E., Ali, F.R., Al-Niaimi, F., 2017. Treatment of keloid scars using light-, laser- and energy-based devices: a contemporary review of the literature. *Lasers Med Sci*, 32, pp.2145–2154.

Freitas, F.C., Depintor, T.S., Agostini, L.T., Luna-Lucena, D., Nunes, F.M., Bitondi, M.M., Simões, Z.L. and Lourenço, A.P., 2019. Evaluation of reference genes for gene expression analysis by real-time quantitative PCR (qPCR) in three stingless bee species (Hymenoptera: Apidae: Meliponini). *Scientific reports*, 9(1), p.17692

Frykberg, R.G.; Banks, J. Challenges in the Treatment of Chronic Wounds. *Adv. Wound Care* 2015, 4, 560–582.

Fu, S.C., Hung, L.K., Shum, W.T., Lee, Y.W., Chan, L.S., Ho, G. and Chan, K.M., 2010. In vivo low-intensity pulsed ultrasound (LIPUS) following tendon injury promotes repair during granulation but suppresses decorin and biglycan expression during remodeling. *journal of orthopaedic & sports physical therapy*, 40(7), pp.422-429.

Fung, C.H., Cheung, W.H., Pounder, N.M., de Ana, F.J., Harrison, A. and Leung, K.S., 2014. Investigation of rat bone fracture healing using pulsed 1.5 MHz, 30 mW/cm<sup>2</sup> burst ultrasound–axial distance dependency. *Ultrasonics*, 54(3), pp.850-859.

Furusawa, Y., Hassan, M.A., Zhao, Q.L., Ogawa, R., Tabuchi, Y. and Kondo, T., 2014. Effects of therapeutic ultrasound on the nucleus and genomic DNA. *Ultrasonics sonochemistry*, 21(6), pp.2061-2068.

Fushida-Takemura, H., Udagawa, N., Suda, T. and Takahashi, N., 1996. The role of macrophage colony-stimulating factor in the regulation of osteoclastogenesis and bone-resorbing activity. *Biochemical and Biophysical Research Communications*, 226(3), pp.639-645.

Gan, B.S., Huys, S., Sherebrin, M.H. and Scilley, C.G., 1995. The effects of ultrasound treatment on flexor tendon healing in the chicken limb. *Journal of Hand Surgery*, 20(6), pp.809-814.

Gao, J., Guo, Z., Zhang, Y., Liu, Y., Xing, F., Wang, J., Luo, X., Kong, Y. and Zhang, G., 2023. Age-related changes in the ratio of Type I/III collagen and fibril diameter in mouse skin. *Regenerative Biomaterials*, 10, p.rbac110.

Gartland, A., Erler, J.T. and Cox, T.R., 2016. The role of lysyl oxidase, the extracellular matrix and the pre-metastatic niche in bone metastasis. *Journal of bone oncology*, 5(3), pp.100-103.

Geiger, B. and Yamada, K.M., 2011. Molecular architecture and function of matrix adhesions. *Cold Spring Harbor perspectives in biology*, 3(5), p.a005033.

Geiger, B. and Yamada, K.M., 2011. Molecular architecture and function of matrix adhesions. *Cold Spring Harbor perspectives in biology*, 3(5), p.a005033.

Gharee-Kermani, M. and Pham, S.H., 2001. Role of cytokines and cytokine therapy in wound healing and fibrotic diseases. *Current pharmaceutical design*, 7(11), pp.1083-1103.

Ghazawi, F.M., Zargham, R., Gilardino, M.S., Sasseville, D. and Jafarian, F., 2018. Insights into the pathophysiology of hypertrophic scars and keloids: how do they differ? *Adv Skin Wound Care*, 31, pp.582–595.

Giampuzzi, M., Botti, G., Di Duca, M., Arata, L., Ghiggeri, G., Gusmano, R., Ravazzolo, R. and Di Donato, A., 2000. Lysyl oxidase activates the transcription activity of human collagen III promoter: Possible involvement of Ku antigen. *Journal of Biological Chemistry*, 275(46), pp.36341-36349.



Gilbert, R.W., Vickaryous, M.K. and Vilorio-Petit, A.M., 2016. Signalling by transforming growth factor beta isoforms in wound healing and tissue regeneration. *Journal of developmental biology*, 4(2), p.21.

Gonzalez-Junca, A., Driscoll, K.E., Pellicciotta, I., Du, S., Lo, C.H., Roy, R., Parry, R., TenVooren, I., Marquez, D.M., Spitzer, M.H. and Barcellos-Hoff, M.H., 2019. Autocrine TGF $\beta$  is a survival factor for monocytes and drives immunosuppressive lineage commitment. *Cancer immunology research*, 7(2), pp.306-320.

Gonzalez, A.C.D.O., Costa, T.F., Andrade, Z.D.A. and Medrado, A.R.A.P., 2016. Wound healing-A literature review. *Anais brasileiros de dermatologia*, 91(5), pp.614-620.

Gosain, A. and DiPietro, L.A., 2004. Aging and wound healing. *World journal of surgery*, 28, pp.321-326.

Greiling, D. and Clark, R.A., 1997. Fibronectin provides a conduit for fibroblast transmigration from collagenous stroma into fibrin clot provisional matrix. *Journal of cell science*, 110(7), pp.861-870.

Grinnell, F., Billingham, R.E. and Burgess, L., 1981. Distribution of fibronectin during wound healing in vivo. *Journal of Investigative Dermatology*, 76(3), pp.181-189.

Grinnell, F., Ho, C.H. and Wysocki, A., 1992. Degradation of fibronectin and vitronectin and vitronectin in chronic wound fluid: analysis by cell blotting, immunoblotting, and cell adhesion assays. *Journal of investigative dermatology*, 98(4), pp.410-416.

Guler, Z. and Roovers, J.P., 2022. Role of fibroblasts and myofibroblasts on the pathogenesis and treatment of pelvic organ prolapse. *Biomolecules*, 12(1), p.94.

Gumucio, Jonathan P., Kristoffer B. Sugg, and Christopher L. Mendias. "TGF- $\beta$  superfamily signaling in muscle and tendon adaptation to resistance exercise." *Exercise and sport sciences reviews* 43, no. 2 (2015): 93-99.

Guo, S.A. and DiPietro, L.A., 2010. Factors affecting wound healing. *Journal of dental research*, 89(3), pp.219-229.

Gutcher, I., Donkor, M.K., Ma, Q., Rudensky, A.Y., Flavell, R.A. and Li, M.O., 2011. Autocrine transforming growth factor- $\beta$ 1 promotes in vivo Th17 cell differentiation. *Immunity*, 34(3), pp.396-408.

Hahn, C. and Schwartz, M.A., 2009. Mechanotransduction in vascular physiology and atherogenesis. *Nature Reviews Molecular Cell Biology*, 10(1), pp.53-62.

Han, G. and Ceilley, R., 2017. Chronic wound healing: a review of current management and treatments. *Advances in therapy*, 34, pp.599-610.

Han, G., Li, F., Singh, T.P., Wolf, P. and Wang, X.J., 2012. The pro-inflammatory role of TGF $\beta$ 1: a paradox? *International Journal of Biological Sciences*, 8(2), p.228.

Hantash, B.M., Zhao, L., Knowles, J.A. and Lorenz, H.P., 2008. Adult and fetal wound healing. *Front Biosci*, 13(1), pp.51-61.

Harn, H.I.C., Wang, Y.K., Hsu, C.K., Ho, Y.T., Huang, Y.W., Chiu, W.T., Lin, H.H., Cheng, C.M. and Tang, M.J., 2015. Mechanical coupling of cytoskeletal elasticity and force generation is crucial for understanding the migrating nature of keloid fibroblasts. *Experimental dermatology*, 24(8), pp.579-584.

Harrison, A. and Alt, V., 2021. Low-intensity pulsed ultrasound (LIPUS) for stimulation of bone healing—A narrative review. *Injury*, 52, pp.S91-S96.

Harrison, A., Lin, S., Pounder, N. and Mikuni-Takagaki, Y., 2016. Mode & mechanism of low intensity pulsed ultrasound (LIPUS) in fracture repair. *Ultrasonics*, 70, pp.45-52.

Hassan, M.A., Buldakov, M.A., Ogawa, R., Zhao, Q.L., Furusawa, Y., Kudo, N., Kondo, T. and Riesz, P., 2010. Modulation control over ultrasound-mediated gene delivery: Evaluating the importance of standing waves. *Journal of controlled release*, 141(1), pp.70-76.

Hassan, M.A., Campbell, P. and Kondo, T., 2010. The role of Ca<sup>2+</sup> in ultrasound-elicited bioeffects: progress, perspectives and prospects. *Drug Discovery Today*, 15(21-22), pp.892-906.

Heybeli, N., Yeşildağ, A., Oyar, O., Gülsoy, U.K., Tekinsoy, M.A. and Mumcu, E.F., 2002. Diagnostic ultrasound treatment increases the bone fracture—healing rate in an internally fixed rat femoral osteotomy model. *Journal of ultrasound in medicine*, 21(12), pp.1357-1363.

Hiebert, P., Antoniazzi, G., Aronoff, M., Werner, S. and Wennemers, H., 2024. A lysyl oxidase-responsive collagen peptide illuminates collagen remodeling in wound healing. *Matrix Biology*, 128, pp.11-20.

Hinz B, Celetta G, Tomasek JJ, Gabbiani G, Chaponnier C (2001) Alpha-smooth muscle actin expression upregulates fibroblast contractile activity. *Mol Biol Cell* 12(9):2730–2741.

Hoffmann, G.A. and Smith, M.L., 2019. New insights into collagen and fibronectin reciprocity during extracellular matrix formation. *Chem*, 5(8), pp.1930-1932.

Holmes, D.F., Lu, Y., Starborg, T. and Kadler, K.E., 2018. Collagen fibril assembly and function. *Current topics in developmental biology*, 130, pp.107-142.

Holzheimer, R.G. and Steinmetz, W.G., 2000. Local and systemic concentrations of pro-and anti-inflammatory cytokines in human wounds. *European journal of medical research*, 5(8), pp.347-355.

Hong, H.H. and Trackman, P.C., 2002. Cytokine regulation of gingival fibroblast lysyl oxidase, collagen, and elastin. *Journal of periodontology*, 73(2), pp.145-152.

Hormozi-Moghaddam, Z., Mokhtari-Dizaji, M., Nilforoshzadeh, M.A. and Bakhshandeh, M., 2021. Low-intensity ultrasound to induce proliferation and collagen I expression of adipose-derived mesenchymal stem cells and fibroblast cells in co-culture. *Measurement*, 167, p.108280.

Hornsby, T.K., Jakhmola, A., Kolios, M.C. and Tavakkoli, J., 2023. A quantitative study of thermal and non-thermal mechanisms in ultrasound-induced nano-drug delivery. *Ultrasound in Medicine & Biology*, 49(5), pp.1288-1298.

Hsu, C.K., Lin, H.H., Harn, H.I., Hughes, M.W., Tang, M.J. and Yang, C.C., 2018. Mechanical forces in skin disorders. *J Dermatol Sci*, 90, pp.232–240.

Huang, C., Murphy, G.F., Akaishi, S. and Ogawa, R., 2013. Keloids and hypertrophic scars: update and future directions. *Plastic and Reconstructive Surgery–Global Open*, 1(4), p.e25.

Hur, S.S., Jeong, J.H., Ban, M.J., Park, J.H., Yoon, J.K. and Hwang, Y., 2020. Traction force microscopy for understanding cellular mechanotransduction. *BMB reports*, 53(2), p.74.

Hurlow J, Bowler PG. Acute and chronic wound infections: microbiological, immunological, clinical and therapeutic distinctions. *J Wound Care*. 2022 May 2;31(5):436-445.

Icenogle, A., Şahin, F., Akkaya, N., Ök, N., Yörükoğlu, Ç., Mete, G. and Akgün, Ş., 2021. Effects of low-density pulsed ultrasound treatment on transforming growth factor-beta, collagen level, histology, biomechanics, and function in repaired rat tendons. *Turkish journal of physical medicine and rehabilitation*, 67(2), p.167.

Ignotz, R.A. and Massague, J., 1986. Transforming growth factor-beta stimulates the expression of fibronectin and collagen and their incorporation into the extracellular matrix. *Journal of Biological Chemistry*, 261(9), pp.4337-4345.

Ingber, D.E., Wang, N., Stamenovic, D., and Butler, J.P., 2003. Tensegrity, cellular biophysics, and the mechanics of living systems. *Reports on Progress in Physics*, 66(11), pp.1367-1409.

Izadifar, Z., Babyn, P. and Chapman, D., 2019. Ultrasound cavitation/microbubble detection and medical applications. *Journal of Medical and Biological Engineering*, 39, pp.259-276.

Jahromi, M.A.M., Zangabad, P.S., Basri, S.M.M., Zangabad, K.S., Ghamarypour, A., Aref, A.R., Karimi, M. and Hamblin, M.R., 2018. Nanomedicine and advanced technologies for burns: Preventing infection and facilitating wound healing. *Advanced drug delivery reviews*, 123, pp.33-64.

Jakab, L., 2014. Connective tissue and inflammation. *Orvosi Hetilap*, 155(12), pp.453-460.

Jamur, M.C. and Oliver, C., 2009. Permeabilization of cell membranes. In *Immunocytochemical methods and protocols* (pp. 63-66). Totowa, NJ: Humana Press.

Janowska, A., Dini, V., Oranges, T., Iannone, M., Loggini, B. and Romanelli, M., 2019. Atypical ulcers: diagnosis and management. *Clinical interventions in aging*, pp.2137-2143.

Jansen, K.A., Licup, A.J., Sharma, A., Rens, R., MacKintosh, F.C. and Koenderink, G.H., 2018. The role of network architecture in collagen mechanics. *Biophysical journal*, 114(11), pp.2665-2678.

Järbrink, K., Ni, G., Sönnnergren, H., Schmidtchen, A., Pang, C., Bajpai, R. and Car, J., 2017. The humanistic and economic burden of chronic wounds: a protocol for a systematic review. *Systematic reviews*, 6, pp.1-7.

Jiang, X., Savchenko, O., Li, Y., Qi, S., Yang, T., Zhang, W. and Chen, J., 2018. A review of low-intensity pulsed ultrasound for therapeutic applications. *IEEE Transactions on Biomedical Engineering*, 66(10), pp.2704-2718.

Jones, N., 2010. Scar tissue. *Current opinion in otolaryngology & head and neck surgery*, 18(4), pp.261-265.

Júnior, S.L.J., Camanho, G.L., Bassit, A.C.F., Forgas, A., Ingham, S.J. and Abdalla, R.J., 2011. Low-intensity pulsed ultrasound accelerates healing in rat calcaneus tendon injuries. *journal of orthopaedic & sports physical therapy*, 41(7), pp.526-531.

Kagan, H.M. and Li, W., 2003. Lysyl oxidase: properties, specificity, and biological roles inside and outside of the cell. *Journal of cellular biochemistry*, 88(4), pp.660-672.

Kagan, H.M., 2000. Intra-and extracellular enzymes of collagen biosynthesis as biological and chemical targets in the control of fibrosis. *Acta tropica*, 77(1), pp.147-152.

Kang, Y., Xu, L., Dong, J., Yuan, X., Ye, J., Fan, Y., Liu, B., Xie, J. and Ji, X., 2024. Programmed microalgae-gel promotes chronic wound healing in diabetes. *Nature communications*, 15(1), p.1042.

Kaplani, K., Koutsi, S., Armenis, V., Skondra, F.G., Karantzelis, N., Tsaniras, S.C. and Taraviras, S., 2018. Wound healing related agents: Ongoing research and perspectives. *Advanced Drug Delivery Reviews*, 129, pp.242-253.

Karimi, K., Odhav, A., Kollipara, R., Fike, J., Stanford, C. and Hall, J.C., 2017. Acute cutaneous necrosis: A guide to early diagnosis and treatment. *J. Cutan. Med. Surg.*, 21, pp.425-437.

Kasowanjete, P., Kumar, S.S.D. and Houreld, N.N., 2023. A review of photobiomodulation on PI3K/AKT/mTOR in wound healing. *Journal of Photochemistry and Photobiology*, p.100215.

Katsuda, S., Okada, Y., Minamoto, T., Oda, Y., Matsui, Y. and Nakanishi, I., 1992. Collagens in human atherosclerosis. Immunohistochemical analysis using collagen type-specific antibodies. *Arteriosclerosis and thrombosis: a journal of vascular biology*, 12(4), pp.494-502.

Kenny, F.N., Marcotti, S., De Freitas, D.B., Drudi, E.M., Leech, V., Bell, R.E., Easton, J., Fleck, R., Allison, L., Philippeos, C. and Manhart, A., 2023. Autocrine IL-6 drives cell and extracellular matrix anisotropy in scar fibroblasts. *Matrix Biology*, 123, pp.1-16.

Kim, Y.M., Kim, E.C. and Kim, Y., 2011. The human lysyl oxidase-like 2 protein functions as an amine oxidase toward collagen and elastin. *Molecular biology reports*, 38, pp.145-149.

Kingwill, A., Barker, G. and Wong, A., 2017. Point-of-care ultrasound: Its growing application in hospital medicine. *British Journal of Hospital Medicine*, 78(9), pp.492-496.

Kiritsi, D. and Nystrom, A., 2018. The role of TGFbeta in wound healing pathologies. *Mech Ageing Dev*, 172, pp.51–58.

Kisling, A., Lust, R.M. and Katwa, L.C., 2019. What is the role of peptide fragments of collagen I and IV in health and disease?. *Life sciences*, 228, pp.30-34.

Knuutinen, A., Kokkonen, N., Risteli, J., Vähäkangas, K., Kallioinen, M., Salo, T., Sorsa, T. and Oikarinen, A., 2002. Smoking affects collagen synthesis and extracellular matrix turnover in human skin. *British Journal of Dermatology*, 146(4), pp.588-594.

Kong, W., Lyu, C., Liao, H. and Du, Y., 2021. Collagen crosslinking: effect on structure, mechanics and fibrosis progression. *Biomedical Materials*, 16(6), p.062005.

Koskinas, K.C., Sukhova, G.K., Baker, A.B., Papafaklis, M.I., Chatzizisis, Y.S., Coskun, A.U., Quillard, T., Jonas, M., Maynard, C., Antoniadis, A.P. and Shi, G.P., 2013. Thin-capped atheromata with reduced collagen content in pigs develop in coronary arterial regions exposed to persistently low endothelial shear stress. *Arteriosclerosis, thrombosis, and vascular biology*, 33(7), pp.1494-1504

Krieg, Thomas, and Monique Aumailley. "The extracellular matrix of the dermis: flexible structures with dynamic functions." *Experimental dermatology* 20, no. 8 (2011): 689-695.

Kubow, K.E., Vukmirovic, R., Zhe, L., Klotzsch, E., Smith, M.L., Gourdon, D., Luna, S. and Vogel, V., 2015. Mechanical forces regulate the interactions of fibronectin and collagen I in extracellular matrix. *Nature communications*, 6(1), p.8026.

Kular, J.K., Basu, S. and Sharma, R.I., 2014. The extracellular matrix: Structure, composition, age-related differences, tools for analysis and applications for tissue engineering. *Journal of tissue engineering*, 5, p.2041731414557112.

Kumari, S., Panda, T.K. and Pradhan, T., 2017. Lysyl oxidase: its diversity in health and diseases. *Indian Journal of Clinical Biochemistry*, 32, pp.134-141.

Laczko, R. and Csiszar, K., 2020. Lysyl oxidase (LOX): functional contributions to signaling pathways. *Biomolecules*, 10(8), p.1093.

Lambert, R.J.W., Skandamis, P.N., Coote, P.J. and Nychas, G.J., 2001. A study of the minimum inhibitory concentration and mode of action of oregano essential oil, thymol and carvacrol. *Journal of applied microbiology*, 91(3), pp.453-462.

Langton, A.K., Griffiths, C.E., Sherratt, M.J. and Watson, R.E., 2013. Cross-linking of structural proteins in ageing skin: an in situ assay for the detection of amine oxidase activity. *Biogerontology*, 14, pp.89-97.

Larson, B.J., Longaker, M.T. and Lorenz, H.P., 2010. Scarless fetal wound healing: a basic science review. *Plastic and reconstructive surgery*, 126(4), pp.1172-1180.

Las Heras, K., Igartua, M., Santos-Vizcaino, E. and Hernandez, R.M., 2020. Chronic wounds: Current status, available strategies and emerging therapeutic solutions. *Journal of controlled release*, 328, pp.532-550.

Lazarus, G.S., Cooper, D.M., Knighton, D.R., Margolis, D.J., Percoraro, R.E., Rodeheaver, G. and Robson, M.C., 1994. Definitions and guidelines for assessment of wounds and evaluation of healing. *Wound repair and regeneration*, 2(3), pp.165-170.

Lazzarini, P.A., Cramb, S.M., Golledge, J., Morton, J.I., Magliano, D.J. and Van Netten, J.J., 2023. Global trends in the incidence of hospital admissions for diabetes-related foot disease and amputations: a review of national rates in the 21st century. *Diabetologia*, 66(2), pp.267-287.

Le, H.A. and Mayor, R., 2023. Cell–matrix and cell–cell interaction mechanics in guiding migration. *Biochemical Society Transactions*, 51(4), pp.1733-1745.

LeBleu, V.S. and Neilson, E.G., 2020. Origin and functional heterogeneity of fibroblasts. *The FASEB Journal*, 34(3), pp.3519-3536.

Lee, C.H., Hong, C.H., Chen, Y.T., Chen, Y.C. and Shen, M.R., 2012. TGF-beta1 increases cell rigidity by enhancing expression of smooth muscle actin: keloid-derived fibroblasts as a model for cellular mechanics. *Journal of dermatological science*, 67(3), pp.173-180.

Lee, H.P., Alisafaei, F., Adebawale, K., Chang, J., Shenoy, V.B. and Chaudhuri, O., 2021. The nuclear piston activates mechanosensitive ion channels to generate cell migration paths in confining microenvironments. *Science advances*, 7(2), p.eabd4058.

Lee, W., Georgas, E., Komatsu, D.E. and Qin, Y.X., 2024. Daily low-intensity pulsed ultrasound stimulation mitigates joint degradation and pain in a post-traumatic osteoarthritis rat model. *Journal of Orthopaedic Translation*, 44, pp.9-18.

Leithner, A., Eichner, A., Müller, J., Reversat, A., Brown, M., Schwarz, J., Merrin, J., de Gorter, D.J., Schur, F., Bayerl, J. and De Vries, I., 2016. Diversified actin protrusions promote environmental exploration but are dispensable for locomotion of leukocytes. *Nature cell biology*, 18(11), pp.1253-1259.

Lekka, M., Gnanachandran, K., Kubiak, A., Zieliński, T. and Zemła, J., 2021. Traction force microscopy–Measuring the forces exerted by cells. *Micron*, 150, p.103138.

Lenselink, E.A., 2015. Role of fibronectin in normal wound healing. *International wound journal*, 12(3), pp.313-316.

Li, B. and Wang, J.H.C., 2011. Fibroblasts and myofibroblasts in wound healing: force generation and measurement. *Journal of tissue viability*, 20(4), pp.108-120.

Li, J., Chen, J. and Kirsner, R., 2007. Pathophysiology of acute wound healing. *Clinics in dermatology*, 25(1), pp.9-18.

Li, J.K.J., Lin, J.C.A., Liu, H.C., Sun, J.S., Ruaan, R.C., Shih, C. and Chang, W.H.S., 2006. Comparison of ultrasound and electromagnetic field effects on osteoblast growth. *Ultrasound in medicine & biology*, 32(5), pp.769-775.



Li, X., Guo, L., Yang, X., Wang, J., Hou, Y., Zhu, S., Du, J., Feng, J., Xie, Y., Zhuang, L. and He, X., 2020. TGF- $\beta$ 1-induced connexin43 promotes scar formation via the Erk/MMP-1/collagen III pathway. *Journal of Oral Rehabilitation*, 47, pp.99-106.

Li, Y., Li, W., Liu, X., Liu, X., Zhu, B., Guo, S., Wang, C., Wang, D., Li, S. and Zhang, Z., 2023. Effects of Low-Intensity Pulsed Ultrasound in Tendon Injuries. *Journal of Ultrasound in Medicine*, 42(9), pp.1923-1939.

Li, Y., Li, W., Liu, X., Liu, X., Zhu, B., Guo, S., Wang, C., Wang, D., Li, S. and Zhang, Z., 2023. Effects of Low-Intensity Pulsed Ultrasound in Tendon Injuries. *Journal of Ultrasound in Medicine*, 42(9), pp.1923-1939.

Liarte, S., Bernabé-García, Á. and Nicolás, F.J., 2020. Role of TGF- $\beta$  in skin chronic wounds: a keratinocyte perspective. *Cells*, 9(2), p.306.

Lichtman, M.K., Otero-Vinas, M. and Falanga, V., 2016. Transforming growth factor beta (TGF- $\beta$ ) isoforms in wound healing and fibrosis. *Wound Repair and Regeneration*, 24(2), pp.215-222.

Liu, L., Geng, X., McDermott, J., Shen, J., Corbin, C., Xuan, S., Kim, J., Zuo, L. and Liu, Z., 2016. Copper deficiency in the lungs of TNF- $\alpha$  transgenic mice. *Frontiers in physiology*, 7, p.234.

Liu, X., Wu, H., Byrne, M., Krane, S. and Jaenisch, R., 1997. Type III collagen is crucial for collagen I fibrillogenesis and for normal cardiovascular development. *Proceedings of the National Academy of Sciences*, 94(5), pp.1852-1856.

Löffek, S., Schilling, O. and Franzke, C.W., 2011. Biological role of matrix metalloproteinases: a critical balance. *European Respiratory Journal*, 38(1), pp.191-208.

Lomakin, A.J., Cattin, C.J., Cuvelier, D., Alraies, Z., Molina, M., Nader, G.P.F., Srivastava, N., Sáez, P.J., Garcia-Arcos, J.M., Zhitnyak, I.Y. and Bhargava, A., 2020. The nucleus acts as a ruler tailoring cell responses to spatial constraints. *Science*, 370(6514), p.eaba2894.

Longstreth, J.H. and Wang, K., 2024. The role of fibronectin in mediating cell migration. *American Journal of Physiology-Cell Physiology*, 326(4), pp.C1212-C1225.

Lopes, T.S., dos Santos Videira, L.M.M., Saraiva, D.M.R.F., Agostinho, E.S. and Bandarra, A.J.F., 2020. Multicentre study of pressure ulcer point prevalence in a Portuguese region. *Journal of Tissue Viability*, 29(1), pp.12-18.

López-Otín, C. and Matrisian, L.M., 2007. Emerging roles of proteases in tumour suppression. *Nature reviews cancer*, 7(10), pp.800-808.

Lovell, C.R., Smolenski, K.A., Duance, V.C., Light, N.D., Young, S. and Dyson, M., 1987. Type I and III collagen content and fibre distribution in normal human skin during ageing. *British Journal of Dermatology*, 117(4), pp.419-428.

Lu, M., Qin, Q., Yao, J., Sun, L. and Qin, X., 2019. Induction of LOX by TGF- $\beta$ 1/Smad/AP-1 signaling aggravates rat myocardial fibrosis and heart failure. *IUBMB life*, 71(11), pp.1729-1739.

Lucero, H.A. and Kagan, H.M., 2006. Lysyl oxidase: An oxidative enzyme and effector of cell function. *Cell Mol Life Sci.*, 63, pp.2304–2316.

Lukjanenko, L., Jung, M.J., Hegde, N., Perruisseau-Carrier, C., Migliavacca, E., Rozo, M., Karaz, S., Jacot, G., Schmidt, M., Li, L. and Metairon, S., 2016. Loss of fibronectin from the aged stem cell niche affects the regenerative capacity of skeletal muscle in mice. *Nature medicine*, 22(8), pp.897-905.

Lukjanenko, L., Karaz, S., Stuelsatz, P., Gurriaran-Rodriguez, U., Michaud, J., Dammone, G., Sizzano, F., Mashinchian, O., Ancel, S., Migliaccio, E., Feige, J.N., Sizzano, F., and M. Bentzinger, C.F., 2016. Fibronectin is required for maintenance of myofiber integrity and satellite cell self-renewal during aging. *Nature Medicine*, 22, pp.897-905.

Lutz, R., Sakai, T. and Chiquet, M., 2010. Pericellular fibronectin is required for RhoA-dependent responses to cyclic strain in fibroblasts. *Journal of cell science*, 123(9), pp.1511-1521.

Maeda, T., Masaki, C., Kanao, M., Kondo, Y., Ohta, A., Nakamoto, T. and Hosokawa, R., 2013. Low-intensity pulsed ultrasound enhances palatal mucosa wound healing in rats. *Journal of prosthodontic research*, 57(2), pp.93-98.

Mahoney, C.M., Morgan, M.R., Harrison, A., Humphries, M.J. and Bass, M.D., 2009. Therapeutic ultrasound bypasses canonical syndecan-4 signaling to activate rac1. *Journal of biological chemistry*, 284(13), pp.8898-8909.

Maione, A.G., Smith, A., Kashpur, O., Yanez, V., Knight, E., Mooney, D.J., Veves, A., Tomic-Canic, M. and Garlick, J.A., 2016. Altered ECM deposition by diabetic foot ulcer-derived fibroblasts implicates fibronectin in chronic wound repair. *Wound repair and regeneration*, 24(4), pp.630-643.

Maione, A.G., Smith, A., Kashpur, O., Yanez, V., Knight, E., Mooney, D.J., Veves, A., Tomic-Canic, M. and Garlick, J.A., 2016. Altered ECM deposition by diabetic foot ulcer-derived fibroblasts implicates fibronectin in chronic wound repair. *Wound repair and regeneration*, 24(4), pp.630-643.

Maitra, A., 2005. Calcium phosphate nanoparticles: second-generation nonviral vectors in gene therapy. *Expert Review of Molecular Diagnostics*, 5(6), pp.893-905.

Mäki, J.M., Sormunen, R., Lippo, S., Kaarteenaho-Wiik, R., Soininen, R. and Myllyharju, J., 2005. Lysyl oxidase is essential for normal development and function of the respiratory system and for the integrity of elastic and collagen fibers in various tissues. *The American journal of pathology*, 167(4), pp.927-936.

Manka, S.W., Bihan, D. and Farndale, R.W., 2019. Structural studies of the MMP-3 interaction with triple-helical collagen introduce new roles for the enzyme in tissue remodelling. *Scientific reports*, 9(1), p.18785.

Marconi, G.D., Fonticoli, L., Rajan, T.S., Lanuti, P., Della Rocca, Y., Pierdomenico, S.D., Trubiani, O., Pizzicannella, J. and Diomedea, F., 2021. Transforming growth factor-beta1 and human gingival fibroblast-to-myofibroblast differentiation: molecular and morphological modifications. *Frontiers in physiology*, 12, p.676512.

Marcos-Garcés, V., Molina Aguilar, P., Bea Serrano, C., García Bustos, V., Benavent Seguí, J., Ferrández Izquierdo, A. and Ruiz-Saurí, A., 2014. Age-related dermal collagen changes during development, maturation and ageing—a morphometric and comparative study. *Journal of anatomy*, 225(1), pp.98-108.

Margolis, D.J., Kantor, J., Santanna, J., Strom, B.L. and Berlin, J.A., 2000. Risk factors for delayed healing of neuropathic diabetic foot ulcers: a pooled analysis. *Archives of dermatology*, 136(12), pp.1531-1535.

Mari, W., Alsabri, S.G., Tabal, N., Younes, S., Sherif, A. and Simman, R., 2015. Novel insights on understanding of keloid scar: article review. *Journal of the American College of Clinical Wound Specialists*, 7(1-3), pp.1-7.

Martin, P., 1997. Wound healing--aiming for perfect skin regeneration. *Science*, 276(5309), pp.75-81.

Mathew-Steiner, S.S., Roy, S. and Sen, C.K., 2021. Collagen in wound healing. *Bioengineering*, 8(5), p.63.

Mathew-Steiner, S.S., Roy, S. and Sen, C.K., 2021. Collagen in wound healing. *Bioengineering*, 8(5), p.63.

Matsui, R., Osaki, K.I., Konishi, J., Ikegami, K. and Koide, M., 1996. Evaluation of an artificial dermis full-thickness skin defect model in the rat. *Biomaterials*, 17(10), pp.989-994.

McDonald, J.A., Kelley, D.G. and Broekelmann, T.J., 1982. Role of fibronectin in collagen deposition: Fab' to the gelatin-binding domain of fibronectin inhibits both fibronectin and collagen organization in fibroblast extracellular matrix. *The Journal of cell biology*, 92(2), pp.485-492.

McMillan, J.R., Akiyama, M. and Shimizu, H., 2003. Epidermal basement membrane zone components: ultrastructural distribution and molecular interactions. *Journal of dermatological science*, 31(3), pp.169-177.

Merkel JR, DiPaolo BR, Hallock GG, Rice DC. Type I and type III collagen content of healing wounds in fetal and adult rats. *Proc Soc Exp Biol Med* 1988;187:493-497.

Merkel, J.R., DiPaolo, B.R., Hallock, G.G. and Rice, D.C., 1988. Type I and type III collagen content of healing wounds in fetal and adult rats. *Proceedings of the Society for Experimental Biology and Medicine*, 187(4), pp.493-497.

Mervis, J.S. and Phillips, T.J., 2019. Pressure ulcers: Prevention and management. *Journal of the American Academy of Dermatology*, 81(4), pp.893-902.

Michael, M. and Parsons, M., 2020. New perspectives on integrin-dependent adhesions. *Current opinion in cell biology*, 63, pp.31-37.

Midwood, K.S., Williams, L.V. and Schwarzbauer, J.E., 2004. Tissue repair and the dynamics of the extracellular matrix. *The international journal of biochemistry & cell biology*, 36(6), pp.1031-1037.

Moretti, F.A., Chauhan, A.K., Iaconcig, A., Porro, F., Baralle, F.E. and Muro, A.F., 2007. A major fraction of fibronectin present in the extracellular matrix of tissues is plasma-derived. *Journal of Biological Chemistry*, 282(38), pp.28057-28062.

Morgan, M.R., Hamidi, H., Bass, M.D., Warwood, S., Ballestrem, C. and Humphries, M.J., 2013. Syndecan-4 phosphorylation is a control point for integrin recycling. *Developmental cell*, 24(5), pp.472-485.

Mostaço-Guidolin, L., Rosin, N.L. and Hackett, T.L., 2017. Imaging collagen in scar tissue: developments in second harmonic generation microscopy for biomedical applications. *International journal of molecular sciences*, 18(8), p.1772.

Mostafa, N.Z., Uludağ, H., Dederich, D.N., Doschak, M.R. and El-Bialy, T.H., 2009. Anabolic effects of low-intensity pulsed ultrasound on human gingival fibroblasts. *archives of oral biology*, 54(8), pp.743-748.

Munro, J., Steeghs, K., Morrison, V., Ireland, H. and Parkinson, E.K., 2001. Human fibroblast replicative senescence can occur in the absence of extensive cell division and short telomeres. *Oncogene*, 20(27), pp.3541-3552.

Muntz, I., Fenu, M., van Osch, G.J. and Koenderink, G.H., 2022. The role of cell–matrix interactions in connective tissue mechanics. *Physical biology*, 19(2), p.021001.

Mustoe, T.A., Cooter, R.D., Gold, M.H., Hobbs, F.R., Ramelet, A.A., Shakespeare, P.G., Stella, M., Téot, L., Wood, F.M., Ziegler, U.E. and International Advisory Panel on Scar Management, 2002. International clinical recommendations on scar management. *Plastic and reconstructive surgery*, 110(2), pp.560-571.

Ng, C.O., Ng, G.Y., See, E.K. and Leung, M.C., 2003. Therapeutic ultrasound improves strength of Achilles tendon repair in rats. *Ultrasound in medicine & biology*, 29(10), pp.1501-1506.

Ng, K.W. and Lau, W.M., 2015. Skin deep: the basics of human skin structure and drug penetration. *Percutaneous penetration enhancers chemical methods in penetration enhancement: drug manipulation strategies and vehicle effects*, pp.3-11.

Noble, N.A., Harper, J.R. and Border, W.A., 1992. In vivo interactions of TGF- $\beta$  and extracellular matrix. *Progress in Growth Factor Research*, 4(4), pp.369-382.

Nuthakki, V.K., Fleser, P.S., Malinzak, L.E., Seymour, M.L., Callahan, R.E., Bendick, P.J., Zelenock, G.B. and Shanley, C.J., 2004. Lysyl oxidase expression in a rat model of arterial balloon injury. *Journal of vascular surgery*, 40(1), pp.123-129.

Nuutila, K., Siltanen, A., Peura, M., Bizik, J., Kaartinen, I., Kuokkanen, H., Nieminen, T., Harjula, A., Aarnio, P., Vuola, J. and Kankuri, E., 2012. Human skin transcriptome during superficial cutaneous wound healing. *Wound Repair and Regeneration*, 20(6), pp.830-839.

O’Kane, S. and Ferguson, M.W.J., 1997. Transforming growth factor  $\beta$ s and wound healing. *The International Journal of Biochemistry & Cell Biology*, 29(1), pp.63-78.

Olaso, E., Lin, H.C., Wang, L.H. and Friedman, S.L., 2011. Impaired dermal wound healing in discoidin domain receptor 2-deficient mice associated with defective extracellular matrix remodeling. *Fibrogenesis & tissue repair*, 4, pp.1-9.

Ongenaes, K.C., Phillips, T.J. and Park, H.Y., 2000. Level of fibronectin mRNA is markedly increased in human chronic wounds. *Dermatologic surgery*, 26(5), pp.447-451.

Page-McCaw, A., Ewald, A.J. and Werb, Z., 2007. Matrix metalloproteinases and the regulation of tissue remodelling. *Nature reviews Molecular cell biology*, 8(3), pp.221-233.

Paquette, D. and Falanga, V., 2002. Leg ulcers. *Clinics in geriatric medicine*, 18(1), pp.77-88.

Parri, M. and Chiarugi, P., 2010. Rac and Rho GTPases in cancer cell motility control. *Cell Communication and Signaling*, 8(1), p.23.

Pathi, S.D., Acevedo, J.F., Keller, P.W., Kishore, A.H., Miller, R.T., Wai, C.Y. and Word, R.A., 2012. Recovery of the injured external anal sphincter after injection of local or intravenous mesenchymal stem cells. *Obstetrics & Gynecology*, 119(1), pp.134-144.

Patten, J. and Wang, K., 2021. Fibronectin in development and wound healing. *Advanced drug delivery reviews*, 170, pp.353-368.

Pelham Jr, R.J. and Wang, Y.L., 1997. Cell locomotion and focal adhesions are regulated by substrate flexibility. *Proceedings of the national academy of sciences*, 94(25), pp.13661-13665.

Penn, J.W., Grobbelaar, A.O. and Rolfe, K.J., 2012. The role of the TGF- $\beta$  family in wound healing, burns and scarring: a review. *International journal of burns and trauma*, 2(1), p.18.

Penn, J.W., Grobbelaar, A.O., Rolfe, K.J., 2012. The role of the TGF-b family in wound healing, burns and scarring: a review. *Int J Burns Trauma*, 2, pp.18–28.

Petrie, R.J., Koo, H. and Yamada, K.M., 2014. Generation of compartmentalized pressure by a nuclear piston governs cell motility in a 3D matrix. *Science*, 345(6200), pp.1062-1065.

Pfisterer, K., Levitt, J., Lawson, C.D., Marsh, R.J., Heddlestone, J.M., Wait, E., Ameer-Beg, S.M., Cox, S. and Parsons, M., 2020. FMNL2 regulates dynamics of fascin in filopodia. *Journal of Cell Biology*, 219(5).

Pfisterer, K., Shaw, L.E., Symmank, D. and Weninger, W., 2021. The extracellular matrix in skin inflammation and infection. *Frontiers in cell and developmental biology*, 9, p.682414.

Phillips, C.J., Humphreys, I., Fletcher, J., Harding, K., Chamberlain, G. and Macey, S., 2016. Estimating the costs associated with the management of patients with chronic wounds using linked routine data. *J Cutan. Med. Surg.*, 20, pp.221–229.

Pittenger, M.F., Discher, D.E., Péault, B.M., Phinney, D.G., Hare, J.M. and Caplan, A.I., 2019. Mesenchymal stem cell perspective: cell biology to clinical progress. *NPJ Regenerative medicine*, 4(1), p.22.

Plotnikov, S.V., Pasapera, A.M., Sabass, B. and Waterman, C.M., 2012. Force fluctuations within focal adhesions mediate ECM-rigidity sensing to guide directed cell migration. *Nature Cell Biology*, 14(6), pp. 606-616.

Potekaev, N.N., Borzykh, O.B., Medvedev, G.V., Pushkin, D.V., Petrova, M.M., Petrov, A.V., Dmitrenko, D.V., Karpova, E.I., Demina, O.M. and Shnayder, N.A., 2021. The role of extracellular matrix in skin wound healing. *Journal of Clinical Medicine*, 10(24), p.5947.

Qiu, Z., Kwon, A.H. and Kamiyama, Y., 2007. Effects of plasma fibronectin on the healing of full-thickness skin wounds in streptozotocin-induced diabetic rats. *Journal of Surgical Research*, 138(1), pp.64-70.

Rafiq, N.B.M., Nishimura, Y., Plotnikov, S.V., Thiagarajan, V., Zhang, Z., Shi, S., Natarajan, M., Viasnoff, V., Kanchanawong, P., Jones, G.E. and Bershadsky, A.D., 2019. A mechano-signalling network linking microtubules, myosin IIA filaments and integrin-based adhesions. *Nature materials*, 18(6), pp.638-649.

Rajpaul, K., 2015. Biofilm in wound care. *British journal of community nursing*, 20(Sup3), pp.S6-S11.

Rangaraj, A., Harding, K. and Leaper, D., 2011. Role of collagen in wound management. *Wounds uk*, 7(2), pp.54-63.

Rantanen, J., Thorsson, O., Wollmer, P., Hurme, T. and Kalimo, H., 1999. Effects of therapeutic ultrasound on the regeneration of skeletal myofibers after experimental muscle injury. *The American journal of sports medicine*, 27(1), pp.54-59.

Ray, A., Slama, Z.M., Morford, R.K., Madden, S.A. and Provenzano, P.P., 2017. Enhanced directional migration of cancer stem cells in 3D aligned collagen matrices. *Biophysical journal*, 112(5), pp.1023-1036.

Ray, A., Slama, Z.M., Morford, R.K., Madden, S.A. and Provenzano, P.P., 2017. Enhanced directional migration of cancer stem cells in 3D aligned collagen matrices. *Biophysical Journal*, 112(5), pp.1023-1036.

Redden, R.A. and Doolin, E.J., 2003. Collagen crosslinking and cell density have distinct effects on fibroblast-mediated contraction of collagen gels. *Skin research and technology*, 9(3), pp.290-293.

Remst, D.F.G., Blom, A.B., Vitters, E.L., Bank, R.A., Van Den Berg, W.B., Blaney Davidson, E.N. and Van Der Kraan, P.M., 2014. Gene expression analysis of murine and human osteoarthritis synovium reveals elevation of transforming growth factor  $\beta$ -responsive genes in osteoarthritis-related fibrosis. *Arthritis & rheumatology*, 66(3), pp.647-656.

Ren, L.L., Li, X.J., Duan, T.T., Li, Z.H., Yang, J.Z., Zhang, Y.M., Zou, L., Miao, H. and Zhao, Y.Y., 2023. Transforming growth factor- $\beta$  signaling: from tissue fibrosis to therapeutic opportunities. *Chemico-biological interactions*, 369, p.110289.

Ricard-Blum, S., 2011. The collagen family. *Cold Spring Harbor perspectives in biology*, 3(1), p.a004978.



Riching, K.M., Cox, B.L., Salick, M.R., Pehlke, C., Riching, A.S., Ponik, S.M., Bass, B.R., Crone, W.C., Jiang, Y., Weaver, A.M. and Eliceiri, K.W., 2014. 3D collagen alignment limits protrusions to enhance breast cancer cell persistence. *Biophysical journal*, 107(11), pp.2546-2558.

Rolfe, K.J. and Grobbelaar, A.O., 2012. A review of fetal scarless healing. *International Scholarly Research Notices*, 2012(1), p.698034.

Roper, J.A., Williamson, R.C., Bally, B., Cowell, C.A., Brooks, R., Stephens, P., Harrison, A.J. and Bass, M.D., 2015. Ultrasonic stimulation of mouse skin reverses the healing delays in diabetes and aging by activation of Rac1. *Journal of Investigative Dermatology*, 135(11), pp.2842-2851.

Roy SG, Nozaki Y, Phan SH (2001) Regulation of alpha-smooth muscle actin gene expression in myofibroblast differentiation from rat lung fibroblasts. *Int J Biochem Cell Biol* 33(7):723– 734.

Rozario, T. and DeSimone, D.W., 2010. The extracellular matrix in development and morphogenesis: a dynamic view. *Developmental biology*, 341(1), pp.126-140.

Saba, T.M. and Jafe, B., 1980. The physiology and pathology of plasma fibronectin. *Blood*, 56(3), pp.405-419.

Sabass, B., Gardel, M.L., Waterman, C.M. and Schwarz, U.S., 2008. High resolution traction force microscopy based on experimental and computational advances. *Biophysical journal*, 94(1), pp.207-220.

Sabass, B., Gardel, M.L., Waterman, C.M. and Schwarz, U.S., 2008. High resolution traction force microscopy based on experimental and computational advances. *Biophysical journal*, 94(1), pp.207-220.

Saito, M., Soshi, S., Tanaka, T. and Fujii, K., 2004. Intensity-related differences in collagen post-translational modification in MC3T3-E1 osteoblasts after exposure to low-and high-intensity pulsed ultrasound. *Bone*, 35(3), pp.644-655.

Samuels, J.A., Weingarten, M.S., Margolis, D.J., Zubkov, L., Sunny, Y., Bawiec, C.R., Conover, D. and Lewin, P.A., 2013. Low-frequency (< 100 kHz), low-intensity (< 100

mW/cm<sup>2</sup>) ultrasound to treat venous ulcers: A human study and in vitro experiments. *The Journal of the Acoustical Society of America*, 134(2), pp.1541-1547.

Satish, L., Gallo, P.H., Baratz, M.E., Johnson, S. and Kathju, S., 2011. Reversal of TGF- $\beta$  1 stimulation of  $\alpha$ -smooth muscle actin and extracellular matrix components by cyclic AMP in Dupuytren's-derived fibroblasts. *BMC musculoskeletal disorders*, 12, pp.1-9.

Schiller, M., Javelaud, D., Mauviel, A., 2004. TGF-beta-induced SMAD signaling and gene regulation: consequences for extracellular matrix remodeling and wound healing. *J Dermatol Sci*, 35, pp.83–92.

Schlicher, R.K., Hutcheson, J.D., Radhakrishna, H., Apkarian, R.P. and Prausnitz, M.R., 2010. Changes in cell morphology due to plasma membrane wounding by acoustic cavitation. *Ultrasound in medicine & biology*, 36(4), pp.677-692.

Schortinghuis, J., Stegenga, B., Raghoobar, G.M. and De Bont, L.G., 2003. Ultrasound stimulation of maxillofacial bone healing. *Crit Rev Oral Biol Med*, 14, pp.63-74.

Schwarzbauer, J.E. and DeSimone, D.W., 2011. Fibronectins, their fibrillogenesis, and in vivo functions. *Cold Spring Harbor perspectives in biology*, 3(7), p.a005041.

Sen, C.K., 2021. Human wound and its burden: updated 2020 compendium of estimates. *Advances in wound care*, 10(5), pp.281-292.

Senk, A. and Djonov, V., 2021. Collagen fibers provide guidance cues for capillary regrowth during regenerative angiogenesis in zebrafish. *Scientific reports*, 11(1), p.19520.

Serezani, A.P., Bozdogan, G., Sehra, S., Walsh, D., Krishnamurthy, P., Potchanant, E.A.S., Nalepa, G., Goenka, S., Turner, M.J., Spandau, D.F. and Kaplan, M.H., 2017. IL-4 impairs wound healing potential in the skin by repressing fibronectin expression. *Journal of Allergy and Clinical Immunology*, 139(1), pp.142-151.

Shah, M., Foreman, D.M. and Ferguson, M.W., 1995. Neutralisation of TGF- $\beta$ 1 and TGF- $\beta$ 2 or exogenous addition of TGF- $\beta$ 3 to cutaneous rat wounds reduces scarring. *Journal of cell science*, 108(3), pp.985-1002.

Shi, F., Harman, J., Fujiwara, K., & Sottile, J. (2010). Collagen I matrix turnover is regulated by fibronectin polymerization. *American journal of physiology. Cell physiology*, 298(5).

Shin, J.Y., Yun, S.K., Roh, S.G., Lee, N.H. and Yang, K.M., 2017. Efficacy of 2 representative topical agents to prevent keloid recurrence after surgical excision. *J Oral Maxillofacial Surg*, 75, pp.401.e1–401.e6.

Shiraishi, R., Masaki, C., Toshinaga, A., Okinaga, T., Nishihara, T., Yamanaka, N., Nakamoto, T. and Hosokawa, R., 2011. The effects of low-intensity pulsed ultrasound exposure on gingival cells. *Journal of periodontology*, 82(10), pp.1498-1503.

Shoulders, M.D. and Raines, R.T., 2009. Collagen structure and stability. *Annual review of biochemistry*, 78(1), pp.929-958.

Sible, J.C., Eriksson, E., Smith, S.P. and Oliver, N., 1994. Fibronectin gene expression differs in normal and abnormal human wound healing. *Wound Repair and Regeneration*, 2(1), pp.3-19.

Sigaut, L., Bianchi, M., Von Bilderling, C. and Pietrasanta, L.I., 2021. Correlation of cellular traction forces and dissociation kinetics of adhesive protein zyxin revealed by multi-parametric live cell microscopy. *PLoS One*, 16(5), p.e0251411.

Singh, D., Rai, V. and Agrawal, D.K., 2023. Regulation of collagen I and collagen III in tissue injury and regeneration. *Cardiology and cardiovascular medicine*, 7(1), p.5.

Singh, P., Carraher, C. and Schwarzbauer, J.E., 2010. Assembly of fibronectin extracellular matrix. *Annual review of cell and developmental biology*, 26(1), pp.397-419.

Sinha, M., Sen, C.K., Singh, K., Das, A., Ghatak, S., Rhea, B., Blackstone, B., Powell, H.M., Khanna, S. and Roy, S., 2018. Direct conversion of injury-site myeloid cells to fibroblast-like cells of granulation tissue. *Nature communications*, 9(1), p.936.

Slemp, A.E. and Kirschner, R.E., 2006. Keloids and scars: a review of keloids and scars, their pathogenesis, risk factors, and management. *Current opinion in pediatrics*, 18(4), pp.396-402.

Smith, K.L. and Dean, S.J., 1998. Tissue repair of the epidermis and dermis. *Journal of Hand Therapy*, 11(2), pp.95-104.

Sorg, H., Tilkorn, D.J., Hager, S., Hauser, J. and Mirastschijski, U., 2017. Skin wound healing: an update on the current knowledge and concepts. *European surgical research*, 58(1-2), pp.81-94.

Sorushanova, A., Delgado, L.M., Wu, Z., Shologu, N., Kshirsagar, A., Raghunath, R., Mullen, A.M., Bayon, Y., Pandit, A., Raghunath, M. and Zeugolis, D.I., 2019. The collagen suprafamily: from biosynthesis to advanced biomaterial development. *Advanced materials*, 31(1), p.1801651.

Sowbhagya, R., Muktha, H., Ramakrishnaiah, T.N., Surendra, A.S., Sushma, S.M., Tejaswini, C., Roopini, K. and Rajashekara, S., 2024. Collagen as the Extracellular Matrix Biomaterials in the Arena of Medical Sciences. *Tissue and Cell*, p.102497.

Speed, C.A., 2001. Therapeutic ultrasound in soft tissue lesions. *Rheumatology*, 40(12), pp.1331-1336.

Stark, R., Grzelak, M. and Hadfield, J., 2019. RNA sequencing: the teenage years. *Nature Reviews Genetics*, 20(11), pp.631-656.

Stadelmann, W.K., Digenis, A.G. and Tobin, G.R., 1998. Physiology and healing dynamics of chronic cutaneous wounds. *The American journal of surgery*, 176(2), pp.26S-38S.

Stern, R., McPherson, M. and Longaker, M.T., 1990. Histologic study of artificial skin used in the treatment of full-thickness thermal injury. *The Journal of Burn Care & Rehabilitation*, 11(1), pp.7-13.

Stoffels, J.M., Zhao, C. and Baron, W., 2013. Fibronectin in tissue regeneration: timely disassembly of the scaffold is necessary to complete the build. *Cellular and Molecular Life Sciences*, 70(22), pp.4243-4253.

Stoffels, J.M.J., Zhao, C. and Baron, W., 2013. Fibronectin in tissue regeneration: timely disassembly of the scaffold is necessary to complete the build. *Cell and Tissue Research*, 339(2), pp.245-256.

Style, R.W., Boltyanskiy, R., German, G.K., Hyland, C., MacMinn, C.W., Mertz, A.F., Wilen, L.A., Xu, Y. and Dufresne, E.R., 2014. Traction force microscopy in physics and biology. *Soft matter*, 10(23), pp.4047-4055.

Sun, Q., Tang, L. and Zhang, D., 2023. Molecular mechanisms of uterine incision healing and scar formation. *European Journal of Medical Research*, 28(1), p.496.

Szauter, K.M., Cao, T., Boyd, C.D. and Csiszar, K., 2005. Lysyl oxidase in development, aging and pathologies of the skin. *Pathologie Biologie*, 53(7), pp.448-456.

Tang, H., Wang, C.C.J., Blankschtein, D. and Langer, R., 2002. An investigation of the role of cavitation in low-frequency ultrasound-mediated transdermal drug transport. *Pharmaceutical research*, 19, pp.1160-1169.

Tang, J., Guha, C. and Tomé, W.A., 2015. Biological effects induced by non-thermal ultrasound and implications for cancer therapy: a review of the current literature. *Technology in cancer research & treatment*, 14(2), pp.221-235.

Tavakkoli, J. and Sanghvi, N.T., 2011. Ultrasound-guided HIFU and thermal ablation. *Therapeutic ultrasound: mechanisms to applications*, pp.137-161.

Thornton, N.J., Garcia, B.A., Hoyer, P. and Wilkerson, M.G., 2021. Keloid scars: an updated review of combination therapies. *Cureus*, 13(1).

Tottoli, E.M., Dorati, R., Genta, I., Chiesa, E., Pisani, S. and Conti, B., 2020. Skin wound healing process and new emerging technologies for skin wound care and regeneration. *Pharmaceutics*, 12(8), p.735.

Trace, A.P., Enos, C.W., Mantel, A. and Harvey, V.M., 2016. Keloids and hypertrophic scars: a spectrum of clinical challenges. *Am J Clin Dermatol*, 17, pp.201–223.

Tracy, L.E., Minasian, R.A. and Caterson, E.J., 2016. Extracellular matrix and dermal fibroblast function in the healing wound. *Advances in wound care*, 5(3), pp.119-136.

Tran, T.A., Roger, S., Le Guennec, J.Y., Tranquart, F. and Bouakaz, A., 2007. Effect of ultrasound-activated microbubbles on the cell electrophysiological properties. *Ultrasound in medicine & biology*, 33(1), pp.158-163.

Tsai, W.C., Pang, J.H.S., Hsu, C.C., Chu, N.K., Lin, M.S. and Hu, C.F., 2006. Ultrasound stimulation of types I and III collagen expression of tendon cell and upregulation of transforming growth factor  $\beta$ . *Journal of orthopaedic research*, 24(6), pp.1310-1316.

Tseng, Q., Duchemin-Pelletier, E., Deshiere, A., Balland, M., Guillou, H., Filhol, O. and Théry, M., 2012. Spatial organization of the extracellular matrix regulates cell–cell junction positioning. *Proceedings of the National Academy of Sciences*, 109(5), pp.1506-1511.

Tsirogianni, Afrodite K., Niki Maria Moutsopoulos, and Haralampos M. Moutsopoulos. "Wound healing: immunological aspects." *Injury* 37, no. 1 (2006): S5-S12.

Tuan, T.L. and Nichter, L.S., 1998. The molecular basis of keloid and hypertrophic scar formation. *Molecular medicine today*, 4(1), pp.19-24.

Ud-Din, S., Volk, S.W. and Bayat, A., 2014. Regenerative healing, scar-free healing and scar formation across the species: current concepts and future perspectives. *Experimental dermatology*, 23(9), pp.615-619.

Uddin, S.M., Komatsu, D.E., Motyka, T. and Petterson, S., 2021. Low-intensity continuous ultrasound therapies—a systematic review of current state-of-the-art and future perspectives. *Journal of clinical medicine*, 10(12), p.2698.

Uitto, J. and Kouba, D., 2000. Cytokine modulation of extracellular matrix gene expression: relevance to fibrotic skin diseases. *Journal of dermatological science*, 24, pp.S60-S69.

Usansky, I., Jaworska, P., Asti, L., Kenny, F.N., Hobbs, C., Sofra, V., Song, H., Logan, M., Graham, A. and Shaw, T.J., 2021. A developmental basis for the anatomical diversity of dermis in homeostasis and wound repair. *The Journal of Pathology*, 253(3), pp.315-325.

Vakonakis, I. and Campbell, I.D., 2007. Extracellular matrix: from atomic resolution to ultrastructure. *Current opinion in cell biology*, 19(5), pp.578-583.

Vallée, A. and Lecarpentier, Y., 2019. TGF- $\beta$  in fibrosis by acting as a conductor for contractile properties of myofibroblasts. *Cell & bioscience*, 9(1), p.98.

Vallet, S.D. and Ricard-Blum, S., 2019. Lysyl oxidases: from enzyme activity to extracellular matrix cross-links. *Essays in biochemistry*, 63(3), pp.349-364.

Van Wamel, A., Kooiman, K., Harteveld, M., Emmer, M., Ten Cate, F.J., Versluis, M. and De Jong, N., 2006. Vibrating microbubbles poking individual cells: drug transfer into cells via sonoporation. *Journal of controlled release*, 112(2), pp.149-155.

Velnar, T., Bailey, T. and Smrkolj, V., 2009. The wound healing process: an overview of the cellular and molecular mechanisms. *Journal of international medical research*, 37(5), pp.1528-1542.

Velnar, T., Bailey, T. and Smrkolj, V., 2009. The wound healing process: an overview of the cellular and molecular mechanisms. *Journal of international medical research*, 37(5), pp.1528-1542.

Venturini, V., Pezzano, F., Castro, F., Häkkinen, H.M., Jiménez-Delgado, S., Colomer-Rosell, M., Marro, M., Tolosa-Ramon, Q., Paz-López, S., Valverde, M.A., Weghuber, J. and Trepap, X., 2020. The nucleus measures shape changes for cellular proprioception to control dynamic cell behavior. *Science*, 370(6514), pp.eabc3643.

Verhaegen, P.D., Van Zuijlen, P.P., Pennings, N.M., Van Marle, J., Niessen, F.B., Van Der Horst, C.M. and Middelkoop, E., 2009. Differences in collagen architecture between keloid, hypertrophic scar, normotrophic scar, and normal skin: an objective histopathological analysis. *Wound repair and regeneration*, 17(5), pp.649-656.

Volk, S.W., Iqbal, S.A. and Bayat, A., 2011. Interactions of the extracellular matrix and progenitor cells in cutaneous wound healing. *Advances in Wound Care*, 2(1), pp.261-272.

Volk, S.W., Wang, Y., Mauldin, E.A., Liechty, K.W. and Adams, S.L., 2011. Diminished type III collagen promotes myofibroblast differentiation and increases scar deposition in cutaneous wound healing. *Cells Tissues Organs*, 194(1), pp.25-37.

Voloshenyuk, T.G., Landesman, E.S., Khoutorova, E., Hart, A.D. and Gardner, J.D., 2011. Induction of cardiac fibroblast lysyl oxidase by TGF- $\beta$ 1 requires PI3K/Akt, Smad3, and MAPK signaling. *Cytokine*, 55(1), pp.90-97.

Wall, I.B., Moseley, R., Baird, D.M., Kipling, D., Giles, P., Laffafian, I., Price, P.E., Thomas, D.W. and Stephens, P., 2008. Fibroblast dysfunction is a key factor in the non-healing of chronic venous leg ulcers. *Journal of Investigative Dermatology*, 128(10), pp.2526-2540.

Walters, K.A. and Roberts, M.S., 2002. The structure and function of skin. In *Dermatological and transdermal formulations* (pp. 19-58). CRC press.

Wang, J., Dodd, C., Shankowsky, H.A., Scott, P.G., Tredget, E.E. and Wound Healing Research Group, 2008. Deep dermal fibroblasts contribute to hypertrophic scarring. *Laboratory investigation*, 88(12), pp.1278-1290.

Wang, J.H. and Li, B., 2010. Application of cell traction force microscopy for cell biology research. *Cytoskeleton Methods and Protocols*, pp.301-313.

Wang, J.H. and Lin, J.S., 2007. Cell traction force and measurement methods. *Biomechanics and modeling in mechanobiology*, 6, pp.361-371.

Wang, K., Wen, D., Xu, X., Zhao, R., Jiang, F., Yuan, S., Zhang, Y., Gao, Y. and Li, Q., 2023. Extracellular matrix stiffness—The central cue for skin fibrosis. *Frontiers in Molecular Biosciences*, 10, p.1132353.

Wang, R., Ghahary, A., Shen, Q., Scott, P.G., Roy, K. and Tredget, E.E., 2000. Hypertrophic scar tissues and fibroblasts produce more transforming growth factor- $\beta$ 1 mRNA and protein than normal skin and cells. *Wound Repair and Regeneration*, 8(2), pp.128-137.

Wang, W.Y., Pearson, A.T., Kutys, M.L., Choi, C.K., Wozniak, M.A., Baker, B.M. and Chen, C.S., 2018. Extracellular matrix alignment dictates the organization of focal adhesions and directs uniaxial cell migration. *APL bioengineering*, 2(4).

Wang, X.J., Han, G., Owens, P., Siddiqui, Y. and Li, A.G., 2006. Role of TGF $\beta$ -mediated inflammation in cutaneous wound healing. *Journal of Investigative Dermatology Symposium Proceedings*, 11(1), pp.112-117.

Wei, S., Gao, L., Wu, C., Qin, F. and Yuan, J., 2020. Role of the lysyl oxidase family in organ development. *Experimental and Therapeutic Medicine*, 20(1), pp.163-172.

Werner, S., Krieg, T. and Smola, H., 2007. Keratinocyte–fibroblast interactions in wound healing. *Journal of investigative dermatology*, 127(5), pp.998-1008.

Wershof, E., Park, D., Barry, D.J., Jenkins, R.P., Rullan, A., Wilkins, A., Schlegelmilch, K., Roxanis, I., Anderson, K.I., Bates, P.A. and Sahai, E., 2021. A FIJI macro for quantifying pattern in extracellular matrix. *Life science alliance*, 4(3).



White, L.A., Mitchell, T.I. and Brinckerhoff, C.E., 2000. Transforming growth factor  $\beta$  inhibitory element in the rabbit matrix metalloproteinase-1 (collagenase-1) gene functions as a repressor of constitutive transcription. *Biochimica et Biophysica Acta (BBA)-Gene Structure and Expression*, 1490(3), pp.259-268.

Widgerow, A.D., King, K., Tocco-Tussardi, I., Banyard, D.A., Chiang, R., Awad, A., Afzel, H., Bhatnager, S., Melkumyan, S., Wirth, G. and Evans, G.R., 2015. The burn wound exudate—An under-utilized resource. *Burns*, 41(1), pp.11-17.

Wild, S., Roglic, G., Green, A., Sicree, R. and King, H., 2004. Global prevalence of diabetes: estimates for the year 2000 and projections for 2030. *Diabetes care*, 27(5), pp.1047-1053.

Wolf, K., Te Lindert, M., Krause, M., Alexander, S., Te Riet, J., Willis, A.L., Hoffman, R.M., Figdor, C.G., Weiss, S.J. and Friedl, P., 2013. Physical limits of cell migration: control by ECM space and nuclear deformation and tuning by proteolysis and traction force. *The Journal of cell biology*, 201(7), p.1069.

Wong, V.W., Gurtner, G.C. and Longaker, M.T., 2013, September. Wound healing: a paradigm for regeneration. In *Mayo Clinic Proceedings*, 88 (9), pp. 1022-1031

Wood, V.T., Pinfildi, C.E., Neves, M.A., Parizoto, N.A., Hochman, B. and Ferreira, L.M., 2010. Collagen changes and realignment induced by low-level laser therapy and low-intensity ultrasound in the calcaneal tendon. *Lasers in Surgery and Medicine*, 42(6), pp.559-565.

Wu, J. and Nyborg, W.L., 2008. Ultrasound, cavitation bubbles and their interaction with cells. *Adv Drug Deliv Rev*, 60, pp.1103-1116.

Xie, Y., Yang, Z., Zhou, Y., Yin, X., Yin, Y., Zhang, W. and Zhang, X., 2009. Persistent expression of integrin  $\alpha\beta 6$  induces chronic wounds by increasing TGF- $\beta 1$  levels in mice. *Journal of Investigative Dermatology*, 129(1), pp.2463-2471.

Xin, Z., Lin, G., Lei, H., Lue, T.F. and Guo, Y., 2016. Clinical applications of low-intensity pulsed ultrasound and its potential role in urology. *Transl Androl Urol*, 5, pp.255-266.

Xue, M. and Jackson, C.J., 2015. Extracellular matrix reorganization during wound healing and its impact on abnormal scarring. *Advances in wound care*, 4(3), pp.119-136.

Y.F. Zhou, 2011. High intensity focused ultrasound in clinical tumor ablation. *World J. Clin. Oncol.*, 2, pp.8–27.

Yamada, K.M. and Sixt, M., 2019. Mechanisms of 3D cell migration. *Nature Reviews molecular cell biology*, 20(12), pp.738-752.

Yang, K.H., Parvizi, J., Wang, S.J., Lewallen, D.G., Kinnick, R.R., Greenleaf, J.F. and Bolander, M.E., 1996. Exposure to low-intensity ultrasound increases aggrecan gene expression in a rat femur fracture model. *Journal of Orthopaedic Research*, 14(5), pp.802-809.

Yang, S.W., Geng, Z.J., Ma, K., Sun, X.Y. and Fu, X.B., 2016. Comparison of the histological morphology between normal skin and scar tissue. *Journal of Huazhong University of Science and Technology [Medical Sciences]*, 36(2), pp.265-269.

Yeung, D.A. and Kelly, N.H., 2021. The role of collagen-based biomaterials in chronic wound healing and sports medicine applications. *Bioengineering*, 8(1), p.8.

Yue, B., 2014. Biology of the extracellular matrix: an overview. *Journal of glaucoma*, 23, pp.S20-S23.

Yue, B., 2014. Biology of the extracellular matrix: an overview. *Journal of glaucoma*, 23, pp.S20-S23.

Yue, Y., Yang, X., Zhang, L., Xiao, X., Nabar, N.R., Lin, Y., Hao, L., Zhang, D., Huo, J., Li, J. and Cai, X., 2016. Low-intensity pulsed ultrasound upregulates pro-myelination indicators of Schwann cells enhanced by co-culture with adipose-derived stem cells. *Cell Proliferation*, 49(6), pp.720-728.

Zhang, Z.J., Huckle, J., Francomano, C.A. and Spencer, R.G., 2003. The effects of pulsed low-intensity ultrasound on chondrocyte viability, proliferation, gene expression and matrix production. *Ultrasound in medicine & biology*, 29(11), pp.1645-1651.

Zhang, E., Gao, B., Yang, L., Wu, X. and Wang, Z., 2016. Notoginsenoside Ft1 promotes fibroblast proliferation via PI3K/Akt/mTOR signaling pathway and benefits wound healing in genetically diabetic mice. *Journal of pharmacology and experimental therapeutics*, 356(2), pp.324-332.

Zhong, F., Cao, S., Yang, L., Liu, J., Gui, B., Wang, H., Jiang, N., Zhou, Q. and Deng, Q., 2024. Low intensity pulsed ultrasound accelerates diabetic wound healing by ADSC derived exosomes via promoting the uptake of exosomes and enhancing angiogenesis. *International Journal of Molecular Medicine*, 53(3), pp.1-13.

Zhou, S., Schmelz, A., Seufferlein, T., Li, Y., Zhao, J. and Bachem, M.G., 2004. Molecular mechanisms of low intensity pulsed ultrasound in human skin fibroblasts. *Journal of Biological Chemistry*, 279(52), pp.54463-54469.

Zollinger, A.J. and Smith, M.L., 2017. Fibronectin, the extracellular glue. *Matrix Biology*, 60, pp.27-37.

Zura, R., Della Rocca, G.J., Mehta, S., Harrison, A., Brodie, C., Jones, J. and Steen, R.G., 2015. Treatment of chronic (> 1 year) fracture nonunion: heal rate in a cohort of 767 patients treated with low-intensity pulsed ultrasound (LIPUS). *Injury*, 46(10), pp.2036-2041.

Zwolinski, C.M., Ellison, K.S., DePaola, N. and Thompson, D.M., 2011. Generation of cell-derived three dimensional extracellular matrix substrates from two dimensional endothelial cell cultures. *Tissue Engineering Part C: Methods*, 17(5), pp.589-595.